

THE RADIO AND ELECTRONIC ENGINEER

The Journal of the Institution of Electronic and Radio Engineers

FOUNDED 1925 INCORPORATED BY ROYAL CHARTER 1961

"To promote the advancement of radio, electronics and kindred subjects by the exchange of information in these branches of engineering."

VOLUME 32

SEPTEMBER 1966

NUMBER 3

Q R Y

QRY—the Quality and Reliability Year—which is to be inaugurated on 20th October next has been planned by the British Productivity Council in association with the National Council for Quality and Reliability. The Institution was one of the founder members of the latter body and has given it active support throughout its life of something more than four years. The history of the first two years of N.C.Q.R. has been recorded in our *Journal*; for the present purpose it suffices to add that its subsequent life has seen a widening and strengthening of its membership and structure with a corresponding increase in its influence on the imperative need for positive action directed to the enhancement of quality and reliability of all classes of products and services.

It is both proper and realistic that N.C.Q.R. should make no attempt to dictate a detailed plan of operation for its member bodies during QRY—nor for that matter at any other time. The Institution's Council have unreservedly endorsed the principles underlying QRY and are making known to all Standing Committees and Local Sections their wish that every opportunity is taken during the year to identify their programmes, discussions and tasks with the theme of quality and reliability. It has done so in the knowledge that our professional history already has seen a great concentration on the topic with no little success and that our membership has a high potential for valuable support to the many and varied events during—and indeed subsequent to—QRY.

Corporate collaboration is thus assured, but this still leaves a pressing need for our members individually to identify themselves with the principles and efforts underlying QRY. The Chartered Engineer and all who aspire to this responsible status have a special duty to the general public, whether the latter is regarded as individuals or collectively as a nation. As individuals we have a rightful expectation of an appropriate standard of quality and reliability in our personal purchases, be they products or services. Collectively as a nation we have a proud quality record behind us which in present circumstances needs increasing concentration not only to maintain but to enhance.

Apart from the leading events of the QR Year planned on a national level—among the first is the important Inter-Industry Conference in Blackpool from 8th to 10th November—the 89 permanently organized QR Groups attached to the Local Productivity Associations of the British Productivity Council will be orienting their own local activities toward the wider objective of national advancement in the principles and practices essential to quality and reliability progress. They will also look to the Year as an opportunity for gaining increased support for their purely local objectives. Many of these special events will be listed in the Institution's *Proceedings* or brought otherwise to the attention of members in the Local Sections.

Furthermore, the two major Conferences to be organized nationally by the Institution during 1967 will bear directly or indirectly on QRY: these are on 'Design for Production', with which the Institution of Production Engineers will be associated, and on 'Radio Frequency Measurements and Standards' which will have the similar support of the Institution of Electrical Engineers.

The moral support of our membership and the participation of all who can render practical support during and after the Quality and Reliability Year is urged as our professional duty in aid of what has been very aptly called the most valuable commodity this country can offer.

F. G. DIVER

INSTITUTION NOTICES

Discussion on Progress in Automated Assembling

At the request of the Minister of Technology, the United Kingdom Automation Council is promoting a discussion on 'Progress in Automated Assembling', which will be held at the University of Nottingham on 3rd and 4th January 1967. The organization of the meeting is being undertaken by the Institution of Production Engineers.

The Minister of Technology, The Rt. Honourable Anthony Wedgwood Benn, M.P., will give the opening address to the meeting and the seven sessions will be on the following subjects:

- Automatic Sub-Assembly;
- Automatic Assembling Machines: Examples of Current Practice;
- Operator-Paced or Machine-Paced Automatic Assembling Machines;
- The Economics of Automatic Assembling;
- Component and Product Design for Automatic Assembling;
- Quality Control and Automatic Inspection for Automatic Assembling;
- The Shape of Things to Come: a Review of Research Programmes.

Application forms may be obtained from the I.Prod.E., 10 Chesterfield Street, London, W.1. Further details will be announced in the *Proceedings of the I.E.R.E.*

Centenary of the Royal Aeronautical Society

The Institution was represented at several of the functions held recently to mark the centenary of the founding of the Royal Aeronautical Society.

Over very many years the Institution has had close association with the Royal Aeronautical Society and to mark this notable occasion the Institution has presented to the Society a silver cigarette box suitably inscribed.

Acoustic Noise and its Control

A conference on Acoustic Noise and its Control will be held at the Institution of Electrical Engineers from 23rd to 26th January 1967.

Topics to be discussed will include the subjective aspects of noise problems, the nature of the human perception of noise, and the analysis and measurement of noise. Consideration will be given to the ways in which noise is generated in machines and the techniques that are necessary to reduce it to acceptable levels. Methods of reducing internally the noise generated inside a building and methods of impeding its transmission through the structure will be discussed.

Joint sponsors of the Conference are: the I.E.E. Electronics Division, the Institution of Electronic and Radio Engineers (through its Electro-Acoustics Group Committee), the Institute of Electrical and Electronics Engineers (U.K. and Eire Section), the Institute of Physics and the Physical Society, and the British Acoustical Society.

Registration forms and further details will be available from the I.E.R.E., 8-9 Bedford Square, London, W.C.1.

Electronics and Britain's Future

The first report of the Economic Development Committee for Electronics, set up by the British Government's National Economic Development Council in 1964, has now been issued.*

Whilst touching on the inherent problems of research and development, e.g. capital equipment, the report emphasizes the importance of a thriving electronics industry in the future of Britain's economic development.

A fuller commentary will be given in the Institution's *Proceedings*.

Back Copies of the Journal

Because of the increasing number of requests by new subscribers, several issues of *The Radio and Electronic Engineer* for this year are now out of print, namely, February, April and May 1966 (Volume 31). Members in the United Kingdom who are willing to part with their copies of any or all of the above three issues (which *must* be in good condition) are invited to send them to the Publications Department, I.E.R.E., 8-9 Bedford Square, London, W.C.1; payment of 5s. per copy will be made. Please note that these are the only issues required. In view of the liability to damage in the post, *Journals* should *not* be sent from overseas.

Conference on U.H.F. Television Erroneous Announcement

Announcements that a Conference on U.H.F. Television is to be held under the Institution's auspices in London from 22nd to 23rd November 1966, have recently appeared in error in several publications which list forthcoming international conferences. This Conference in fact took place on the dates mentioned in 1965. Reference is made to the announcements here in order to warn any intending participants who may believe that the Conference has become an annual event. (Copies of the papers read at the 1965 Conference are still available as a complete volume from the Institution, price £2 10s.)

* Obtainable from the Secretary, Electronics E.D.C., National Economic Development Office, Millbank Tower, London, S.W.1.

Improved Radar Visibility of Small Targets in Sea Clutter

By

J. CRONEY, B.Sc., Ph.D.†

Presented at a meeting of the Radar and Navigational Aids Group in London on 19th January 1966.

Summary: An X-band radar has been built with an antenna capable of rotational speeds up to 1400 rev/min, and a display system which follows at these speeds. This enables only one or two pulses per beam-width to be displayed, the pulses received from successive looks at the sea clutter being de-correlated. A conventional fluoride p.p.i. tube and a storage p.p.i. tube were used simultaneously. The resulting improvements from de-correlation and integration are demonstrated.

List of Symbols

x	instantaneous clutter amplitude
σ	r.m.s. clutter amplitude
$P(x) dx$	probability of x lying between x and $x + dx$
θ	azimuth beam-width of antenna in degrees
N_s	revolutions per minute of slowly rotating antenna
P	repetition rate of radar in pulses per second
t_c	de-correlation time of clutter
N_r	revolutions per minute of rapidly rotating antenna
u/c	ratio of un-correlated to correlated pulses
$R(t')$	normalized auto-correlation function of clutter signals
$G(f)$	power spectral density function of clutter signals
Δf	half power band-width of clutter spectrum
f	frequency of clutter spectrum
t'	value of t_c in milliseconds at which the clutter auto-correlation function drops to $1/n$ of its peak value

1. Introduction

One of the difficulties encountered in the use of radar for marine navigation is the obscuration on the c.r.t. of small target echoes by radar returns from the surface of the sea (sea clutter). Even when the target is returning a signal several times greater in power than that from the sea waves in its vicinity (clutter signal) the target signal will still be lost once the clutter signal is large enough fully to brighten (saturate) the p.p.i. display tube. These effects can be particularly troublesome in the picking out of buoyed channels to harbour entrances, and in safe navigation through areas congested by small traffic.

In previous papers¹⁻³ the author has dealt with the design and use of logarithmic receivers for eliminating

† Admiralty Surface Weapons Establishment Extension, Funtington, near Chichester, Sussex.

this saturation effect by sea clutter signals. The techniques there described bring the r.m.s. amplitude of the random clutter signals down to the same r.m.s. amplitude of the random noise background on the display. In spite of this the sea clutter areas on the displays are still readily distinguishable from the receiver noise areas; the clutter areas appear to have a much coarser grain size than the noise areas and look in fact very much like a random collection of signals from targets of small yet significant size. The problem of identifying positively a genuine target signal in such areas is still considerable if the target signal is only a few decibels above the clutter signal. The author has stated³ that this increased coarseness of the clutter area was caused by the strong correlation from pulse to pulse of the sea clutter signals compared with the noise signals, and suggested that ways of destroying this correlation could give further worthwhile improvements in the detection of wanted signals in clutter. The present work is concerned firstly with one method of destroying this correlation in order to smooth out the clutter background and so improve the visibility of a wanted signal against this background. Secondly, it is concerned with improved signal integration techniques to enhance the signal/clutter visibility in the smoothed clutter region.

2. Theoretical Consideration

2.1. Correlation of Sea Clutter

The author has stated the important properties of, and differences between, background noise and sea clutter on a p.p.i. display.³

Considering a fixed element of range (pulse-width) from one trace to the next of a p.p.i. display it was stated that both noise and sea clutter obey more or less a Rayleigh amplitude probability distribution given by

$$P(x) dx = \frac{2x}{\sigma^2} \exp(-x^2/\sigma^2) dx$$

and represented in Fig. 1 where amplitude is plotted as abscissae and probability as ordinate. It is this property which enables the logarithmic receiver to

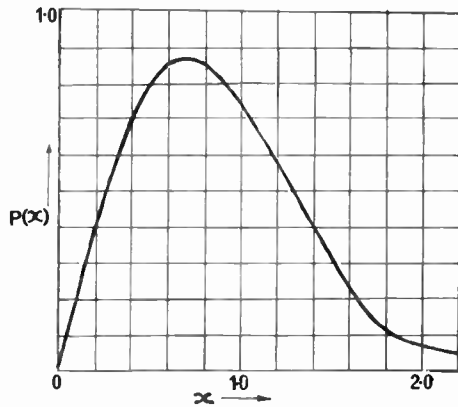


Fig. 1. Curve of Rayleigh distribution of x plotted for scale factor $\sigma = 1.0$.

$$\text{Equation of curve: } P(x) dx = \frac{2x}{\sigma^2} \exp(-x^2/\sigma^2) dx.$$

reduce the r.m.s. amplitudes of sea clutter and background noise to equality. Even so as stated above, the clutter region still has a very different appearance from the noise.

In a typical X-band civil marine radar there will usually be about sixteen successive range traces of the p.p.i. within one beam-width of motion of the antenna. Considering a particular range element of noise we are likely, in the sixteen samples, to run the whole gamut of possible amplitude values on the curve of Fig. 1, because noise is not correlated from trace to trace. But for a range element of sea clutter all sixteen samples may be nearly identical possibly at one extreme near zero, or at the other extreme of very large amplitude. This is because the sea surface changes relatively slowly and the clutter signals can be correlated over the whole beam-width of the antenna. If we looked longer the sea clutter would establish the random nature of its amplitude just the same as the noise. But we cannot in a simple radar. It is the intention of this work to consider a modification to the radar which will enable us to establish the random nature of the clutter in the shortest practicable time of observation, remembering that with a moving platform effective observation times on any element of range are limited.

2.2. De-correlation Gain

Consider a typical civil marine radar with a slowly rotating antenna. Let this antenna rotate at N_s rev/min, and assume the azimuth beam-width to be θ deg. Then the time to sweep through one beam-width in azimuth will be

$$\frac{\theta}{6N_s} \text{ seconds.}$$

If the pulse repetition rate of the radar is p pulses per second there will be

$$\frac{\theta p}{6N_s}$$

pulses on the target.

If the time required between successive transmitted pulses to effect de-correlation of the successive received pulses is t_c seconds, those pulses within every packet pt_c of the above pulses will be correlated. The number of un-correlated samples that we could obtain from any given bearing (target) would therefore be

$$\frac{\theta}{6N_s t_c} \text{ per revolution of the antenna.}$$

Now assume the speed of rotation of the antenna to be increased, keeping the repetition rate the same until a speed N_f is reached where only one pulse is transmitted per beam-width (bearing), the next pulse for that same bearing coming one complete revolution later at an interval of time equal to or greater than t_c seconds. All the pulses are now de-correlated. Also the number of de-correlated pulses received (on any given bearing) during a time corresponding to one revolution of the original slowly rotating antenna will be simply:

$$\frac{N_f}{N_s}$$

having increased from $\frac{\theta}{6N_s t_c}$ to this figure as the antenna speeded up.

We therefore have, for the ratio of un-correlated to correlated pulses,

$$\begin{aligned} u/c &= \frac{N_f}{N_s} \times \frac{6N_s t_c}{\theta} \\ &= \frac{6N_f t_c}{\theta} \end{aligned}$$

Since we have chosen the interval between pulses, $\frac{1}{p}$ seconds, to be equal to the time of passage of the antenna through one beam-width, $\frac{\theta}{6N_f}$ seconds, we have $\frac{6N_f}{\theta} = p$ and therefore

$$u/c = pt_c \dots\dots(1)$$

It was found early in the present work that there are severe losses in sensitivity of the radar system if only one pulse is transmitted per beam-width. This arises from scanning losses of the antenna beam as it sweeps across the target, and the practical limit is to transmit two pulses per antenna beam-width so that we then get un-correlated packets of two pulses for each antenna beam-width. Under these conditions

$$u/c = \frac{pt_c}{2} \dots\dots(2)$$

To assess magnitudes for u/c it is necessary to make some estimate of the de-correlation time t_c of the sea clutter. The following analysis gives an approximate figure.

For a continuously varying function $F(t)$ the normalized auto-correlation function $R(t')$ is defined by

$$R(t') = \frac{\int_{-\infty}^{+\infty} F(t) F(t+t') dt}{\int_{-\infty}^{+\infty} \{F(t)\}^2 dt} \dots\dots(3)$$

The Wiener-Khintchine theorem⁴ states that for a continuous signal the power spectral density $G(f)$ is the Fourier transform of the auto-correlation function. Applying this we get:

$$G(f) = \int_{-\infty}^{+\infty} R(t') \exp(-j\omega t') dt' \dots\dots(4)$$

and by the duality of Fourier transforms

$$R(t') = \int_{-\infty}^{+\infty} G(f) \exp(j\omega t') df \dots\dots(5)$$

The power spectrum of sea clutter has been determined experimentally to be approximately Gaussian⁵ and we may therefore represent this in terms of its half-power band-width Δf by

$$G(f) = \exp\left\{-0.7\left(\frac{2f}{\Delta f}\right)^2\right\} \dots\dots(6)$$

where f is measured as deviation from the maximum ordinate. Substituting in eqn. (5)

$$R(t') = \int_{-\infty}^{+\infty} \exp\left\{-0.7\left(\frac{2f}{\Delta f}\right)^2\right\} \exp(j2\pi f t') df \dots\dots(7)$$

$$= - \int_{-\infty}^{+\infty} \exp\left\{j2\pi f t' - 0.7\left(\frac{2f}{\Delta f}\right)^2\right\} df \dots\dots(8)$$

which may be evaluated as

$$R(t') = \Delta f \sqrt{\frac{\pi}{2.8}} \exp\left\{\frac{-(2\pi t' \Delta f)^2}{11.2}\right\}$$

normalizing

$$R(t') = \exp\left\{\frac{-(2\pi t' \Delta f)^2}{11.2}\right\} \dots\dots(9)$$

The half-power band-width of sea clutter at X-band has been determined⁵ as 60 Hz. Inserting this value, and expressing t' as the time t_c in milliseconds for which the auto-correlation function drops to $1/n$ of its peak value we get

$$\exp(-0.012t^2) \simeq \frac{1}{n} \dots\dots(10)$$

Using this relationship we may derive values of t for a series of values of n . And inserting the values of t so obtained into eqn. (2) we may estimate the likely improvements to be obtained in visibility from de-correlation in the following manner.

For a radar of azimuth beam-width 2 deg and antenna revolution rate $N_p = 1200$ per minute the time to go through one beam-width will be $1/3600$ seconds and we would therefore need a pulse repetition rate of $p = 3600$ per second to give one pulse per beam-width. Inserting this value in eqn. (2) we get for the practical case:

$$u/c = 1.8t_c$$

where t_c is in milliseconds. Assuming a square root relationship for post-detector integration efficiency, we may construct Table I below, to show the visibility improvement in decibels for different values of n in eqn. (10).

Table I

n	t_c (milliseconds)	$\sqrt{u/c}$ dB
2	8	5.8
10	14	6.9
100	20	7.7
1000	24	8.2

It is often assumed that correlation effectively ceases when the auto-correlation function drops to one half ($n = 2$) of its peak value. Other workers however consider correlation to be significant down to much smaller fractions of the peak value even down to the first zero. As the auto-correlation function in our case is Gaussian there is no first zero but even if we let the function drop to one thousandth of its peak value ($n = 1000$) the additional improvement in visibility is not large. It is probably safe to look for an improvement of no more than 6.0 dB.

Although this sounds only a modest improvement it should be remembered that the signal to clutter visibility of a target in sea clutter is inversely proportional to range, other factors being constant.^{6, 11} This implies that the improvement translates directly to an improvement in range into which the target can be tracked as it approaches closer into the clutter.

2.3. Integration Times

The useful integration time will depend either on the time taken for a target to move through one spot size of the p.p.i. tube, or one pulse length whichever is the greater. Assuming the ship to be approaching buoyed channels or harbour entrances, the use of a range scale of 2 miles is not unreasonable. We may also assume a civil marine radar set with a 0.1 μ s pulse to be in use. In the author's view it is unlikely

for a c.r.t. of 12-inch diameter, focused and adjusted for brightness by ships' personnel, to have a spot size less than 0.5 mm. Under these circumstances, on the 4000 yards range scale, both the pulse length and spot size equate approximately to 40 feet.

Assuming the radial component of the relative approach velocity to buoys or small craft to be about 10 knots, this gives possible integration times of 3 seconds. For a four-mile range scale the figures will be 6 seconds and for targets with lower relative velocities (e.g. parallel passage on the beams where antenna beam-width becomes the limiting factor) longer times will be possible.

The integration of pulses on a normal p.p.i. tube is generally considered to lie in a combination of properties of the eye of the observer and the phosphor of the c.r. tube. Blake⁷ suggests a figure of 2 seconds as a conservative value of integration time for this combination. The author doubts if, under typical conditions of adjustment at sea, efficient integration occurs even for this time. This will appear later in considering those results of the present experiments where a storage tube was in use.

3. Description of Equipment

The equipment used in this work was an X-band radar system (about 15 kW peak power, 0.1 μ s pulse length), with a number of special features. These will be briefly outlined here: some of them are dealt with more fully elsewhere.

(i) The antenna (vertically polarized, azimuth beam-width 2 deg, elevation beam-width 16 deg), comprised a linear array enclosed in an aerodynamically designed radome, and designed to rotate at continuously variable speeds from 20 rev/min to 1400 rev/min. This is the subject of a separate paper.⁸

(ii) A modulator in which the repetition rate was continually variable from 1 to 10 kHz.

(iii) The antenna was sited on a bank overlooking the sea, some one hundred feet away from the transmitting, receiving, and display equipment. The X-band signals were therefore piped through circular waveguide, operating in the H_{01} mode to keep losses down. In this way some 5 dB of radar losses were eliminated. This technique was developed by the Marconi Company for radar applications, and a description with a photograph of the actual waveguide run is given in Reference 9.

(iv) The receiving channel was specially designed to have a very uniform logarithmic input output relationship over 100 dB of input range. The bandwidth was 14 MHz to half power points and the r.m.s. noise level was set at about 20 dB up the logarithmic characteristic so that fluctuations 20 dB

below this level remained on the logarithmic characteristic. This was a transistor amplifier and to achieve the very uniform law some new techniques involving long-tailed pairs were employed. This is the subject of a separate paper.¹⁰

(v) Two displays were used side by side. Both had range scales variable from one to ten miles. One used a normal phosphor p.p.i. tube of 12-inch diameter, and the other a newly-developed storage tube of 11-inch diameter (English Electric Valve Co. E712). Special techniques were necessary to give mag-slip transmission revolving at 1200 rev/min. This work will be recorded separately.

4. Observations and Results

The antenna was sited about 45 ft above sea level on a bank above the beach at Southsea. Under these conditions, and with the transmitter power used, it needs rough seas which occur perhaps only two or three times a month throughout the autumn and winter to give clutter out to ranges of a mile or more. More often clutter will extend out to half a mile and so that observations could be made in these more prevalent conditions the first targets were two smooth spheres of 2 ft (61 cm) diameter giving echoing areas of about 0.3 m². From calculations these targets seemed likely to be just visible in a condition of moderate clutter. The targets were supported on 2-inch diameter wooden poles (fibreglass poles were used in later experiments). The poles were secured to floats which just broke the surface of the water. The centres of the spheres were about 6 ft above the water level in calm conditions, but the poles leaned considerably in rough conditions.

The storage tube did not become available until a late stage of the experiments so that the bulk of the work reported here used an ordinary fluoride p.p.i. tube alone. The method of operation was to set the repetition rate of the radar to give 2 pulses per beam-width or less at the high speed rotation of the antenna (1200 rev/min) and observe and photograph the p.p.i. The antenna was then adjusted to normal speed (about 20 rev/min), keeping the repetition rate the same, so that mean transmitted power was constant and the p.p.i. again observed and photographed. From the first observations of the display there seemed no significant difference between the pictures obtained using antenna speeds of 1000 and 1200 rev/min. Although the antenna revolved satisfactorily at 1200 rev/min there seemed no point in adding unnecessarily to the rotational stresses and most of the work was therefore conducted at speeds of 1000 rev/min.

Figure 2 gives a key to the targets present in the clutter during the first set of observations, and to the

range scale in use on the p.p.i. Range marker rings were not used. The range (2000 yards) of South Parade Pier, near the right-hand edge of the p.p.i., was taken as an adequate indication. The two 0.3 m² targets are ringed, other targets present, with estimated echoing areas, are shown by crosses.

In the first comparison (Fig. 3) clutter extends out to about 0.6 mile. The repetition rate was set at 5400 pulses/second and the antenna switched between 20 and 1000 rev/min. The smoothing of the clutter by de-correlation is obvious, giving significant improvement in the identification of the targets. The time of exposure (3 seconds) is sufficiently short to make camera integration effects small. The pictures shown here look similar to the direct observations of the p.p.i. by the eye.

With the antenna set to rotate at 20 rev/min as for Fig. 3(a) three further pictures of the p.p.i. were taken using exposures of 9 seconds, 18 seconds, and 40 seconds respectively. The camera in this process integrates the de-correlated packets of correlated pulses until enough de-correlated pulses have been recorded to establish the random nature of the clutter and smooth it out. Only the longest of these exposures (40 seconds) is reproduced here as Fig. 4. The smoothing achieved is obvious when we compare Fig. 4, 40 seconds integration, with Fig. 3(a), 3 seconds integration. A most interesting comparison is that of Fig. 4 with Fig. 3(b). We notice that we have not perhaps quite achieved the degree of smoothing of the clutter background after 40 seconds of integration from the slowly rotating antenna that we have achieved after only 3 seconds of integration from the rapidly rotating antenna. But the target visibilities are not much different and we may safely say, (making the crude assumption of a square root law for the efficiency of post detector integration) that the high speed system represents an improvement of $\sqrt{(40/3)} = 5.6$ dB in signal to clutter visibility. Of course with moving targets we would never be able to integrate effectively for anything like 40 seconds so the high speed system offers a practical advantage.

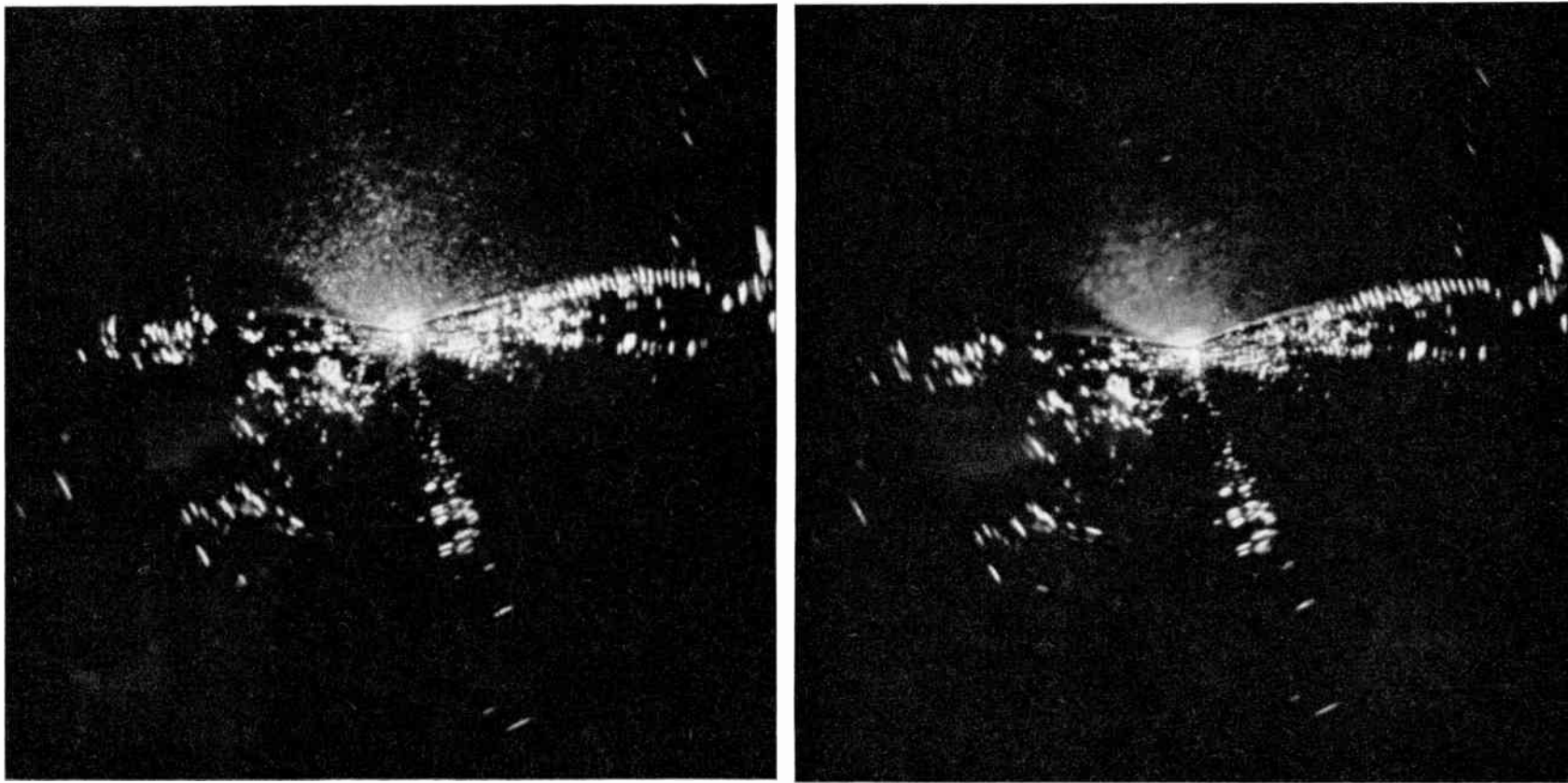
The additional 3 targets (close inshore and at the water's edge, Fig. 4) were small boats of a Royal Marines exercise. These had not appeared when Fig. 3(b) was taken, about 15 minutes earlier.

The 0.3 m² targets were now replaced by 4 targets of 3 to 5 m² so that observations could be made in heavier seas. These were reflecting spheres with some 'omni-directional gain' of the type described in Reference 11. However before any photographic records could be made the outer pair were washed away in a storm. Pictures taken during the later part of this storm are shown in Fig. 5. (To save space the lower half and the edges of each picture have been cut

away.) Figure 5(a) shows one revolution of the p.p.i. with the slowly rotating antenna, 20 rev/min. The p.r.f. was 6000 to give 100 pulses per beam-width with the slowly rotating antenna, and 2 pulses per beam-width with the antenna speeded up to 1000 rev/min.

In these pictures the clutter extends to 1.4 miles (South Parade Pier, 2000 yards, is marked with a cross in Fig. 5(b)). The sea was covered with 'white horses' with waves estimated at 6 ft. Again the smoothing of the clutter between the slowly rotating and rapidly rotating system is illustrated in comparing 5(a) with 5(b); it does not appear to be as marked as with the lower sea state (Fig. 4). The two 3-5 m² targets are ringed in Fig. 5(b) though it is not suggested that an observer would have picked them out in this case. It needs in fact 9 seconds of integration on the rapid scan system, (Fig. 5(c)) before an observer could be reasonably sure of locating these targets. In Fig. 5(d) are shown the result of a 12-second integration of the output from the slowly rotating antenna system. Again there is clearly an advantage in the de-correlated system (Fig. 5(c)). (The successive dark rings in this sequence of pictures were caused by a fault in the video amplifier, which could not be cleared before the clutter subsided.) Unfortunately the two remaining targets were at such close range in these high seas that it needed longer photographic exposures than were taken (30 seconds) in order to establish the improvement between the correlated and de-correlated systems. Even the records that were taken were under-exposed making conclusions difficult. The author at this stage therefore, has formed only a subjective impression (from visual observation) that the improvement in visibility was somewhat less marked than with the slighter seas. It is the intention to take further records in very rough seas.

The next set of observations were made on the 11-inch direct view storage tube (E712) which was placed beside the fluoride tube, both operating together. For the set of recordings then made, clutter extended out to 0.8 miles, 'white horses' being visible to the eye to three-quarters of a mile. Four new collimating spheres of 3-5 m² echoing area¹¹ had been placed in position; they are ringed in Fig. 6 which should be used for assisting identification in the following sequence. A system which enabled the antenna speed to be adjusted continuously rather than in steps had now been installed; the slowest possible speed proved to be 28 rev/min and the slow-speed pictures are all taken at this speed. First we shall look at the results with the fluoride tube. Figures 7(a) and (b) show the comparison between the correlated and de-correlated system. The smoothing of the clutter is rather more obvious than with the rougher seas of Fig. 5. The four targets can be reasonably identified in Fig. 7(b),



(a) Slowly rotating antenna, 20 rev/min, 3 seconds exposure, (1 revolution), one packet of 90 correlated pulses per beam-width.

(b) Rapidly rotating antenna, 1000 rev/min, 3 seconds exposure, (50 revolutions), 50 de-correlated packets of 1.8 pulses per beam-width.

Fig. 3.

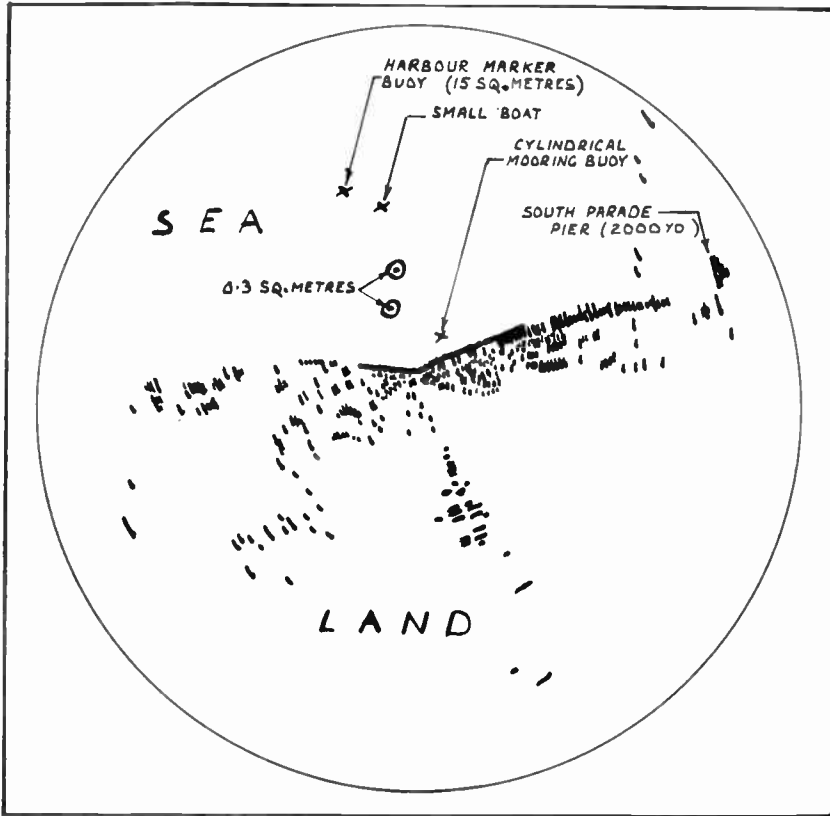


Fig. 2. Key to photographs of Fig. 3.

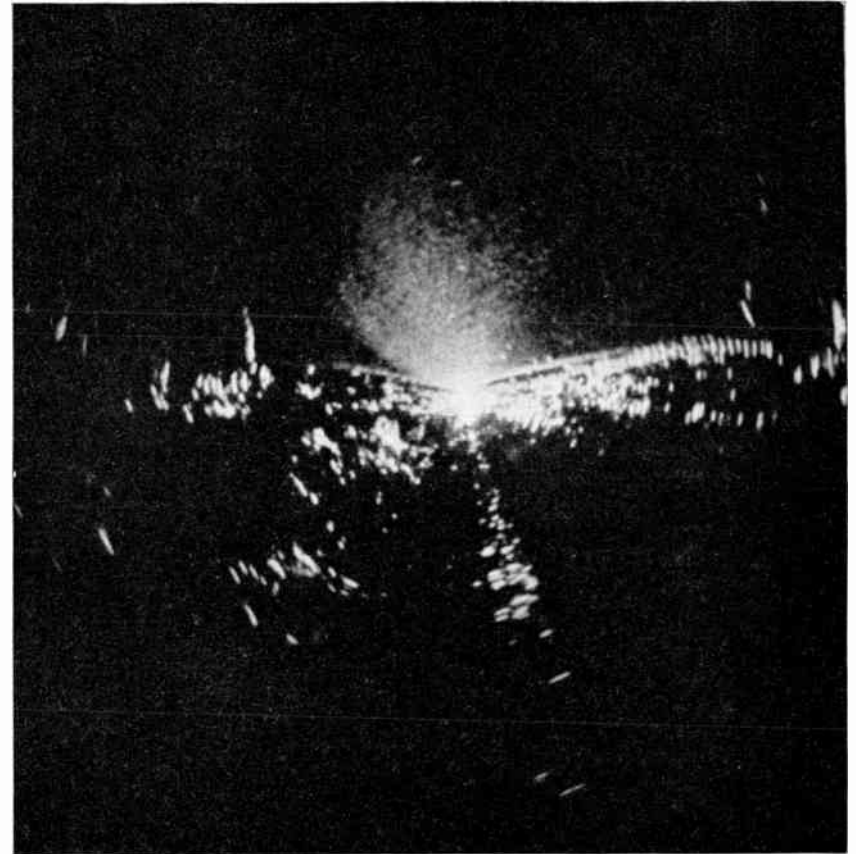
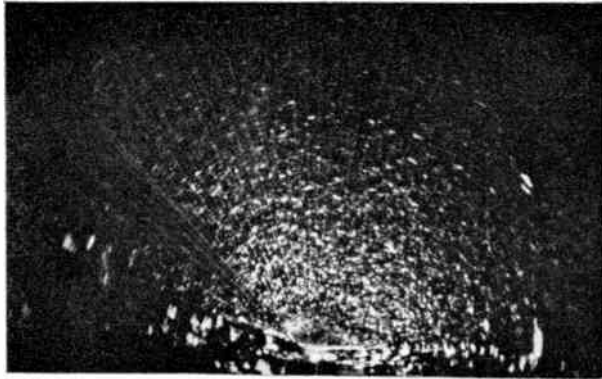
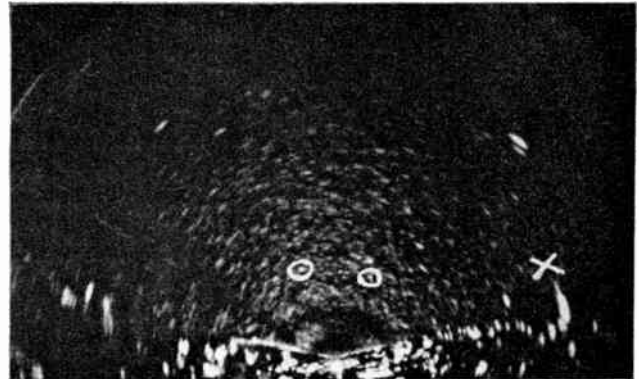


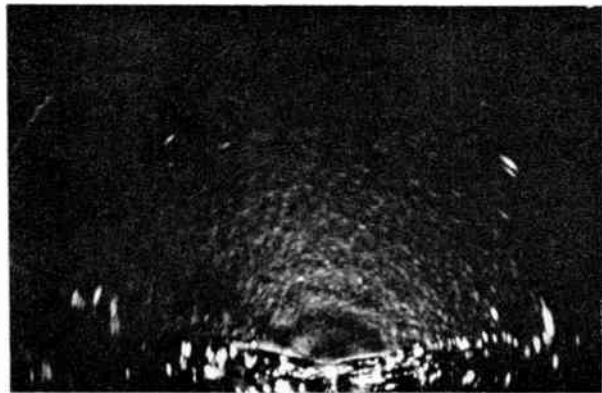
Fig. 4. Slowly rotating antenna, 20 rev/min, 40 seconds exposure (13 revolutions), 13 packets of 90 correlated pulses per beam-width.



(a) 20 rev/min antenna, (1 revolution), 1 packet of 100 correlated pulses per beam-width (3 seconds exposure).



(b) 1000 rev/min antenna, 50 de-correlated packets of 2 pulses per beam-width (3 seconds exposure).



(c) 1000 rev/min antenna, 150 de-correlated packets of 2 pulses per beam-width (9.0 seconds exposure).



(d) 20 rev/min antenna, 4 packets of 100 correlated pulses per beam-width (12 seconds exposure).

Fig. 5.

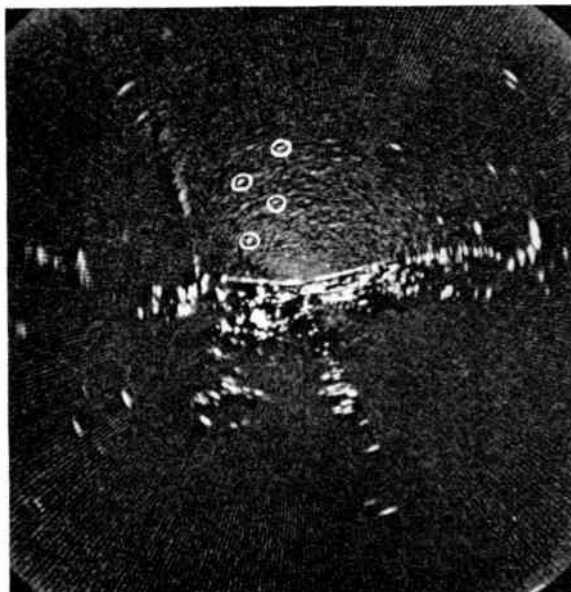
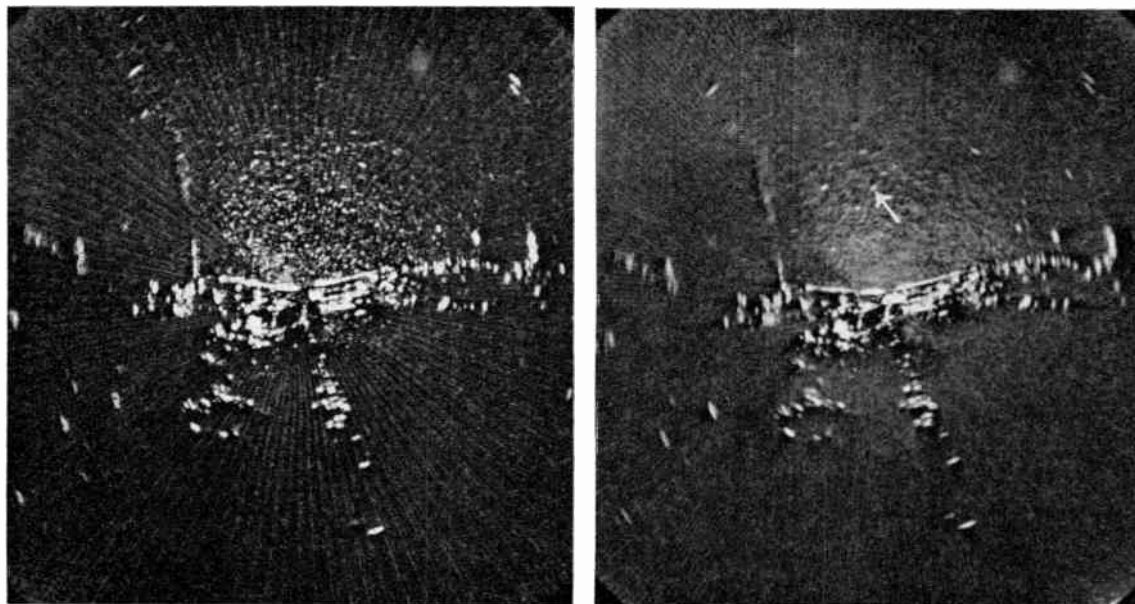


Fig. 6. 1000 rev/min antenna, 1 second exposure, 17 de-correlated packets of 2 pulses/beam-width, 4 spherical targets ringed.

a fifth shown by arrow was a motor boat; there was a fair amount of small boat activity at the time as the area was being surveyed for suitability as a water-skiing course. The motor boat echo should not be looked for in Fig. 7(a) as the fast and slow scan sequences were photographed in succession and several minutes separated a slow scan exposure from its corresponding fast scan exposure.

The sequence of pictures in Fig. 8(a) to (f) shows the effect of camera integration as before. It may be noted that the small mooring buoy just off the water's edge (indicated in key Fig. 2) shows up fairly consistently in the de-correlated sequence on the right. It is again possible to make a rough estimation of the improvement; in Fig. 8(e), 30 seconds integration slow scan, we have approximately achieved the smoothing of clutter shown in 8(b), 2 seconds integration fast scan, so that crudely the improvement is again a shade less than 6 dB which is similar to the estimate made from Fig. 4 for slighter seas.



(a) 28 rev/min antenna, 2 seconds exposure, (1 revolution), 1 packet of 71 correlated pulses.

(b) 1000 rev/min antenna, 2 seconds exposure, (34 revolutions), 34 de-correlated packets of 2 pulses.

Fig. 7.

Finally we come to results with the E712 storage tube. This tube may be controlled by shaped wipe-off pulses to have a storage time varying from less than a second up to several minutes. By suitable adjustment any desired time may therefore be pre-set. The screen is extremely brilliant, giving an easily-viewed picture in a sunlit room. In photographing this tube, film exposures of 1/10th second were used so that any camera integration is negligible. Figure 9(a) shows the result with the tube set to have a memory of approximately 1 second, compared with a 1-second exposure to the fluoride tube (Fig. 9(b)). Figures 10(a) and (b) are for 9 seconds memory. It appears that the storage tube even with 1 second storage time is a more efficient integrator than the fluoride screen plus the eye, or the fluoride screen plus the camera, possibly because the ratio of the flash to the afterglow is so much less with the storage tube. In fact when the room was completely darkened, and the fluoride tube brightness was turned down until the flash was hardly visible in relation to the afterglow, it also gave a better signal to clutter visibility. But it would be too much of a strain to use operationally in these conditions. This technique of turning down the brightness of a fluoride tube in order to achieve integration on the afterglow has been mentioned by Harrison.⁶

The storage tube showed similar advantages with the slowly rotating antenna but with a definite tendency to paint more correlated clutter peaks than

with the high speed antenna. Figure 11 illustrates this point. The track of a speedboat target may be clearly seen at about 10 o'clock (semi-radius) in Fig. 11(b).

5. General Points

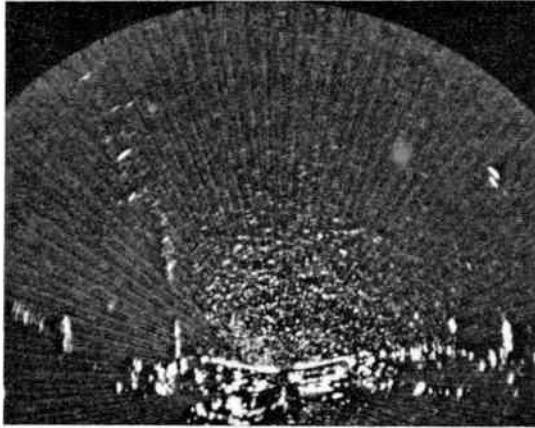
There are a few other points which should be mentioned:

(a) It was noted when running the antenna up to speed that the smoothing of the clutter (de-correlation) seemed to establish itself over the first few hundred revolutions, and to be largely complete at 400-500 revolutions (4 pulses per beam-width at 600 pulses/second). It is possible that a useful system could use much lower speeds than 1000 rev/min.

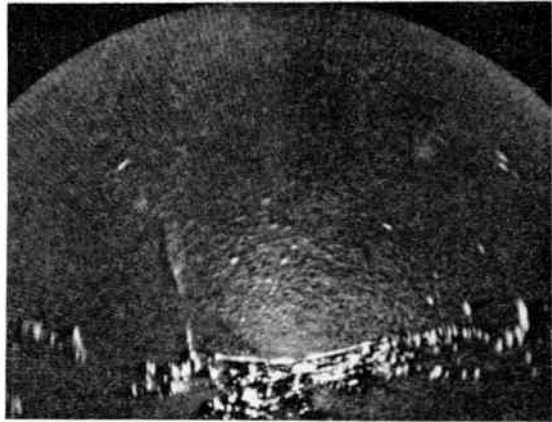
(b) The 1000 rev/min system gave a flickerless display similar to a television picture. It was thought to be more pleasant to view than the slow-moving bright radial of conventional displays.

(c) The high data rate combined with the de-correlation enabled some echoes to be diagnosed which can be most confusing on slow-speed correlated systems. For instance the circling and landing of sea birds could be very clearly followed so that they were identified as harmless targets. The tracking and identification of high-speed targets was similarly easier.

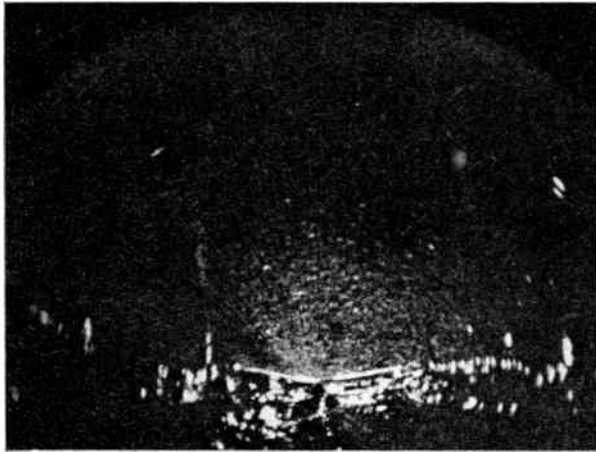
(d) The fading pattern of a target could be followed throughout its whole range of values.



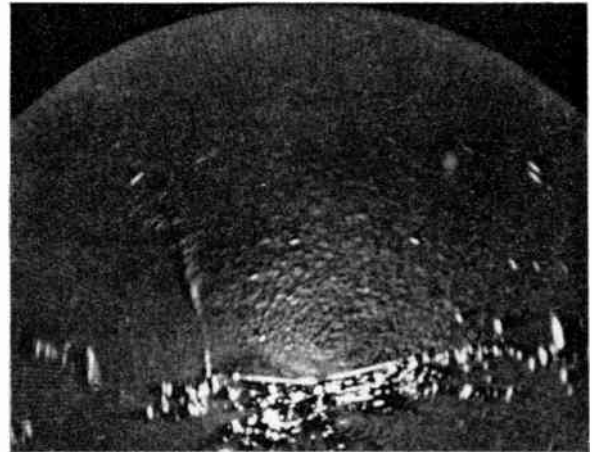
(a) 28 rev/min, 2 seconds exposure (1 revolution), 1 packet of 71 correlated pulses.



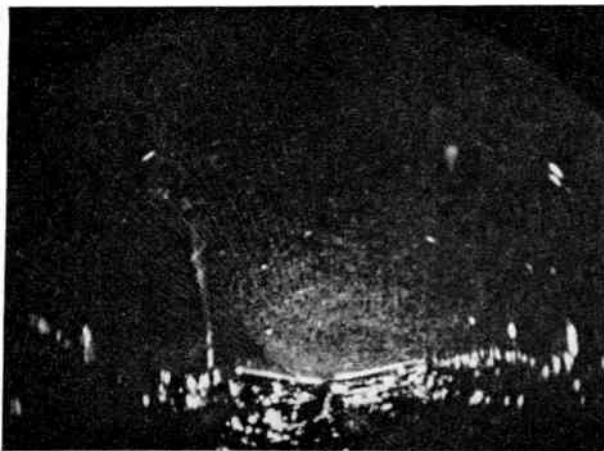
(b) 1000 rev/min, 2 seconds exposure (34 revolutions), 34 de-correlated packets of 2 pulses.



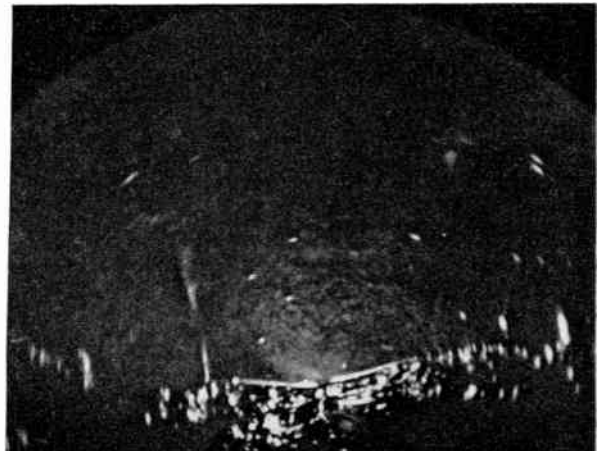
(c) 28 rev/min, 9 seconds exposure (4 revolutions), 4 packets of 71 correlated pulses.



(d) 1000 rev/min, 9 seconds exposure (150 revolutions), 150 de-correlated packets of 2 pulses.



(e) 28 rev/min, 30 seconds exposure (14 revolutions), 14 packets of 71 correlated pulses.

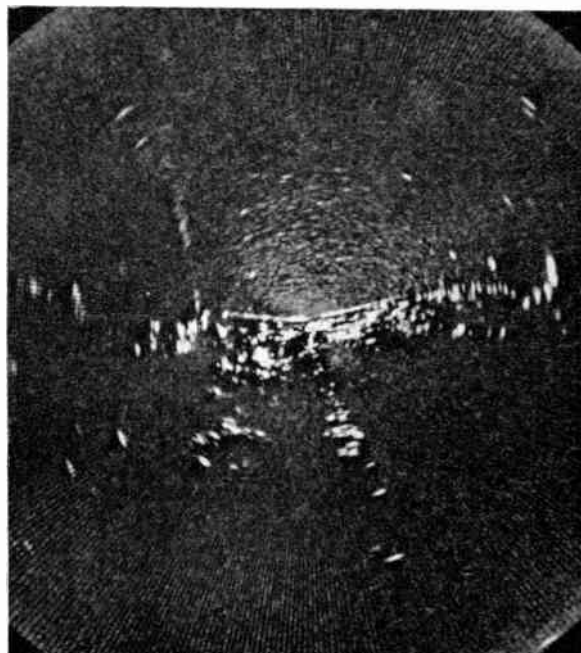


(f) 1000 rev/min, 30 seconds exposure (500 revolutions), 500 de-correlated packets of 2 pulses.

Fig. 8.

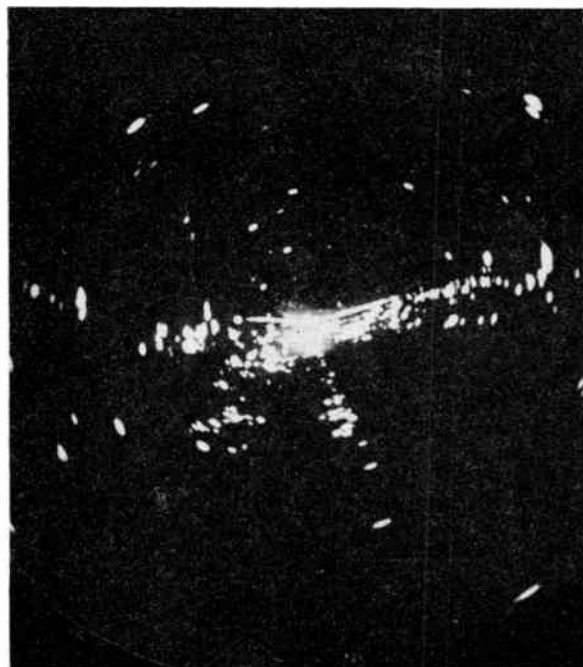


(a) 1000 rev/min, English Electric E712 storage tube set to 1 second storage time. 1/10th second camera exposure.

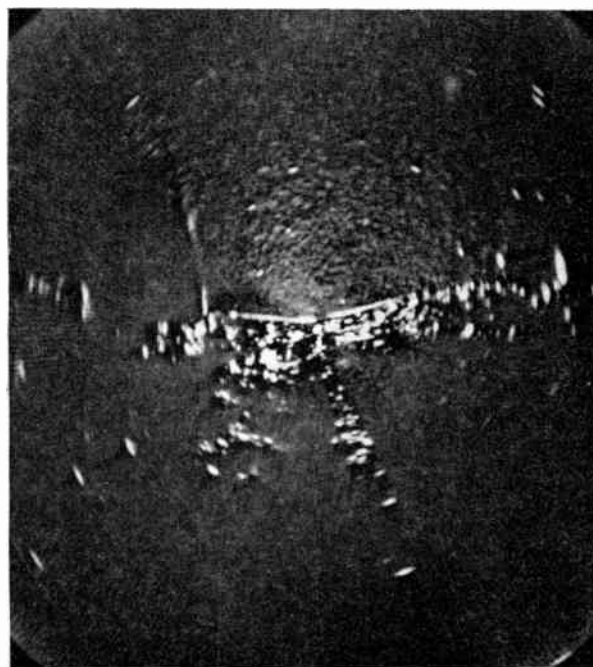


(b) 1000 rev/min, fluoride tube integrated up to 1 second by camera exposure.

Fig. 9.

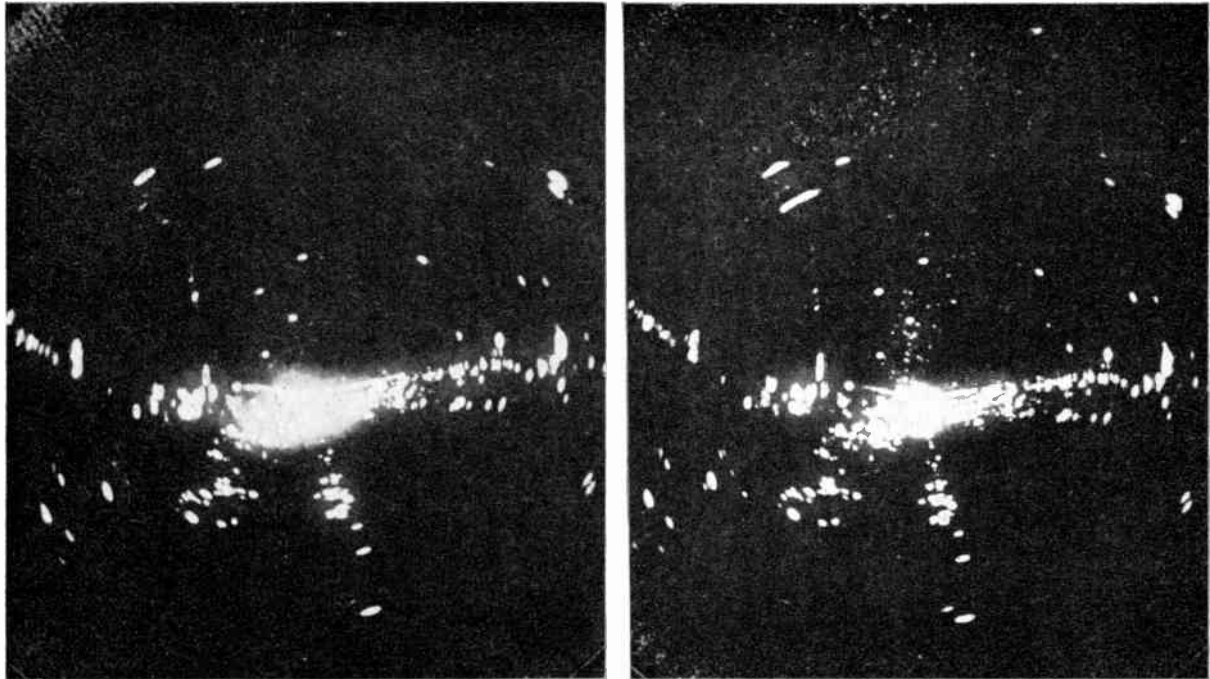


(a) 1000 rev/min, English Electric E712 storage tube set to 9 seconds storage time. 1/10th second camera exposure.



(b) 1000 rev/min, fluoride tube integrated up to 9 seconds by camera exposure.

Fig. 10.



(a) 1000 rev/min antenna, storage tube set for 18 seconds storage time.

(b) 28 rev/min antenna, storage tube set for 18 seconds storage time.

Fig. 11.

6. Conclusions

The high scan rate (1000 rev/min) de-correlated radar system gives improvements of about 6 dB in signal to clutter visibility of small targets in sea clutter, using a p.p.i. and human observer.

From the present series of experiments the author feels that the improvement may become somewhat less in very rough seas, but so far he has only a little subjective evidence for this. If this were so it would imply that the clutter velocity spectrum becomes wider, and the correlation times therefore shorter, eqn. (9), for very rough seas which may be not unreasonable. Ross¹² adduces very guarded evidence for this at least for wavelengths of 10 cm and 55 cm.

By integration (camera or storage tube) considerable further improvements are possible in signal to clutter visibility and a given improvement is obtained in a much shorter time (e.g. 1/13th) for the high scan rate de-correlated system, than for the conventional radar. This is of importance for moving targets.

There is evidence that a storage tube, even with a memory as short as 1 second, is a more efficient integrator than either a fluoride p.p.i. screen plus the eye, or a fluoride p.p.i. screen plus a camera. This is thought to be caused by the high flash to afterglow intensity of a fluoride screen when adjusted for normal

viewing, which does not allow afterglow integration to occur.

The high scan-rate radar gives a number of advantages in the diagnosis of targets and is, at least in the writer's opinion, more pleasant to view than a conventional slowly rotating display.

7. Acknowledgments

The author acknowledges the help of Mr. A. Woroncow on display and receiver circuits associated with this work. The paper is published by permission of the Ministry of Defence (Navy).

8. References

1. J. Croney, 'A simple logarithmic receiver', *Proc. Inst. Radio Engrs*, 39, pp. 807-13, July 1951.
2. J. Croney, 'The reduction of sea and rain clutter', *J. Inst. Navigation*, 7, pp. 175-80, 190-4, April 1954.
3. J. Croney, 'Clutter on radar displays. Reduction by use of logarithmic receivers', *Wireless Engr*, 33, pp. 83-96, April 1956.
4. W. A. Harman, 'Principles of the Statistical Theory of Communication', p. 43 (McGraw-Hill, New York, 1963).
5. D. E. Kerr (Editor), 'Propagation of Short Radio Waves', pp. 570-80 (McGraw-Hill, New York, 1951).
6. A. Harrison, 'Method of distinguishing sea targets from clutter on civil marine radar', *The Radio and Electronic Engineer*, 27, pp. 261-73, April 1964.

7. L. V. Blake, 'A Guide to Basic Pulse-Radar Maximum-Range Calculation', Pt. 1, p. 20, U.S. Naval Research Lab., N.R.L. Report 5868.
 8. W. Delany and R. F. Kyle, 'Antenna for rapid scan de-correlation radar', *The Radio and Electronic Engineer*, 32, No. 3, pp. 156-8, September 1966.
 9. M. H. Cufflin, 'The H_{01} mode and the helix waveguide', *Marconi Rev.*, 28, No. 156, January-March 1965.
 10. A. Woroncow and J. Croney, 'A true i.f. logarithmic amplifier using twin-gain stages', *The Radio and Electronic Engineer*, 32, No. 3, pp. 149-55, September 1966.
 11. J. Croney and W. Delany, 'A new type of omni-azimuthal radar echo enhancer', *Microwave J.*, pp. 105-9, March 1963.
 12. A. W. Ross, 'Sea Clutter Investigations', A.S.R.E. Technical Note R4/50/15.
- Manuscript received by the Institution on 22nd February 1966.
(Paper No. 1063/RNA51).*
- © The Institution of Electronic and Radio Engineers, 1966.

DISCUSSION

Under the Chairmanship of Mr. A. Harrison

Dr. D. C. Cooper: The photographs of the displays for the slow scan and fast scan radar systems appear to show that as the total observation, or integration, time is increased the improvement in performance given by the fast scan system becomes smaller.

Can Mr. Croney give an explanation for this effect?

I would be very interested to learn whether or not the author has had the opportunity of observing the performance of the clutter de-correlation radar in the presence of rain clutter.

Mr. J. Croney (in reply): I think this effect would be expected. As we continue to integrate pulses in both systems the signal to clutter ratio will increase, giving signals from each system which approach nearer to the limiting level of the p.p.i. display at which point differences in intensity will disappear.

I have not looked at the effect on rain clutter of the rapid scan system. As the ordinary logarithmic receiver followed by a high-pass filter usually reduces rain clutter to the same intensity as a noise background I would expect the individual rain clutter pulses to be already de-correlated in a slow scan (20 rev/min, 1000 pulses/second) system, in which case the rapid scan system would offer no advantage. But there are types of rain cloud distributions which do not appear to be eliminated entirely in conventional systems and it may well be worth looking at the effect of the rapid scan system on these.

Mr. R. Voles: I wonder whether Mr. Croney would care to comment on the suggestion that when this kind of de-correlation is used in longer range radar systems having lower pulse repetition frequencies and larger aerials it may be advantageous to exploit the fact that since the returns are then correlated over only a few pulses it should be possible to obtain much of the desired improvement in performance by rapid electronic scanning over a small sector and then rotating the whole aerial mechanically at a relatively slow speed.

If, for instance, the clutter were correlated over a time corresponding to N pulses, then the sector scan angle need be no wider than N beam-widths (or $N/2$ if 2 pulses/beam-width were required) so that the scanning could be achieved by electronic switching between N adjacent horns illuminating a common reflector or by some other form

of limited electronic beam steering. If the time taken to mechanically rotate the aerial once through 360 deg were the same as that taken to build-up the picture in the rapidly-rotating case, then the number of independent integrations obtained would be equal so that the performances of the two systems against targets that were not slowly fading and clutter should be similar.

If the radar data were processed in an automatic detector before being presented to the operator, then since the area over which integration was required would be proportional to only N beam-widths in the sector-scanning arrangement instead of 360 deg in the rapidly-rotating system, the amount of storage required would be reduced by the factor of $(N \text{ beam-widths})/360 \text{ deg}$.

Mr. Croney (in reply): The rapid-scan technique I have described is of course most suitable as it stands for short range radars (12 miles), as one would be worried by second trace echoes with a repetition rate of 6000 pulses/second on longer ranges. In the case of ship-borne X-band radar, sea clutter rarely extends for more than 2 miles, so that long ranges are not required for close navigation in clutter conditions. When switching to longer ranges (20-40 miles) it would be necessary to reduce the repetition rate and antenna revolution speed. As I have said, a compromise might be to use an antenna speed of 500 rev/min.

However, if one tried, as Mr. Voles suggests, to apply such techniques even on the short ranges of long range surveillance radars the great inertia of the large antennas involved would make it essential to adopt some form of low inertia beam scanning and the solution he suggests may be a good economic compromise.

Mr. J. Rowe: I feel that Mr. Croney has amply demonstrated the value of de-correlation in conjunction with the logarithmic receiver, though, having seen the equipment demonstrated at Eastney, I felt that the improvements were less spectacular than integrating photography would suggest. Indeed, I felt that little improvement was gained at speeds below 600 rev/min, though with experience in setting up, this figure might be reduced. However, I am more concerned with practical difficulties.

In view of the cost of the aerial drive unit and of its necessary mounting, quite apart from dangers due to

fouled halyards, it is difficult to envisage the wide use of 3 hp aerial drives in the merchant marine field. Some means may be necessary to avoid the occasional stroboscopic effects resulting from an integral relationship of repetition rate and speed which could result in loss of information at critical moments.

The suggestion made by one speaker, of combining normal rotation speed with a fast beam oscillation, seems to offer a partial solution only unless the angle of fast scan can be very large, since the time over which de-correlation may be spread is reduced in proportion to the fast-scan angle. The effect of uniform tube brightness—a not inconsiderable bonus accruing from the high-speed drive—would also be lost. The Chairman's warning on the potentially dangerous effects of a near-alpha flicker inducing an epileptic condition in the observer is certainly important.

It would be interesting to have Mr. Croney's views on the possibility of producing a high-speed rotating scan without physically rotating the whole aerial.

Mr. Croney (in reply): In my experience the spoking arising from the occasional stroboscopic effect is not troublesome, and does not last long enough to give erroneous information. I think loss of information is very much less likely with the high scan rate system than with a 20 rev/min system where targets may sometimes fail to paint on several successive revolutions of the antenna because the target fading rate has an integral relationship with the antenna revolutions.

I believe the de-correlation is largely complete at a speed of 600 rev/min. I would therefore envisage a mechanically rotating antenna, normally used at say 30 rev/min, but switchable to 600 rev/min for use in clutter conditions. At the present time I feel that a stationary antenna scanning by electronic means continuously through 360 deg in azimuth would be too costly for general application, although quite practicable for the peak powers used in civil marine applications.

Mr. G. A. Egler: I wonder if Mr. Croney is aware of similar work done by Hazeltine for the United States Navy? The radar development I refer to was an airborne S-band search radar, (APS-49). The rotation rate was, I

believe, 900 rev/min and the development was carried out during the early 1950's.

Mr. Croney (in reply): I was not aware of any work in this field by Hazeltine.

Dr. D. E. N. Davies: Mr. Croney's paper shows most impressive improvement in signal to clutter ratio for small targets in sea clutter. It occurs to me however, that in the case of a small craft with about two or three centres of signal reflection, the movement of the sea would cause target fading which might result in de-correlation of the target returns due to the integration. Has the author noticed any such effect during the observation on the experimental radar?

A further interesting point about such radars is that with a scanning rate approaching the limit corresponding to one pulse per target, per beam-width of scan, the two-way directional pattern is no longer the square of the one-way pattern, since the receiver beam-width will have suffered a small angular movement in the time taken for the signals to return from maximum range. This can result in an improvement of the two-way directional pattern which can involve a reduction of both beam-width and sidelobe level. In the limiting case of 1 pulse per beam-width of scan, the beam-width is reduced to about half its original value, but this is also accompanied by a reduction of gain. The interesting feature of this process is that it gives a beam-width which decreases with range, but only by a factor of two.

Mr. Croney (in reply): The frequency of the radar and the motion of the target are not changed, so the echoing polar diagram should be the same, but it is of course sampled much more evenly in time with the high speed antenna. This means the echoing directivity diagram (fading characteristic) is more fully explored in a given time, and certainly this effect is most noticeable in the p.p.i. presentation of floating targets. The whole fading pattern is followed as a continuous process on the display.

The beam-width reduction point is an interesting one and may partly account for the severe losses in range experienced when going from two pulses to one pulse per beam-width, as the effect would apply especially to longer range targets.

A True I.F. Logarithmic Amplifier using Twin-Gain Stages

By

A. WORONCOW, Dipl.Ing.†

AND

J. CRONEY, B.Sc., Ph.D.†

Summary: A true i.f. logarithmic amplifier is described which avoids the successive detection principle and its associated video delay line. Each stage comprises a pair of long-tailed pairs in a complementary role. Transistors are used throughout but 'bottoming' is avoided, and bandwidth variations are negligible. A dynamic range of about 100 dB is possible. A video output may be derived if desired from a single detector after the last stage, but when an output at i.f. is taken, phase variations with amplitude may be of interest, and have been investigated. A technique for correcting such phase variations is described, and a development of the basic amplifier circuit is given which should minimize such phase variations at their source.

1. Introduction

Generally the logarithmic amplifiers at present used in radar systems are of the successive detection type designed in accordance with the techniques discussed by Croney.¹ The logarithmic relationship exists between an input at the intermediate frequency and a rectified output at video frequency. It is not possible from such an amplifier, to extract an intermediate frequency output which is in logarithmic amplitude relationship to the i.f. input, the logarithmic characteristic being really derived at the video frequency.

In some radar applications, for example, moving target indication systems (m.t.i.), it is necessary to perform some of the signal processing before detection, and in such cases an amplifier having a logarithmic relationship between an i.f. input and an i.f. output would be of value. The authors have called such an amplifier a True I.F. Logarithmic Amplifier to distinguish it from the successive detection type.¹

As long ago as 1948, Alred and Reiss² proposed and made a single laboratory model of what was in fact a true i.f. logarithmic amplifier. This comprised a chain of synchronously-tuned i.f. stages with a single detector at the end from which (in their case) a video output was taken, but the tuned load of each i.f. stage was damped by a double-diode, with its two sections reverse-connected to act equally on positive and negative half cycles. For the smallest input signals the damping diodes were inoperative (by a bias adjustment). The i.f. valves were then all operating at maximum gain which was some 20 dB per stage. As the input signal was increased the damping diodes of the final stage were the first to come into play causing the damping load to drop in value

(approximately logarithmically) until it reached a constant value at which the gain of the stage had declined to unity where it stayed. As the input was further increased this happened in a progressive manner to successively earlier stages until for the largest inputs the whole amplifier had a gain of unity. This amplifier may be called the successive damping logarithmic amplifier. It had a number of drawbacks which were:

- (a) Being synchronously tuned it was limited to narrow bandwidth designs.
- (b) As the tuned i.f. circuits suffered progressively heavier damping by the diode loads the bandwidth could vary widely.
- (c) Because of the damping variation the use of critically coupled pairs of circuits was virtually impossible.
- (d) Because of the narrowly prescribed limits within which the diode damping had to vary to obtain a smooth logarithmic characteristic, and a final stage gain of unity, hand selection of diodes was necessary.

Very recently the authors have developed a new type of true i.f. logarithmic amplifier which avoids the above defects. This amplifier which may be called the 'twin-gain stage logarithmic amplifier' is described in the following section.

2. Twin-Gain Stage Logarithmic Amplifier

The amplifier which may have a logarithmic range of up to 100 dB before limiting occurs, comprises n identical stages as shown in Fig. 1. Each stage is a twin-gain stage, described below, and the final output of the n stages may be rectified by a detector as shown, or processed at the intermediate frequency before detection.

† Admiralty Surface Weapons Establishment Extension, Funtington, near Chichester, Sussex.

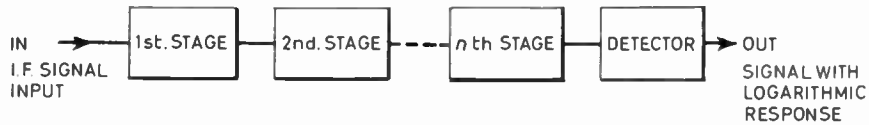


Fig. 1. Block diagram of the logarithmic amplifier.

The principle used to obtain the logarithmic law is again to let each stage have a high gain for the weakest signals, and to make this gain decline progressively as the signal strength increases, until a constant stage gain of unity is reached. However this gain variation is not achieved by a variable damping, the method being quite different from the successive damping technique of Alred and Reiss.

Basically the principle is very simple, and is illustrated by Fig. 2 representing a single stage of the amplifier. Here we see two amplifying devices working in parallel which for convenience we call the 'A' and 'B' amplifiers. These amplifiers feed a common load circuit, the band-pass filter between stages. The 'A' amplifier is designed to have a gain of unity, and to maintain this gain up to the highest level of signal which is to be applied to its input, i.e. it is not limited. The 'B' amplifier is designed to have a high gain for weak signals, but to have its modulation current limited by bias so that its gain falls as the signal strength increases, becoming extremely low for large signals. The combination of the two amplifiers in parallel thus gives a stage which has high gain for weak signals declining to a constant gain of unity for strong signals. In the logarithmic amplifier made up of n such twin-gain stages, as the input signal is gradually increased 'B' amplifier in the last stage goes into the limiting state first, then the penultimate 'B' amplifier and so on, until with the largest signal the 'B' amplifier of the first stage is limiting. This should be the largest signal for which the whole logarithmic

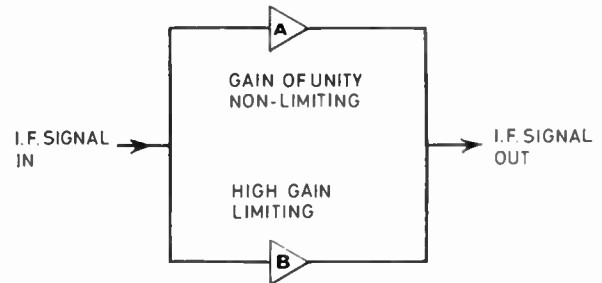


Fig. 2. Principle of operation of each stage of the amplifier.

amplifier is designed, and the 'A' amplifier should still have a gain of unity even for this signal.

A circuit which was found to be very suitable for the 'A' and 'B' amplifiers is the long-tailed pair shown in general form in Fig. 3 which illustrates one stage containing two pairs. Upon application of a signal to TR1 the currents in the transistors change in opposite senses. With sufficiently large modulation, when TR1 is cut off, TR2 conducts all the standing current, and when TR1 is conducting all the standing current, TR2 is cut off. Thus the largest changes of current in TR2 are limited with the result that no transistor is ever 'bottomed'.

The resonant band-pass filter comprising L1-C2 and L2-C4 coupled by the 'top end' capacitor C3 is common to the output circuits of both the 'A' and 'B' amplifiers, and because the transistors are never 'bottomed' the reactive loading on this tuned filter remains the same

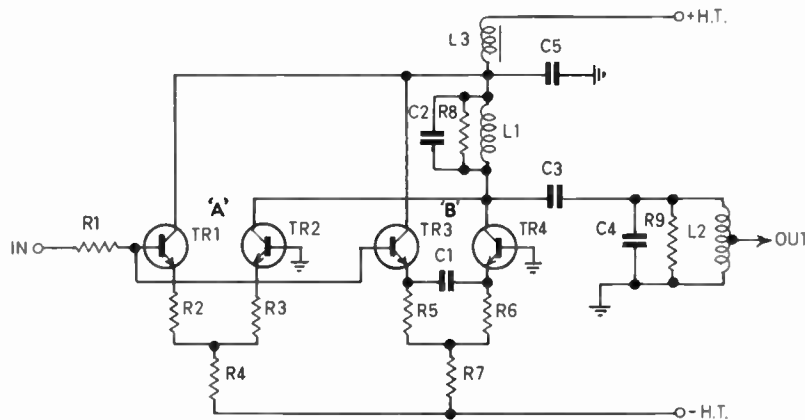


Fig. 3. General circuit diagram of amplifier stage.

for both the limiting and non-limiting state of the 'B' amplifier. This in turn means that its frequency response is not shifted as signal amplitudes in the amplifier change.

The 'A' amplifier has a large standing current which is determined by the resistor R4. Its gain of approximately unity is adjusted by the values of resistors R2 and R3. These resistors should be approximately equal in order to make the standing currents in TR1 and TR2 approximately equal. The standing current in 'B' amplifier is small and is determined by the resistor R7. The current equalizing resistors R5 and R6 are made as small as possible for effective balancing and are by-passed by capacitor C1. The gain of the 'B' long-tailed pair is therefore high, but is quickly limited. Current equalizing resistors are essential in transistor long-tailed pairs, because the currents in the pairs will sometimes become very unequal through 'thermal runaway' by which one of the transistors tends to take over all the current.

Other circuit details of Fig. 3 are as follows. R1 is a base stopper resistor of a few tens of ohms; it suppresses parasitic oscillations in a similar way to the grid stopper used in valve circuits. Resistors R8 and R9 are damping resistors selected to give critical coupling and the required bandwidth of the filter circuit in combination with the coupling capacitor C3. The input signal to the following stage is fed from a tapping point on the inductor L2. Since the input of the following stage represents a resistive load of a few hundred ohms, which increases significantly as

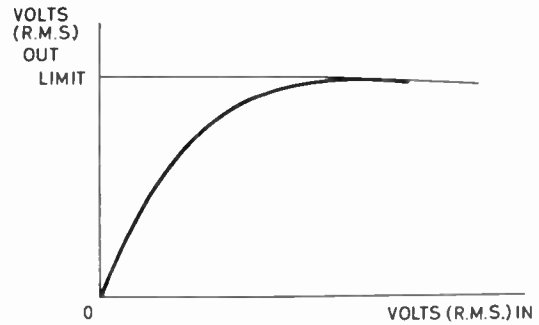


Fig. 4. Gain response of the limiting long-tailed pair, 'B' amplifier.

the 'B' amplifier goes from the non-limiting to the limiting state, this tapping-down reduces the shunting effect of the input load on the resistor R9. The resulting variations in bandwidth of the coupling filter are thus kept within close limits. L3 and C5 provide h.t. decoupling.

A typical gain characteristic of the limiting long-tailed pair is shown in Fig. 4. When i.f. output voltage is measured against input voltage the gain is at first high and remains constant up to a certain value. Beyond that the input voltage drives the transistor gradually into cut-off and the gain decreases as the output voltage approaches the limiting level asymptotically. This characteristic produces a good fit to a logarithmic curve and a logarithmic amplifier made of only a few twin-gain stages is capable of giving a uniform logarithmic input-output law.

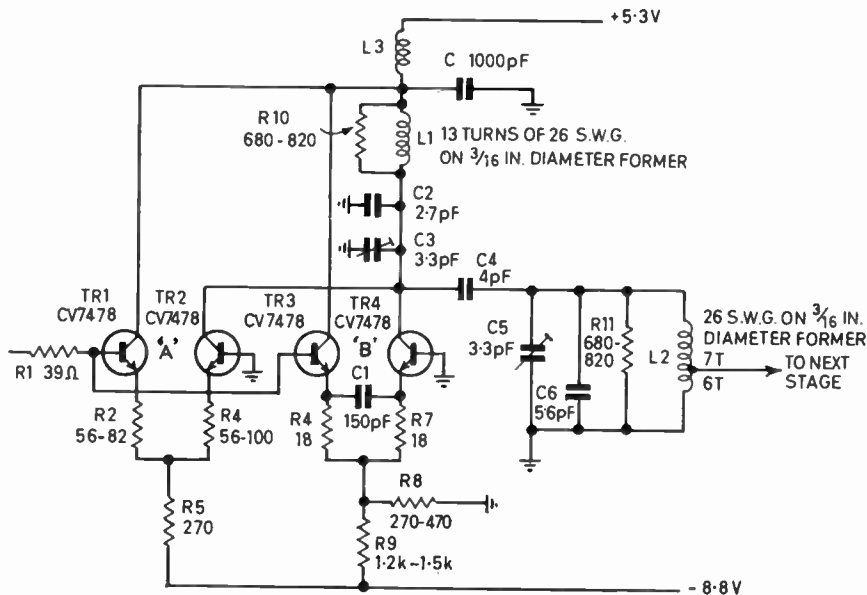


Fig. 5. Circuit details of one stage.

3. An Experimental Twin-Gain Stage Logarithmic Amplifier

An experimental amplifier (of six stages) at 60 MHz intermediate frequency and with 12 MHz bandwidth was built in accord with the principle and general circuit outlined above. The circuit diagram of a typical stage is shown in Fig. 5. The use of R8 as a bleeder resistor to earth allows the value of R9 to be kept smaller, and thus keeps the time-constant formed by this resistance and the base-emitter capacitance of the transistors to a minimum. Such precautions are necessary to avoid paralysis after strong radar signals.

The logarithmic response is shown in Fig. 6. It was very good even on initial assembly before any adjustment of components. Smoothing of the logarithmic law may be made by adjustments to some of the component values. Thus changes in R8 and R9 (Fig. 5) change the contribution of a particular stage to the logarithmic curve and changes in R2 and R4 change the gain of the 'A' amplifiers and so affect the slope of the curve. These adjustments are not critical: a change of 25% in the value of these resistors only modifies the appropriate part of the input-output curve slightly, enabling fine control of the law to be made.

Figure 7 shows the frequency response curves for the amplifier at various levels of i.f. signal. It will be

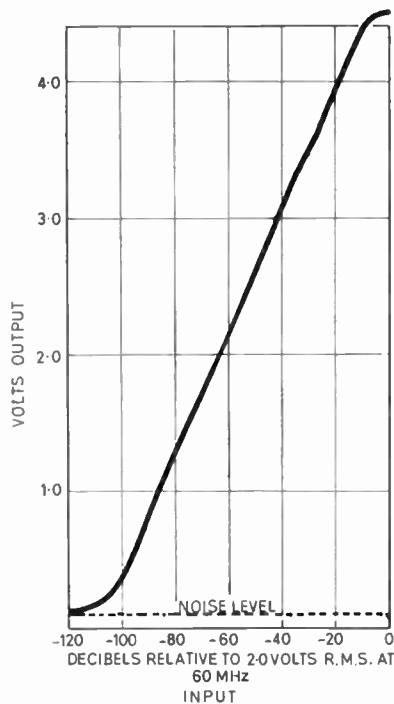


Fig. 6. Input-output law of true i.f. logarithmic amplifier (60 MHz).

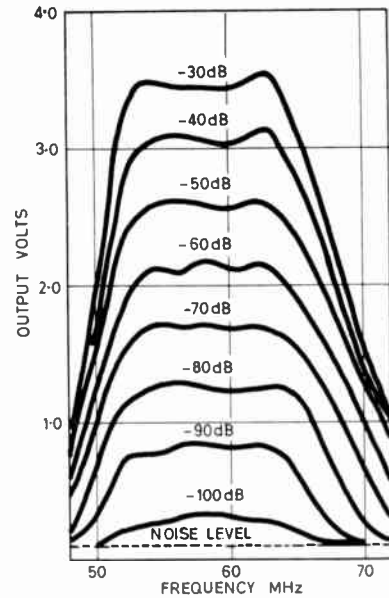


Fig. 7. Response curves of twin-gain stage logarithmic i.f. amplifier. Curves are labelled for inputs in decibels relative to 2.0 volts r.m.s.

seen that the bandwidth only varies slightly with change of input signal level. The amplifier was very stable, resulting from the use of long-tailed pairs in which the base of the second transistor provides an earthed screen between output and input.

It has been found that for video detection at an i.f. of 60 MHz a cascode detector has a better performance than the ordinary triode detector shown in Fig. 8(a). The capacitance between the base and the collector of the transistor introduces some feedback from the collector circuit into the base circuit, and the i.f. ripple in the output circuit of the triode detector appreciably reduces its efficiency. Also this capacitance, being non-linear and depending on the instantaneous values of collector voltage and current, has a detuning effect on the final i.f. circuit. These effects are reduced by using the cascode detector shown in Fig. 8(b). The base of the upper transistor, TR2, is at constant potential and so is its emitter, and therefore the collector of the lower transistor TR1. Detection with considerable amplification is obtainable from the cascode detector if required.

4. Phase Stability of Twin-Gain Stage Amplifier

As this amplifier could be of value in systems involving pre-detector signal processing (e.g. m.t.i.) the phase stability was examined over a wide range of amplitude and frequency of input.

An 0.2 μs pulse at 60 MHz was fed to the i.f. amplifier and the i.f. output (before detection) was displayed on a sampling oscilloscope. This input

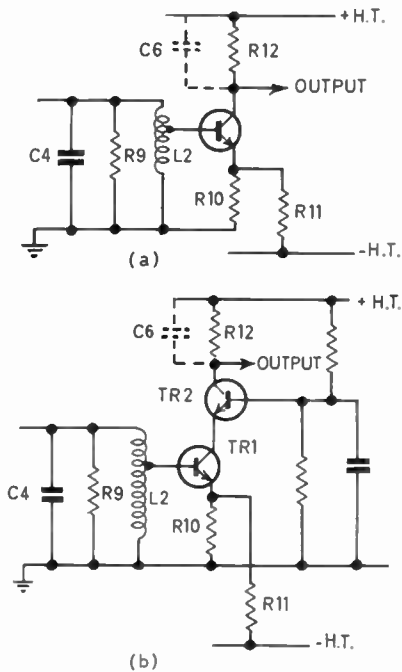


Fig. 8. Types of detector circuit.

pulse is shown in Fig. 9(a) above a reference datum step. After passage through the amplifier the result of Fig. 9(b) was obtained. The group delay of the pulse caused by passage through the amplifier can be read against the reference datum and is approximately 0.065 microseconds, i.e. about 4 cycles at 60 MHz.

The theoretical time delay through a critically coupled pair of single tuned circuits is given by:

$$t = \frac{1}{\pi \Delta F}$$

where ΔF is the bandwidth of a single tuned circuit. Since the effective bandwidth of a single tuned circuit is about 25 MHz and there are six coupled pairs, the

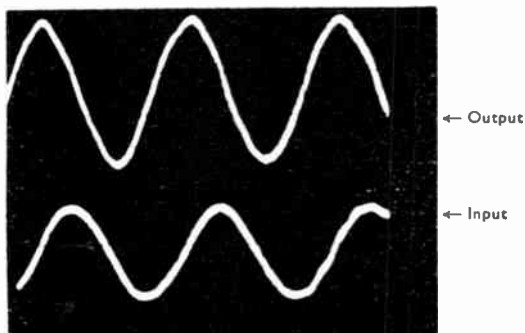
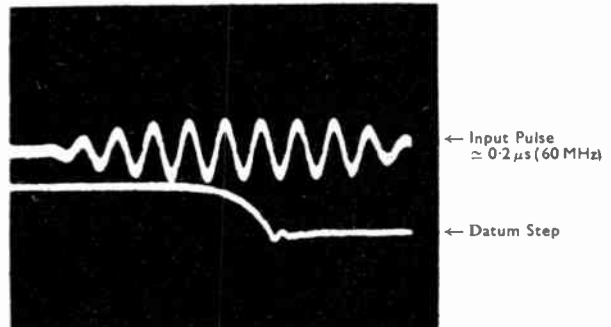


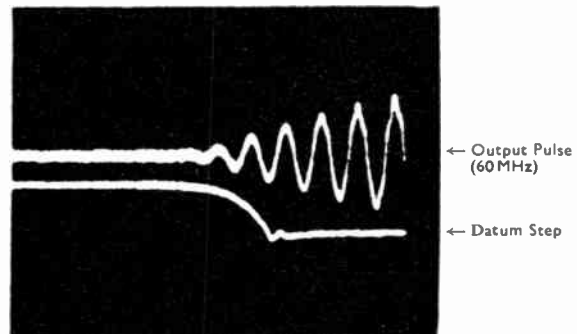
Fig. 10. Typical oscillograms of c.w. input and output of logarithmic amplifier.

delay thus calculated would be approximately 0.07 μ s about $4\frac{1}{2}$ cycles at 60 MHz, which is in sensible agreement, with the accuracy of the measurements.

The actual phase angle variation through the amplifier was then measured as a function of frequency using a c.w. signal. A typical oscillogram is shown in Fig. 10. Results were obtained at two signal levels. For the first signal level (a high one), all the 'B' amplifiers were limiting. The second signal level was



(a) Oscillogram of input to logarithmic amplifier.



(b) Oscillogram of output from logarithmic amplifier.

Fig. 9. Input and output of logarithmic amplifier showing pulse delay.

set at 50 dB below the first one; the available instruments did not permit measurements to be made for lower inputs than this as the amplitudes were too small to be displayed. From the oscillogram results the curves of Fig. 11 were drawn. They are reasonably straight lines throughout the pass-band as would be expected. If the straight lines are projected backwards towards the origin they intersect the zero frequency ordinate at about -1440 deg which is an integral multiple of π (i.e. 8π). According to Wolf³ this is a

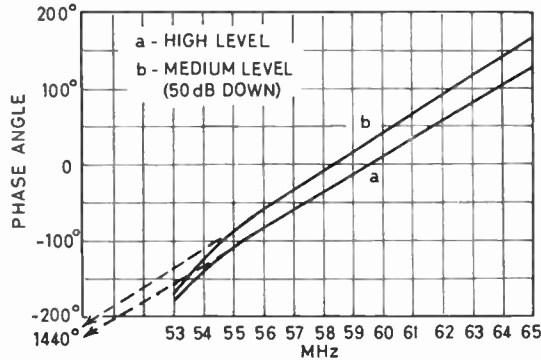


Fig. 11. Phase angle v. Frequency.

requisite condition for the group delay to be constant within the band-pass of the amplifier. The difference between these two curves represents the change of phase shift through the amplifier with change of signal level, and this difference has been plotted against frequency in Fig. 12, curve (a). The change of phase shift is as much as 40 deg at the upper end of the frequency band. This error would be rather high for systems using intermediate frequency cancellation and possibilities of correcting it were considered. From Fig. 11 it may be seen that the phase delay is less at the higher amplitudes of signal, that is when the 'A' amplifiers are making the major contribution. Now the transistors of the 'A' amplifiers have some resistors in the emitters which reduce the gain of the long-tailed pair to unity. These resistors cause the 'A' amplifiers to represent a different complex impedance with different phase angle from that of the 'B' amplifiers. To modify the phase angle of the 'A' amplifiers, a small resistor R_C was placed in series with the base of the input transistor of the pair, and the base was connected to earth by a small capacitor C_C . When R_C was made $100\ \Omega$ and C_C $1\ \text{pF}$ the result of Fig. 12 curve (b) was obtained, and with $R_C = 82\ \Omega$ and $C_C = 1.5\ \text{pF}$ that of Fig. 12 curve (c). The variation is now $\pm 10\ \text{deg}$ over the pass-band which is very small and should be readily acceptable for most applications.

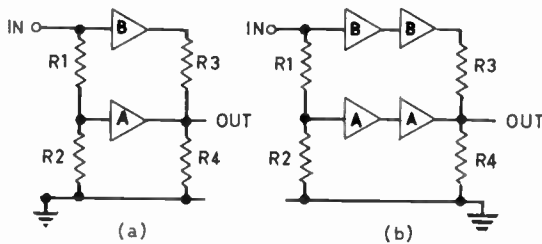
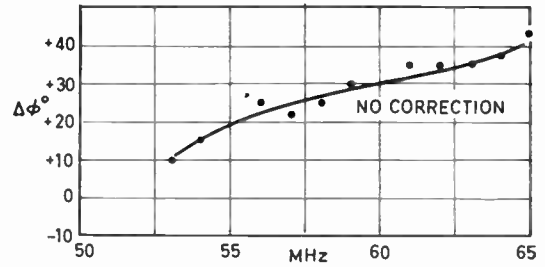
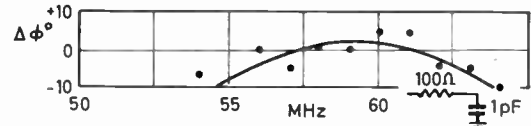


Fig. 13. (a) Single logarithmic stages using identically operated amplifying units.

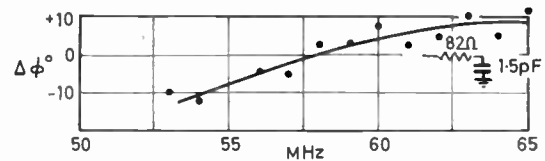
(b) Arrangement of amplifiers in cascade.



(a)



(b)



(c)

Fig. 12. Change of phase angle for 50 dB change of signal.

5. Further Developments

From experience derived with the above amplifier, two possibilities seemed worth pursuing. The smoothness of the logarithmic law suggested that it might be possible to use fewer stages each with a higher gain for small signals, but with unity gain as before for large signals. Also the results of the phase shift measurements suggested that if possible the actual current gains of the 'A' and 'B' amplifiers should be kept as near as possible identical, so that damping and capacitance effects would be the same through both branches, the different gain characteristics being derived by passive elements.

This led to the arrangements shown schematically in Figs. 13(a) and 13(b). Referring to Fig. 13(a) the high gain is provided by amplifier 'B' the output being divided down several times by the step-down network R3 and R4, which may consist of a transformer or a tapped interstage filter. The output must be stepped down as many times as there are stages in the whole amplifier. For example, if there are five stages in the whole logarithmic amplifier the output of 'B' amplifier should be stepped down to one-fifth of the full output. Although the amplifier 'A' has the same current gain as the actual amplifying

device 'B', its effective gain between input and output ports (Fig. 13(a)) is adjusted to unity by means of the step-down network R1/R2. By these step-down techniques the amplifier 'A' with its effective unity gain, can be made to accommodate the cumulative signals from five limited 'B' amplifiers before it begins to saturate, yet the two devices themselves are operating under the same dynamic conditions. It should be appreciated that the amplification of signals by the entire stage can be made aperiodic, but i.f. filters are still necessary for the proper operation of an i.f. amplifier especially where the actual i.f. cycles are to be displayed or phase processed. This is because the limiting action of the 'B' amplifier introduces harmonics, which are filtered out by appropriate inter-stage filters of conventional design.

The arrangement of Fig. 13(a) demands that the high gain 'B' amplifying device gives more gain than in the earlier circuit arrangement and this is easily achieved by cascading the amplifying units in the manner shown in Fig. 13(b). An amplifier using cascaded long-tail pairs for the 'A' and 'B' amplifiers, as shown in Fig. 13(b), has been constructed using 5 similar stages, to give an overall gain of 100 dB (20 dB per stage) with a bandwidth of 20 MHz at 60 MHz intermediate frequency. The input-output law is shown in Fig. 14.

The possibility of constructing these amplifying stages from integrated circuit chips is under consideration.

6. Acknowledgment

The authors gratefully acknowledge the permission of the Ministry of Defence for the publication of this paper.

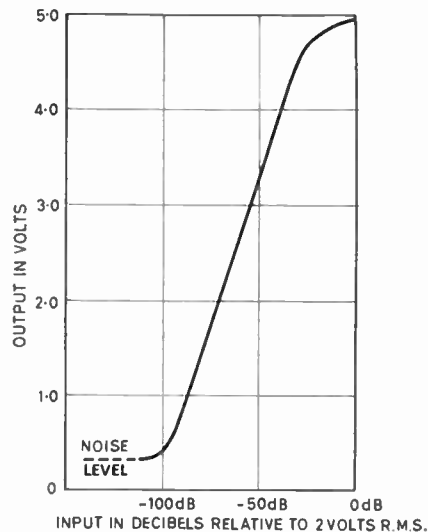


Fig. 14. Input-output law of logarithmic amplifier of bandwidth 20 MHz at 60 MHz intermediate frequency.

7. References

1. J. Croney, 'A simple logarithmic receiver', *Proc. Inst. Radio Engrs*, 39, pp. 807-13, July 1951.
2. R. V. Alred and A. Reiss, 'An anti-clutter radar receiver', *Proc. Instn Elect. Engrs*, 95, Pt. III, No. 38, pp.459-65, November 1948.
3. H. Wolf, 'Phase delay and group delay times', *Nachrichten-technische Zeitschrift*, 16, No. 9, pp. 457-60, September 1963.

Manuscript received by the Institution on 27th April 1966.
(Paper No. 1064/RNA52).

© The Institution of Electronic and Radio Engineers, 1966

Antenna for Rapid Scan Decorrelation Radar

By

W. D. DELANY, B.Sc.(Eng.)†

AND

R. F. KYLE, B.A.‡

Summary: The mechanical design of an X-band antenna suitable for rotational speeds up to 1400 rev/min is described. The microwave design and performance are briefly outlined.

1. Introduction

In connection with the work on de-correlation of sea-clutter described in an accompanying paper,‡ there was a requirement for an X-band radar antenna capable of speeds of revolution up to 1400 rev/min. The antenna developed consisted basically of a linear array in the form of a single length of size 16 waveguide, 4 feet long with shunt displaced slots cut in the broad face of the waveguide feeding a flare through parallel plates, to give a vertically polarized fan beam (2 deg × 16 deg). The array, enclosed in an aerodynamically shaped envelope of glass fibre, could be rotated about a vertical axis at any speed up to 1400 rev/min.

2. Design Requirements

The main limitation imposed by mechanical considerations in designing a high rotation speed aerial is the size of the aperture. The air drag and hence the horsepower required to drive it is greatly increased by extending the length of the array or its height, together or separately.

It can be shown experimentally that a streamlined enclosure having a projected area of 4 ft × 4 inches rotating in still air about an axis at right angles to its length at mid-position will absorb at 1200 rev/min about 3 hp, which will increase to about 8 hp at 1500 rev/min. These dimensions were chosen as a reasonable compromise between radar beam-widths and horsepower.

A mechanical requirement of secondary importance was to reduce the weight of the aerial as much as possible. A mass rotating at 1200 rev/min at a radius of 2 ft is subject to 1000 g. The design had to be strong enough to withstand the forces involved. Stresses could not be reduced simply by increasing the area of the load carrying sections at the ends of the aerial, as the increased mass would cause further increase in stress.

An electrical requirement was that the slotted

waveguide should be very accurately centred in its flare, in good contact with the parallel plate region.

3. Method of Construction

The method that was eventually adopted in constructing the aerial is of some interest in that all the electrical requirements of the design were met in a single unit which also had a high degree of mechanical safety (See Fig. 1). At the same time the method was found to be particularly suitable for the construction of experimental units, only one of which would be required for each design.

The array itself consisted of one continuous straight length of brass waveguide. The slots were cut by jig-borer to the specified displacements. The feed was attached by sweating a length of waveguide bent in the H-plane to the back of the array, the dimensions of the 180 deg corner having been determined by previous experiment. A dummy length of waveguide was attached to the back between centre and load end to make the whole item symmetrical. The v.s.w.r. and radiation patterns were then measured.

A male mould of the flare was coated with a film of silicone grease, and then covered in aluminium foil. Detachable pins, for subsequent accurate location of the array relative to the flare, were pressed through the foil into holes in the mould. A thin layer of a proprietary silver cement was applied over the aluminium foil, and to the slotted face of the waveguide, which was located on the pins and pressed down on to the mould. Before curing, the waveguide was inspected to ensure that it was central.

Glass cloth and epoxy resin were later laminated to the external surfaces of waveguide and aluminium foil, care being taken at the ends, which were rounded, to ensure good overlaps of glass cloth.

At an early stage in the laying-up process, two tinned brass counterweights were added at the ends of the flare (Fig. 1), and the central mounting pad was progressively built up into the main structure. In this way it was ensured that some glass cloth would run continuously from mounting pad to the ends. Similarly a continuous pad was built up around a central axis to carry the radome enclosure. On completion of the laying-up process, these pads were

† Admiralty Surface Weapons Establishment Extension, Funtington, near Chichester, Sussex.

‡ J. Croney, 'Improved radar visibility of small targets in sea clutter', *The Radio and Electronic Engineer*, 32, No. 3, pp. 135-48, September 1966.

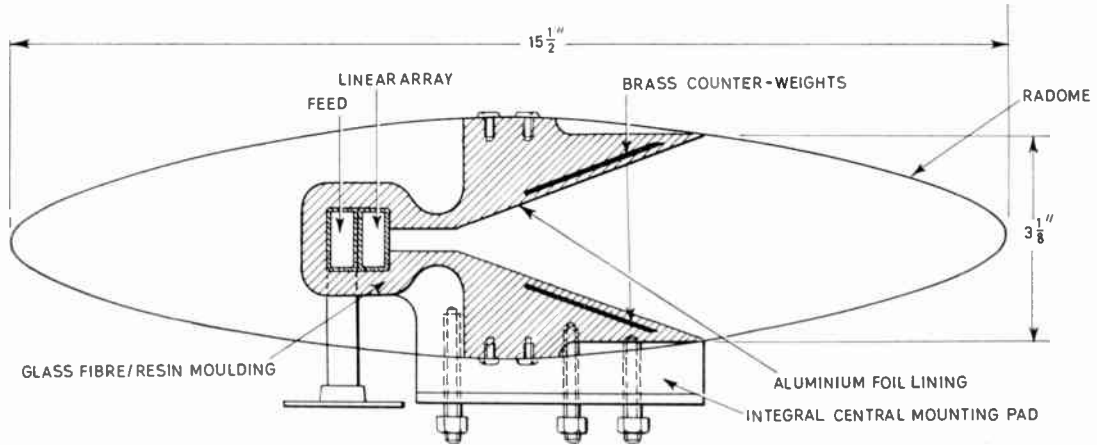


Fig. 1. Sectional view of the aerial.

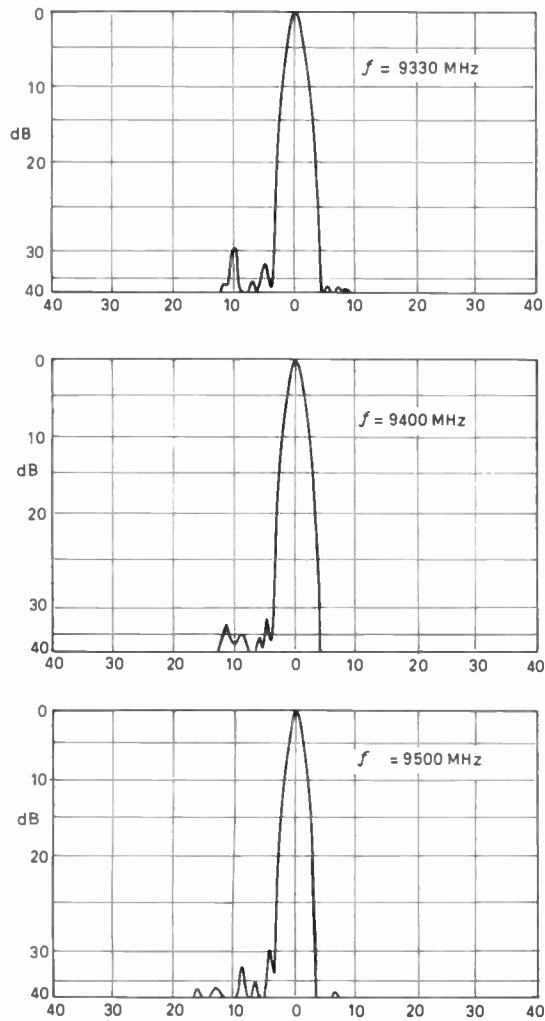
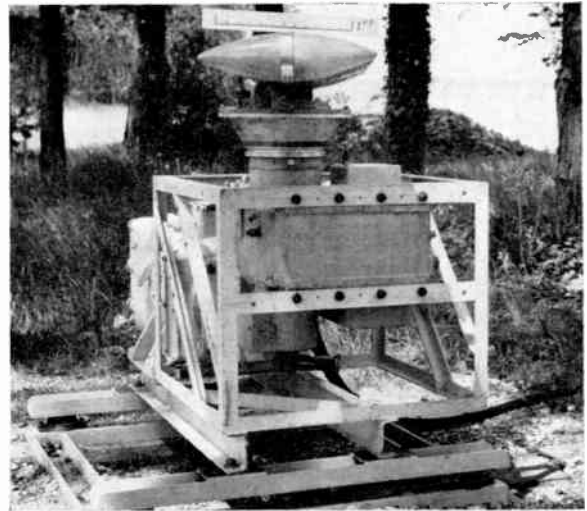
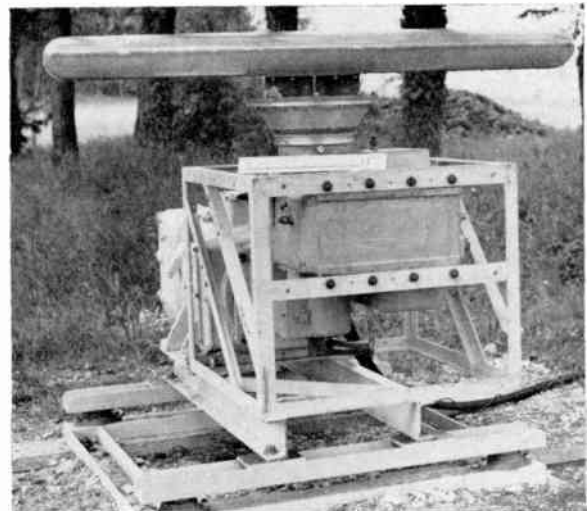


Fig. 2. Horizontal radiation patterns of high speed aerial complete with radome.



Crown Copyright Reserved



Crown Copyright Reserved

Figs. 3 and 4. Different views of completed antenna.

machined and metal inserts were cemented in the radome mounting pad, and studs tapped into the central mounting pad and locked with epoxy resin.

When the moulding was withdrawn, the aluminium foil was cut away from the central region of the waveguide exposing the slots, leaving a good fillet of aluminium foil at the joint of waveguide and flare.

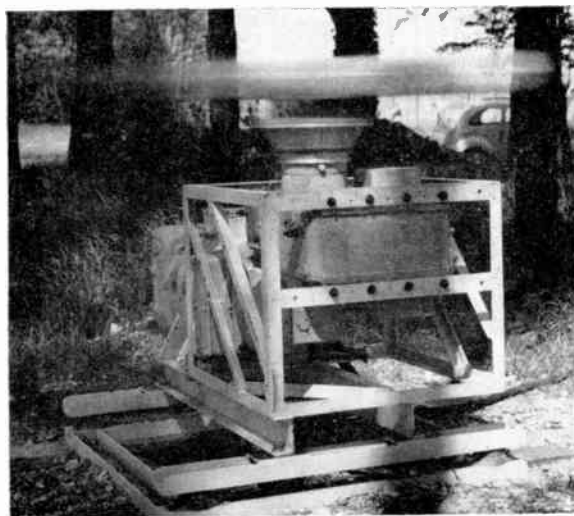
The completed item was therefore a single unit, which had no internal fastenings inside the radome. All fastenings, i.e. nuts on the main pedestal and screws for the radome were external and could be readily examined.

This antenna was bolted to the end flange of a steel tube mounted on two 4-inch ball bearings, at the bottom end of which was a waveguide rotating joint. The unit was chain driven through a bevel gear box by a 6 hp d.c. motor, the speed of which could be readily varied. Included in the mechanical drive was a synchro operating at 4.5 kHz to give positional data. The two photographs of Figs. 3 and 4 show different views of the completed antenna and Fig. 5 is a view of the antenna in speed.

The antenna was connected through low-loss waveguide to a laboratory building about 30 yards away, the speed being remotely controlled from this latter position.

4. Antenna Measurements

A comparison between design and the experimental results is given in Table 1, and the horizontal radiation patterns over the band are shown in Fig. 2. These experimental results were obtained on the complete antenna including radome.



Crown Copyright Reserved

Fig. 5. Photograph showing antenna in speed.

Table 1

	Design	Experimental
Side-lobe level	36 dB	30 dB (9330 MHz) 33 dB (9400 MHz) 30 dB (9500 MHz)
Horizontal beam-width	1.9 deg	2.0 deg (9330 MHz) 2.0 deg (9400 MHz) 1.9 deg (9500 MHz)
Vertical beam-width	16 deg	16 deg
Gain	30.7 dB	30.4 dB
Power in load	5%	5.35%
Squint	5 deg 48 min	5.9 deg
V.S.W.R.		0.93

5. Precessional Forces on Bearings due to Gyroscopic Action when Ship Mounted

Given the following data:

Weight of aerial	50 lb
Speed of rotation	1200 rev/min
Distance between bearings	12 inches
Length of aerial	50 inches
Height of aerial	4 inches

Assuming the following values for ship's motion:

Maximum angle of roll	± 15 deg
Period	12 seconds
Factor for non-simple harmonic motion conditions	1.2

Calculation shows that the maximum load on the bearings at peak values of angular velocity of roll is 47.2 lb. The design load of these bearings at this speed is 1700 lb.

6. Conclusion

The mechanical design of this aerial is strong enough to withstand the various forces involved in rotation at the speeds required. The method of manufacture is quick and easy, and very suitable for making a single experimental aerial of this type. The electrical performance gives low side-lobes and satisfactory beamwidths for use with the radar system.

7. Acknowledgment

This paper is published by permission of Ministry of Defence (Navy).

Manuscript received by the Institution on 27th May 1965 (Contribution No. 89/RNA53.)

© The Institution of Electronic and Radio Engineers, 1966.

The Design of Parallel Counters Using the Map Method

By

K. J. DEAN, B.Sc., C.Eng.
(Member)†

Summary: This paper describes how a counter may be designed to follow any desired code. The method is illustrated by the design of a parallel counter operating in the 5211 binary-coded decimal mode and which uses J-K flip-flops. The modules for the complete design are available as silicon integrated circuits. The minimized input conditions for a number of other coded decade counters are also stated.

The use of Veitch¹ diagrams and Karnaugh² maps are well established as techniques for the minimization of logical functions. By suitable choice of axes these two methods have been shown to be similar.³ It has also been shown^{4, 5} that this method may be applied to the logic and input equations of flip-flops, but in some cases the analysis which has been put forward has stopped at the point where most logical designers find it most interesting—that is, at the point of design of a practical counter.

The logical designer must often use a commercially available flip-flop in his design, whose input conditions may not be those of the ideal J-K flip-flop.⁶ In addition, he may wish to devise a counter to follow a predetermined code, and to use the minimum number of gates in doing so.

To illustrate the way in which such a problem may be solved, the design of a counter operating in 5211 b.c.d. will be considered. This binary-decimal code has the advantage that it is little used, so that the solution will not be immediately obvious to everyone, as it might have been had 8421 or 2421 b.c.d. been used. This code is used, however, in conjunction with other counters in some pulse-ratio-type square root extractors.

It is often stated that a J-K flip-flop is a bistable element in which there is no uncertainty regarding the state of its output when both inputs are at the '1' level. This is achieved by ensuring that when both inputs are at this level, the element is triggered into changing state. In fact, this is not always the case. Some bistable elements which are described as J-K flip-flops in their manufacturer's literature have inputs which are labelled \bar{J} and \bar{K} . It might therefore be better to define a J-K flip-flop as an element in which there is no uncertainty regarding the state of its output, whatever the input states might be. Truth tables for two bistable elements are shown in Table 1.

† Department of Science and Electrical Engineering, Letchworth College of Technology, Letchworth, Herts.

Table 1

(a) Truth table for ideal J-K flip-flop			(b) Truth table for J-K flip-flop having inputs J and K		
J	K	Q ₁	\bar{J}	\bar{K}	Q ₁
0	0	Q	0	0	\bar{Q}
0	1	0	0	1	1
1	0	1	1	0	0
1	1	\bar{Q}	1	1	Q

Note: Q is the output state after n pulses and Q₁ is the state after $n+1$ pulses.

The design procedure will be illustrated using ideal elements obeying truth Table 1(a), with additional gates to form a parallel decade counter. The design can be easily extended to the case where other types of J-K flip-flops are used.

The code in which the counter operates is set out in Table 2, so that the disposition of the decimal numbers 0-9 which correspond to the ten coded states may be determined on the Veitch-Karnaugh map. This map, with these decimal digits inserted,

Table 2
5211 weighted binary-decimal code

	A	B	C	D
0	0	0	0	0
1	0	0	0	1
2	0	0	1	1
3	0	1	0	1
4	0	1	1	1
5	1	0	0	0
6	1	0	0	1
7	1	0	1	1
8	1	1	0	1
9	1	1	1	1

is given in Table 3. The positions of unused code combinations are denoted by the letter X.

It is now necessary to deduce the minimum sufficient conditions for the transitions of logical level between counts. Alternatively, if the level remains unaltered between counts, as the level of D, for example, when the transition of the count takes place from 1 to 2, then in order that D shall remain at the '1' level, it is only necessary for K to be held at the '0' level. In this case, the level of J is immaterial. This may be denoted on subsequent maps by the letter X. Similarly, the transition from '1' to '0' can be made if K is '1', whatever the level of J. These typical conditions are determined by the characteristics of the logical modules which are used and which are stated in Table 1(a). They are summarized in Table 4, for both ideal and non-ideal flip-flops.

Table 3

Veitch-Karnaugh map for 5211 b.c.d.

AB CD	00	01	11	10
00	0	X	X	5
01	1	3	8	6
11	2	4	9	7
10	X	X	X	X

Table 4

	(a)		(b)	
	Ideal J-K flip-flop		Flip-flop with inputs \bar{J} and \bar{K}	
	J	K	\bar{J}	\bar{K}
Change '1' to '0'	X	1	X	0
Change '0' to '1'	1	X	0	X
Maintain '1'	X	0	X	1
Maintain '0'	0	X	1	X

Veitch-Karnaugh maps must now be drawn up for the input conditions which must apply to each of the flip-flops on each of the counts, so that in each case, the clock pulse routing shall be correct for the next desired state in the sequence. To illustrate this, consider the sequence of the element D, from the count of 0 in Table 2. It will be seen that after the count of 0, it must be possible for the output of D to change from '0' to '1'. When the count of 1 has been made, this element must be held at this '1' level for the count of 2. This is so again at the count of 2, in readiness for the count of 3, and also at 3 for the

count of 4. But after the count of 4 there must be a transition of the output to the '0' level for the count of 5. Again, after the count of 5, it must be possible for the transition to the '1' level to occur for the count of 6. The '1' level is then maintained until after the count of 9 when the output changes to the '0' level for the count of 0.

From this information two Veitch-Karnaugh maps can be drawn up as shown in Table 5 to illustrate the input conditions for the flip-flop D. It is from these maps that the minimized conditions for controlling the inputs of the flip-flop D can be deduced, and the advantage of the map method is the ease with which this can be done.

Table 5

Input conditions for the flip-flop D based on the use of ideal J-K flip-flops

AB CD	00	01	11	10
00	1	X	X	1
01	X	X	X	X
11	X	X	X	X
10	X	X	X	X

$D_J = 1$

AB CD	00	01	11	10
00	X	X	X	X
01	0	0	0	0
11	0	1	1	0
10	X	X	X	X

$D_K = BC$

It will be seen from Table 5 that there are two '1' conditions for D_J and that the remainder of the cells on the map are immaterial. In order to obtain the simplest condition for D_J any of the X positions we wish may be assigned the '0' or the '1' level, as may be convenient. Therefore, in this case we may regard them all as being '1's. Thus, the minimized condition for D_J is '1'.

In solving the conditions on the map for D_K it can be seen that there are two '1' conditions, and by looping these with the two X positions adjacent to them we may obtain the input condition. This assumes that these two cells are also regarded as '1's. This loop yields the desired condition for D_K as BC.

In the same way we may treat the conditions for the inputs to the flip-flops A, B and C. The Veitch-Karnaugh maps from which their input conditions may be derived are given in Table 6. It will be noticed that in the case of C_K we again have the minimized condition of '1'.

From Tables 5 and 6 the following minimized input conditions using ideal J-K flip-flops are obtained.

$$A_J = BC; A_K = BC; B_J = C; B_K = C; C_J = D; C_K = 1; D_J = 1; D_K = BC.$$

Table 6

Input conditions for the flip-flops A, B and C based on the use of ideal J-K flip-flops

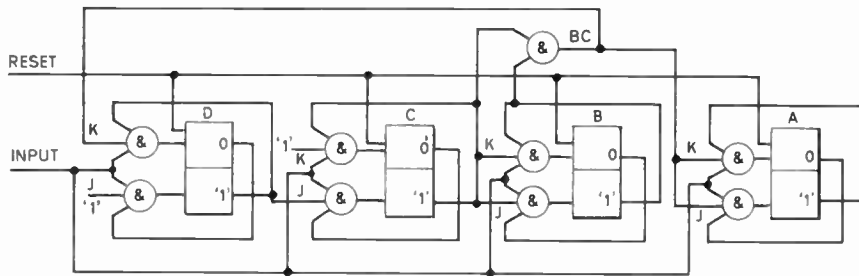
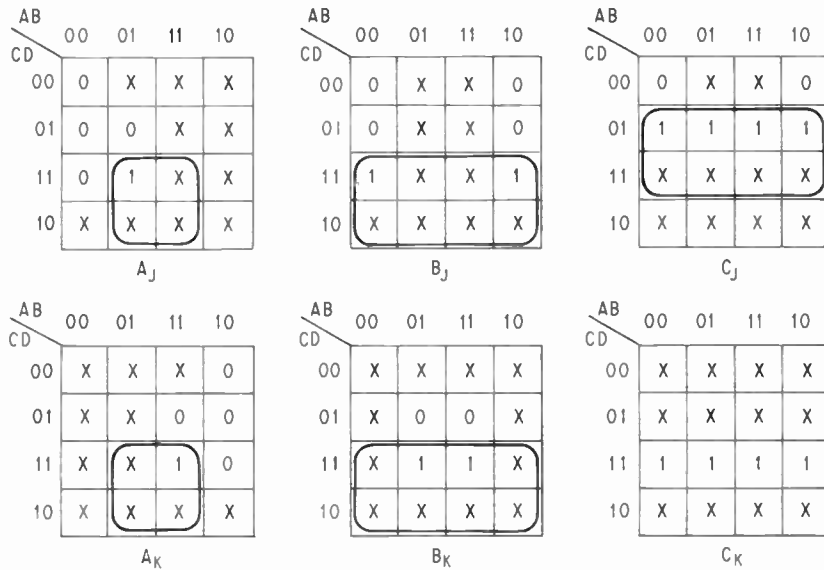


Fig. 1. Logical circuit of the complete counter.

All the data are now available from which the counter can be designed.

Figure 1 shows the complete counter. Since the design is that of a parallel counter, the pulse input must be taken to each of the stages as shown in the figure. The logical representation in the figure is that of four bistable elements, each modified by two AND gates to act as J-K flip-flops, and one additional AND gate to provide the BC output.

A silicon integrated J-K flip-flop will, of course, not require the two AND gates, since they will be incorporated in the design of the flip-flop itself.

In the foregoing discussion it was suggested that not all J-K flip-flops conformed to the ideal convention. For example, if a positive logical convention is used, the SGS-Fairchild Industrial range of Micrologic elements have inputs, \bar{J} and \bar{K} , and thus conform to the truth Table 1(b). Hence, their input

conditions must be deduced from Table 4(b). These lead to minimized expressions which are the negations of the conditions derived here.

The method which has been described can be employed to design counters and sequence generators with a wide variety of codes, of which the example

Table 7

	8421 BCD	2421 BCD	7421 BCD	Gray Code
A_J	BCD	BCD	BC	\overline{BCD}
A_K	D	D	B	D
B_J	CD	CD	$AC+CD$	\overline{CD}
B_K	CD	AD	AC	AD
C_J	\overline{AD}	D	D	\overline{BD}
C_K	D	$AD+\overline{BD}$	$A+B+\overline{D}$	BD
D_J	1	1	$\overline{AB}+\overline{C}$	$\overline{AC}+\overline{BC}+BC$
D_K	1	1	1	$\overline{BC}+\overline{BC}$

quoted here is perhaps one of the simplest. Table 7 gives a summary of some of these counters and the input conditions which are necessary to steer them.

Acknowledgment

The work described in this article and the verification of the codes using silicon integrated circuits has been carried out at the Letchworth College of Technology and the author wishes to thank the Principal of the College for permission to publish it.

References

1. E. W. Veitch, 'A chart method for simplifying truth functions', *Proc. Assoc. Computing Machinery*, p. 127, May 1952.

2. M. Karnaugh, 'The map method for synthesis of combinational logic circuits', *Communications and Electronics*, No. 9, p. 539, November 1953.
 3. N. N. Biswas, 'Veitch-Karnaugh map', *Control*, 79, No. 82, p. 185, April 1965. (Letters to Editor.)
 4. P. Lucas, 'Shortcut to logic design of sequential-counter gating', *Electronic Design*, p. 32, 6th December 1965.
 5. N. N. Biswas, 'The logic and input equations of flip-flops', *Electronic Engineering*, 38, No. 456, p. 107, February 1966.
 6. M. Phister, 'Logical Design of Digital Computers', p. 128, (John Wiley & Sons Ltd., London, 1958).

Manuscript first received by the Institution on 17th February 1966 and in final form on 26th April 1966. (Contribution No. 90/C86.)

© The Institution of Electronic and Radio Engineers, 1966.

STANDARD FREQUENCY TRANSMISSIONS

(Communication from the National Physical Laboratory)

Deviations, in parts in 10^{10} , from nominal frequency for August 1966

August 1966	24-hour mean centred on 0300 U.T.			August 1966	24-hour mean centred on 0300 U.T.		
	GBZ 19.6 kHz	MSF 60 kHz	Droitwich 200 kHz		GBZ 19.6 kHz	MSF 60 kHz	Droitwich 200 kHz
1	- 299.3	- 300.7	+ 3.4	16	- 301.4	- 299.1	+ 1.1
2	- 300.6	- 301.0	+ 3.2	17	- 300.4	- 299.4	+ 1.9
3	- 300.9	- 300.5	+ 3.3	18	- 299.9	- 300.0	+ 1.7
4	- 301.2	- 299.9	+ 3.0	19	- 300.8	- 300.2	+ 1.3
5	- 301.7	- 300.0	+ 3.2	20	- 300.8	- 299.6	+ 1.5
6	- 303.0	- 299.9	+ 3.0	21	- 300.8	- 300.0	+ 1.6
7	- 302.4	- 300.8	+ 3.4	22	- 300.7	- 299.9	+ 1.5
8	- 301.1	- 301.0	+ 3.4	23	- 301.6	- 300.1	+ 1.8
9	- 300.9	- 300.2	+ 3.2	24	- 301.6	- 299.5	+ 1.8
10	- 300.5	- 299.9	-	25	- 302.2	- 299.6	+ 2.3
11	- 299.5	- 299.3	+ 0.2	26	- 301.9	- 300.0	+ 2.1
12	- 300.3	- 300.3	- 0.1	27	- 301.6	- 300.4	+ 2.3
13	- 300.3	- 300.0	- 0.5	28	- 301.2	- 300.5	+ 1.6
14	- 300.4	-	- 0.9	29	- 301.4	- 300.6	+ 0.8
15	- 300.7	-	+ 0.8	30	- 300.8	- 301.1	+ 0.3
				31	- 302.5	- 300.4	0.0

Nominal frequency corresponds to a value of 9 192 631 770.0 Hz for the caesium $F_m(4,0)-F_m(3,0)$ transition at zero field.

U.H.F. Television Reception with Incident Field Strength of under 100 microvolts per metre

By

B. W. OSBORNE, M.Sc., C.Eng.
(Member)†

A short contribution read at the International Conference on U.H.F. Television held in London on 23rd November 1965.

Summary: Techniques in current use for the reception of the B.B.C.-2 programme at u.h.f. are illustrated, with reference to operational unmanned remote site installations. At u.h.f. an engineered receiving site can be designed for 20 dB better signal/noise ratio than is practicable and economic on domestic television installations.

In order to give the B.B.C.-2 u.h.f. television programme as soon as possible and to as many people as possible on the wired television distribution networks, it was necessary to ensure that aerials and pre-amplifiers of high performance were used at the more distant aerial sites. To determine the performance requirements before the start of test transmissions, the diffraction path attenuation to these sites was computed and the likely minimum field strength determined. In many places this made it possible to erect the necessary aerials and other equipment before transmissions were available, as the aerial gain and pre-amplifier noise figure required could generally be predicted.

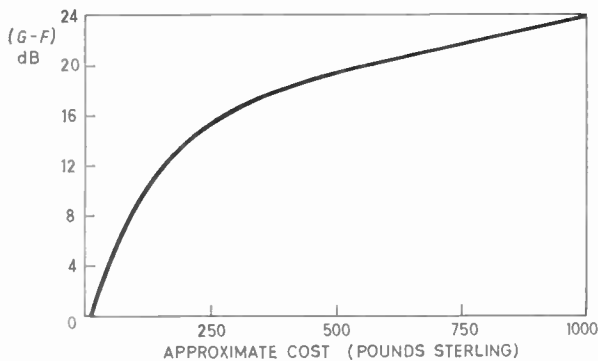


Fig. 1. The approximate relationship between performance and cost of u.h.f. aerials and pre-amplifiers.

The signal to noise requirements at a receiving site can be expressed in terms of the path attenuation x , the aerial gain G (ref. dipole) and the receiving site noise figure F .‡ For a given value of x , G and F must be chosen so as to obtain the desired signal to

† Rediffusion Research Ltd., Kingston-upon-Thames, Surrey.

‡ B. W. Osborne, 'The reception of substantially noise-free u.h.f. television signals over long distance paths', *The Radio and Electronic Engineer*, 28, No. 4, pp. 236-46, October 1964.

noise ratio. x will of course vary from day to day, the attenuation on some days being much less than that calculated from the diffraction path; and on the more difficult sites it is advisable to cross-check the computed signal level against field strength recordings and to look for any unpredicted local field strength variations on site.

Thus $(G-F)$, less any attenuation in the aerial feeder, is a figure of merit for the aerial site installation.

To limit the cost of the aerial and pre-amplifiers it is advisable not to aim unnecessarily high. A $(G-F)$ of 16 dB may cost about £250; whereas a $(G-F)$ of 24 dB may cost £1,000, i.e. about £100 per dB improvement. Thus the cost of making the noise imperceptible, at low field-strength sites, may not always be justified, involving as it does an aerial four times the size of that required (with a given pre-amplifier) to make the noise 'just perceptible'.

The aerial used generally needs to be mounted on a self-supporting mast, or on a pole. A recent design of a 22 dB aerial is shown in Fig. 2. This AE100 aerial has a gain of 22 dB.

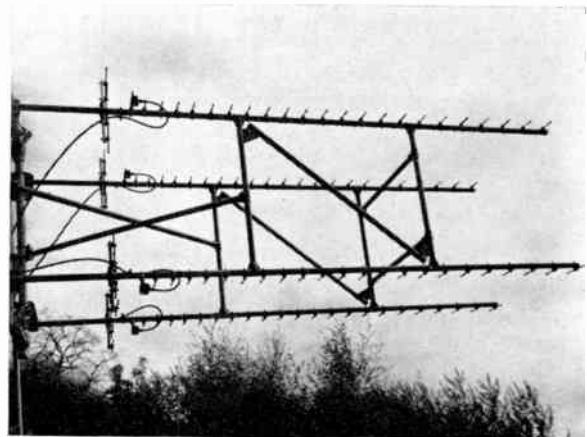


Fig. 2. The AE100 aerial of 22 dB gain.

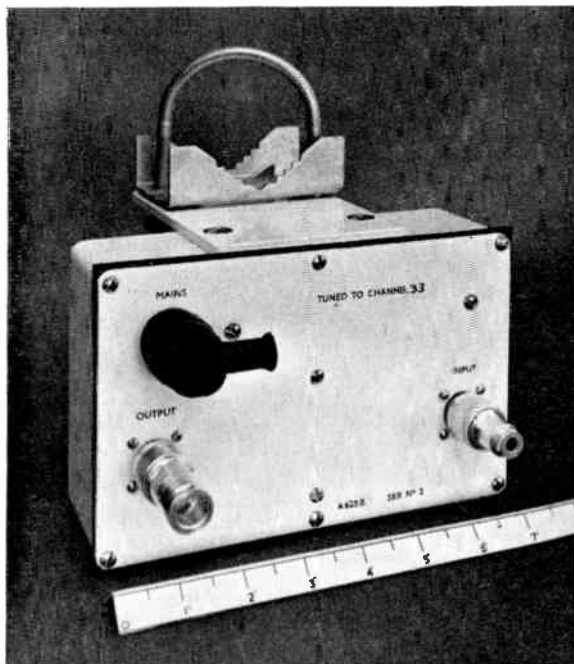


Fig. 3. The A625C very-low-noise transistor pre-amplifier.

Aerials of this size are now in use at the aerial sites used to feed B.B.C.-2 signals over 50-mile paths to subscribers in Exeter (Wenvoe ch. 51 transmitter) and in Kendal (Winter Hill ch. 62 transmitter).

A larger aerial having a gain of 25 dB is used where the highest gain is required, for example when receiving Emley Moor at Hull, over a path of computed attenuation 170 dB. (The initial path attenuation was in fact higher due to the low height of the temporary Emley Moor aerial.) The 25 dB gain can be realized when the incident wavefront is plane.

On the more distant sites where the highest values of $(G-F)$ are required, these large aerials have been used with varactor parametric amplifiers. These amplifiers have given satisfactory performance on unattended sites, the main reliability hazard being the pump klystron and its power supply. The parametric amplifier has to be backed by a second stage, which may typically be a transistor pre-amplifier, such as the A625C shown in Fig. 3. The most recent version of this unit has a noise figure of 4 dB at channel 33.

The 'fail-safe' characteristic of the parametric amplifier ensures that in the event of klystron failure the signal is passed on from the circulator to the

second stage. It is obviously desirable to have the 'stand-by' noise figure of the second stage as good as possible.

The A625C second-stage transistor pre-amplifier is also suitable for masthead mounting, and may be used by itself on sites where a parametric amplifier is not needed, or is not economically justified.

Let us now compare u.h.f. reception on high performance sites with domestic reception where each house has to become a separate receiving site. The inherent technical and economic advantages of wired television distribution in getting a good quality picture in every home are enhanced at u.h.f. for the following reasons:

- (a) The figure of merit of a receiving site is $(G-A-F)$, where A is the feeder attenuation between aerial and pre-amplifier. On typical domestic receiving installations at u.h.f. (or indeed at v.h.f.) it is unusual to find values of $(G-A-F)$ of better than 4 dB; whereas it is practicable to obtain 24 dB;
- (b) This 20 dB improvement in signal-to-noise ratio over domestic reception is additional to any increase in received field strength resulting from proper choice of the receiving site location, and by avoiding any local shadowing by high ground, trees or buildings; and
- (c) It is generally practicable to make good use of this improved signal-to-noise performance. Though we have yet to experience the worst effects of u.h.f. co-channel interference, the use of special aerial systems of spaced aerials can do a great deal of good. The aerials used are very much more directional than any likely to be used on private houses, and this helps to reduce the effect of echoes. Any residual off-air echo can be dealt with by an echo equalizer at the h.f. distribution frequency.

For 'just perceptible' noise impairment at 500 MHz when using a 25 dB aerial and a parametric varactor pre-amplifier, the required field strength is 80 $\mu\text{V}/\text{m}$. For the same noise impairment a domestic receiving installation using a 12 dB aerial, with 2 dB feeder loss and 10 dB noise figure, needs 1.2 mV/m.

This note is presented by permission of the Directors of Rediffusion Research Limited.

Manuscript first received by the Institution on 24th November 1965 and in final form on 12th January 1966. (Contribution No. 91/T36.)

© The Institution of Electronic and Radio Engineers, 1966

The Series Resistance of Varactor Diodes

By

C. TOKER, B.Sc., Ph.D.†

AND

Professor

F. J. HYDE, D.Sc., C.Eng.

(Member)‡

Summary: A series resonance method of determining the equivalent series resistance of the semiconductor region of varactor diodes at u.h.f. has been investigated in some detail. Data are presented for commercial samples of both silicon and gallium arsenide types. It has been found that there is a component of apparent series resistance which decreases approximately as $1/\omega^2$ in the v.h.f. and u.h.f. bands.

1. Introduction

The accurate determination of the parameters of the equivalent circuit¹ of a varactor diode shown in Fig. 1 is of importance in assessing the relative usefulness of different diodes in practical applications.² In this figure C_A and C_B represent the stray capacitance

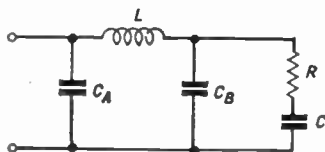


Fig. 1. Small-signal equivalent circuit of a varactor diode.

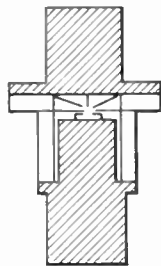


Fig. 2. Cross-section of the diodes used.

and L the stray inductance of the diode capsule. R and C are the equivalent series combination of resistance and capacitance attributed to the semiconductor region. On the basis of a one-dimension model R and C can be considered invariant with frequency until skin effect becomes significant.^{3,4} However, when the surface properties of the semiconductor in the vicinity of the periphery of the p-n junction are taken into consideration there is evidence that R and C are not invariant with frequency. Marked frequency dependence of R at v.h.f. and lower u.h.f. has been reported.^{5,6} The fact that the semiconductor surface is involved is indicated by the observed dependence of R on the gaseous ambient of the semiconductor region. The assessment of the frequency-dependence of R is likely to be obscured by the effects of frequency-dependent losses in the measuring system.^{1,7}

In this paper results are presented for encapsulated diodes having the form shown in Fig. 2, which show

† Middle East Technical University, Ankara, Turkey; formerly at University College of North Wales.

‡ School of Engineering Science, University College of North Wales, Bangor.

the effect of frequency and bias voltage on R . The effect of loss in the measuring system is taken into account.

2. The Measuring System

This is illustrated schematically in Fig. 3. The diode is incorporated in the central conductor of a transmission line of characteristic impedance $Z_0 = 50\Omega$. The main transmission line has the dimensions of the General Radio 874 system. The section in which the diode is mounted has an inner conductor whose reduced diameter is of the order of the outside dimensions of the diodes and is chosen so that when supported by the p.t.f.e. cylinder shown in Fig. 3 the characteristic impedance of this section is also 50Ω . Behind the diode an adjustable short-circuit is located. The technique of measurement is to adjust the position of this short-circuit until minimum voltage-standing-wave-ratio (v.s.w.r.), S , is measured to the left of the diode, using a standard slotted line system. The convention used in this paper is that $S > 1$.

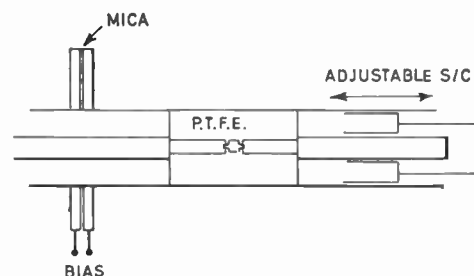


Fig. 3. Schematic diagram of diode mounted in the measuring apparatus.

Values of the equivalent circuit parameters for a typical diode as obtained by measurements at X-band are: $C_A \approx C_B \approx 0.15$ pF, $L \approx 5 \times 10^{-10}$ H, $C \approx 0.5$ pF at zero bias, $R \approx 5-10\Omega$, also at zero bias. Accepting these as a basis it follows that, at frequencies below

about 2000 MHz, L can be ignored in relation to C_A and C_B , so that the effective series impedance of the diode is represented by

$$R_d = R \frac{C^2}{(\omega CRC_s)^2 + (C + C_s)^2} \approx \frac{R}{(1 + C_s/C)^2} \dots\dots(1)$$

$$C_d = \frac{(C + C_s)^2 + (\omega CRC_s)^2}{C + C_s + \omega^2 C^2 R^2 C_s} \approx C + C_s \dots\dots(2)$$

where $C_s = C_A + C_B$. When S is a minimum the reactance of the effective capacitance C_d resonates with that of the inductance due to the length of short-circuited line behind the diode, and then

$$S = \frac{Z_0}{R_d + r} \dots\dots(3)$$

Here r is the effective series resistance of the short-circuited line at the plane of the semiconductor in the diode. This resistance represents the transformed loss due to imperfection in the short-circuit itself and the distributed losses in the line. Provided that r is known for the actual line-length used to produce resonance for each condition of bias and frequency, it follows that R_d can be calculated from equation (3) and hence R from equation (1). The assumption is made that $C_d = C + C_s$ and is invariant with frequency. However, variation of C_d with bias through C is considered. C_s and C can be determined in the manner described in Reference 1. Equation (3), with $S > 1$, is consistent with the observation that $R_d + r < Z_0$.

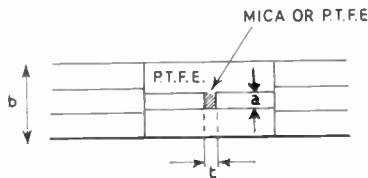


Fig. 4. Passive capacitor section.

3. Evaluation of r

The determination of r for the range of short-circuited line lengths involved can conveniently be carried out by replacing the varactor by a series of lossless capacitors of different values, each one requiring a different line length for resonance. S is measured for each resonant condition and the appropriate value of r thereby determined. The form of construction for the capacitors is shown in Fig. 4. A plane-parallel section of the central conductor, of thickness t , is removed and replaced by a mica or p.t.f.e. disk having the same dimensions. To give support to the sections of the inner conductor the length of line involved is filled with p.t.f.e.; to keep the characteristic impedance uniform the diameter of

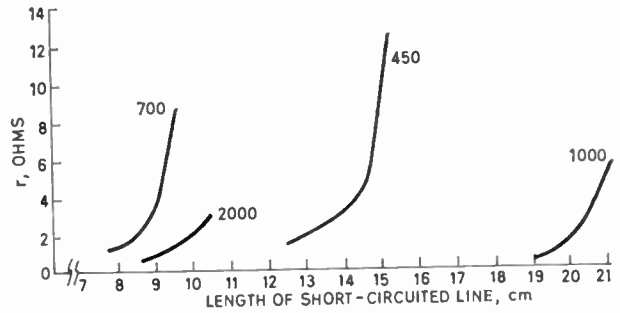


Fig. 5. Dependence of series input resistance on the length of short-circuited line. Frequency in MHz is the parameter. The curves extend over the actual line lengths used. At 450 and 700 MHz $l < \lambda/4$ and at 1000 and 2000 MHz $\lambda/2 < l < 3\lambda/4$ for physical reasons.

the inner conductor in this section is reduced as in the actual diode mount. The capacitance created is the sum of the parallel-plate capacitance C_p and the fringing capacitance C_f given respectively by⁹

$$C_p = 0.0694 \frac{\epsilon a^2}{t} \text{ pF} \dots\dots(4)$$

$$C_f = 0.0884 a \epsilon' \log_e \frac{b-a}{t} \text{ pF} \dots\dots(5)$$

Here a and b are measured in cm, ϵ is the relative permittivity of the dielectric spacer and ϵ' that of the supporting p.t.f.e. cylinder. C_f is of the order of 10% of C_p . The actual values used are:

- $a = 0.427 \text{ cm}; b = 1.427 \text{ cm};$
- $\epsilon' = 2.12; \epsilon = 2.12 \text{ for p.t.f.e. and } 7.0 \text{ for mica};$
- $t = 0.023\text{--}0.076 \text{ cm for p.t.f.e. and } 0.013\text{--}0.025 \text{ cm for mica.}$

The dependence of r on the length of short-circuited line, as obtained from $S = Z_0/r$, is shown in Fig. 5, with frequency as parameter. The distances are measured from the plane of the adjustable short-

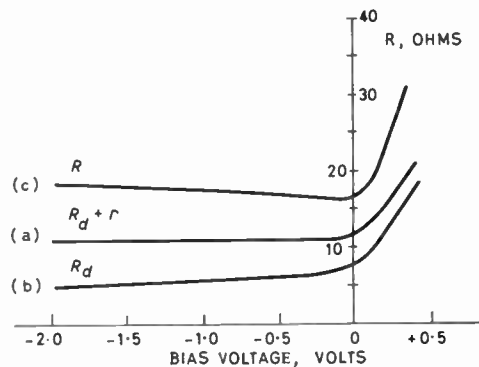


Fig. 6. Reduction of data for a silicon diode type ZC20E. (a) $R_d + r$; (b) R_d ; (c) R in Ω .

circuit to the plane of the capacitor plate nearest to it and this was arranged to correspond with that of the semiconductor region in the diode.

4. Results

The stages in the reduction of the data are illustrated graphically in Fig. 6 for a silicon diode type ZC20E, for a frequency of 450 MHz. Curve (a) shows the direct dependence of $R_d + r$ on bias voltage, calculated from equation (3) using the

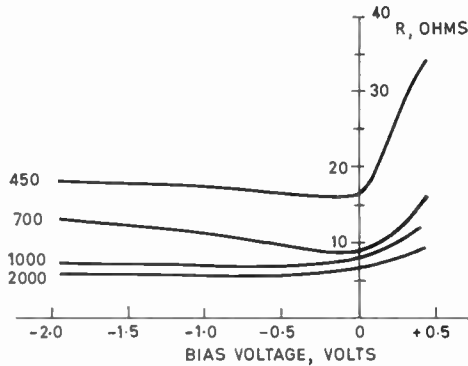


Fig. 7. Dependence of R on bias voltage for a ZC20E silicon diode. Frequency in MHz is the parameter.

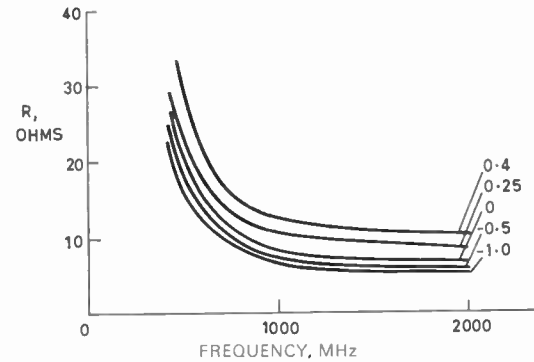


Fig. 8. Dependence of R on frequency for a ZC20E silicon diode. Bias in volts is the parameter.

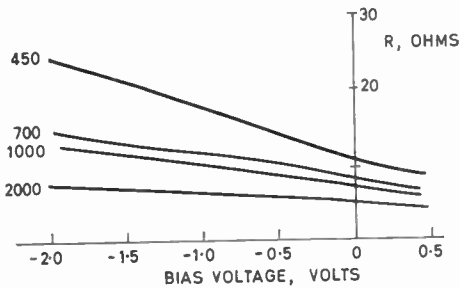


Fig. 9. Dependence of R on bias voltage for a VX3368 gallium arsenide diode. Frequency in MHz is the parameter.

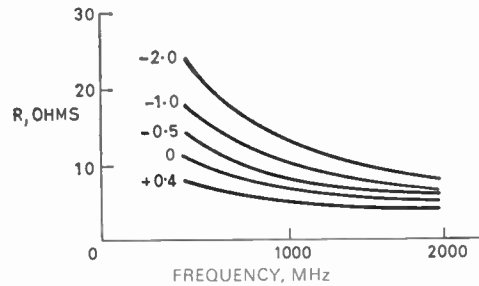


Fig. 10. Dependence of R on frequency for a gallium arsenide diode. Bias in volts is the parameter.

measured values of S . Curve (b) shows the corresponding variation of R_d , the appropriate values of r being subtracted from the points on curve (a). Finally, curve (c) shows the variation of R itself, calculated from the points in curve (b) using equation (1), with the assumption¹ that $C_s = 0.3$ pF.

Collected data for this diode showing the overall dependence of R on bias and frequency respectively are presented in Figs. 7 and 8. Corresponding data for a gallium arsenide diode type VX3368 are shown in Figs. 9 and 10. The zero bias capacitance of the actual junction was 0.58 pF for the silicon diode and 0.35 pF for the gallium arsenide diode.

5. Discussion

It will be noted that for both the silicon and gallium arsenide diodes R decreases with frequency approaching asymptotic values in the vicinity of 2000 MHz. For both diodes R decreases with decreasing reverse bias, more so for the gallium arsenide diode. With increasing forward bias the behaviour is different. R increases for the silicon diode, but continues to fall for the gallium arsenide diode. The increase in resistance with forward bias for the

silicon diode can be explained in terms of the narrowing of the depletion layer with the consequent additional contribution to the bulk resistance of regions of comparatively high resistivity.¹⁰ In view of the greater diffusion potential of the gallium arsenide diode the effect would be expected to be less for this diode over the bias range shown.

Both Eng and Solomon⁶ and Sawyer⁵ have suggested that the frequency-dependence of R is due to surface effects and distributed C-R models have been proposed to represent these. In view of the nature of the present measurements which were made on encapsulated diodes no attempt will be made to

extend these models here. It is of interest, however, to consider the frequency-dependence of the components of R in Figs. 8 and 10 in excess of the asymptotic values. This follows more nearly the $1/\omega^2$ dependence observed by Eng and Solomon, rather than the $1/\omega$ behaviour reported by Sawyer.

It is evident from the nature of these experiments that the accuracy of determination of r is greatest at a given frequency when the length of short-circuited line required to resonate the diode capacitance is small; i.e. when the diode capacitance is comparatively large. The rapid increase in R as this length approaches $\lambda/4$ means that care must be taken in determining this length. There is some uncertainty in specifying the length because the passive capacitors used have finite extent and the semiconductor region is not truly a plane. Errors are therefore likely to be greater at lower frequencies.

6. Conclusion

In a series resonance method of determining the equivalent series resistance of varactor diodes account has been taken of the effective series resistance associated with the length of short-circuited line used to produce the resonance. When this has been done it has been found that there is a component of equivalent series resistance which decreases approximately as $1/\omega^2$. It could be concluded that this is a real effect, which is probably associated with surface conditions at the semiconductor as suggested by earlier workers. The frequency-dependence of the equivalent loss resistance associated with a short-circuited length of line does not appear to be sufficient to account for the observed variation of resistance as determined directly from v.s.w.r. measurements.

7. Acknowledgments

The authors wish to acknowledge the support of this investigation as part of a wider programme by the Science Research Council. The mechanical work was performed by Mr. R. Jones.

8. References

1. F. J. Hyde, S. Deval and C. Toker, 'Varactor diode measurements', *The Radio and Electronic Engineer*, **31**, No. 2, p. 67, 1966.
2. L. A. Blackwell and K. L. Kotzebue, 'Semiconductor-Diode Parametric Amplifiers', (Prentice-Hall, Englewood Cliffs, N.J., 1961).
3. K. E. Mortenson, 'Alloyed, thin-base diode capacitors for parametric amplification', *J. Appl. Phys.*, **30**, p. 1542, 1959.
4. H. V. Shurmer, 'Intrinsic frequency limitations for semiconductor microwave devices', *The Radio and Electronic Engineer*, **31**, No. 2, p. 93, 1966.
5. D. E. Sawyer, 'Surface-dependent losses in variable reactance diodes', *J. Appl. Phys.*, **30**, p. 1689, 1959.
6. S. T. Eng and R. Solomon, 'Frequency dependence of the equivalent series resistance for a germanium parametric amplifier diode', *Proc. Inst. Radio Engrs*, **48**, p. 358, 1960.
7. A. Uhler, 'Apparent frequency dependence of series resistance of varactor diodes', *Proc. I.E.E.E.*, **51**, p. 1246, 1963.
8. D. A. E. Roberts and K. Wilson, 'Evaluation of high quality varactor diodes', *The Radio and Electronic Engineer*, **31**, No. 5, p. 277, 1966.
9. G. L. Matthaei, L. Young and E. M. T. Jones, 'Microwave Filters, Impedance Matching Networks and Coupling Structures', p. 538 (McGraw-Hill, New York, 1964).
10. A. H. Benny, 'Silicon variable capacitance diodes for use at low temperatures', Proceedings of the Symposium on 'Microwave Applications of Semiconductors', London, 1965. Paper No. 1. (I.E.R.E. Conference Proceedings No. 5.)

Manuscript first received by the Institution on 17th August 1965 and in final form on 13th December 1965. (Paper No. 1065.)

© The Institution of Electronic and Radio Engineers, 1966

A Fast Off-line Digital Correlator using Magnetic Tape for Storage, Repetition and Scanning

By

D. P. FRANKLIN†

Based on a short paper presented at the International Conference on Magnetic Recording held in London in July 1964.

Summary: Special purpose digital apparatus is described for off-line correlation of time varying functions in analogue form. The necessary storage, repetition and relative scanning are afforded by an instrumentation magnetic tape recorder through the extension of its 'closed loop'. A new value of lag coincides with the complete replacement of that length of tape contained within the 'closed loop', and a fresh value of correlation coefficient is printed out for each lag. The method takes up only two tracks, so those remaining can be used in the normal acquisition role at any convenient speed, later transferring their signals at high speed to the analysis circuits.

1. Introduction

It often becomes necessary to extract significant information from electrical signals which are predominantly random (e.g. signals near the threshold of detection, signals derived from system fluctuations or perturbations), or others which are of such a variable nature (e.g. video signals) that they can be dealt with only by statistical methods.

A process of fundamental statistical importance is correlation: by it the average of the instantaneous product of two input variables is obtained. Thus, for input functions $x(t)$ and $y(t)$,

$$\text{correlation coefficient} = \overline{x(t) \cdot y(t)}$$

If, now, one of the functions is displaced in time by an amount τ , and the process repeated, we have

$$\text{correlation coefficient} = R(\tau) = \overline{x(t) \cdot y(t - \tau)}$$

and its variation with respect to τ is termed the cross correlation function of x and y . If y is identical with x , we have the autocorrelation function.

Practical situations in which the utility of correlation functions is demonstrated, such as testing the transient response of a system (e.g. an industrial process^{1, 2, 3} or a concert auditorium^{4, 5}) without the use of a large amplitude step or impulsive input, analysis of seismological records,^{6, 7} analysis of e.e.g. records,⁸ spectral analysis,^{9, 10} are subjects of interest in their own right, and will not be further discussed here.

The extraction of the correlation function from a set of data without computational aid can be a very tedious process because, to obtain reasonable precision, the averaging involved has to be taken over a large population (infinitely large, ideally). Regular use of

the technique therefore presupposes the adoption of some form of mechanization. Most commonly, the input functions are first transduced into electrical analogue form but, from this stage onwards, there are a number of alternative courses, depending upon the principles used for providing the relative lag, τ , forming the instantaneous product and deriving the average. There is another distinction to be made according to whether it is permissible for the computation time to be unrelated to the acquisition time of the relevant data (off-line operation), or whether the working speed, resolution and precision have to be so determined that the required output keeps pace with the incoming data (on-line operation). For the second alternative a somewhat degraded performance is usually acceptable in the interests of operating speed.

For off-line working, it is necessary to record or store both input functions for at least a time sufficient to give the required precision and, frequently, they are recorded over a long period so that the selection of the excerpt which is to undergo analysis can be postponed until expedient. The most convenient recording medium currently in use is magnetic tape.

When the signals are 'live' and stationary, it may suffice to introduce storage of a temporary character in one channel only in order to provide the required lag. If, however, it is not certain that the process is stationary, the same excerpts of the functions should be used for all values of lag. In exceptional cases simultaneous (parallel) analysis for each of a number of lags can be justified, but repetition of the signals for successive values of lag is the more common practice and clearly necessitates storage in both channels.

A number of machines have been described in which an excerpt is recorded on a loop of magnetic tape or on a coated drum to permit iterative analysis, and the lag is

† E.M.I. Electronics Ltd., Wells, Somerset.

varied by a physical movement of a transducer head.^{11, 12, 13} The formation of the instantaneous product and the integration, inherent in deriving the average, make use of conventional analogue computing techniques adapted for higher bandwidths. Practical difficulties arising during the design of this type of correlator are the limited storage capacity of a single turn of a drum, the slight instability of tape motion, and the need either to suppress the transient caused by the tape join or to place the join away from the excerpts. Drift in the computing elements over the total analysis time has also to be watched.

As an alternative, the signals may be represented in digital form and dealt with by a standard digital computer.⁹ Unless high speed analogue/digital converters and magnetic tape stores are to hand, the time spent in feeding the information into the system is often uneconomic. Furthermore, the simplicity of the computation is ill-matched to the capability of a general-purpose machine and, if called for frequently, may well justify a small, special-purpose instrument.¹⁴

In this paper, such a system† will be described in which the data, although originating as voltage analogues, are handled in digital form; in it signal storage, repetition and relative scanning between the two channels are all provided using a simple adaptation of the conventional instrumentation magnetic tape deck used to reproduce the input functions.

For on-line applications, the tape deck is not essential, and the same system approach may be retained, with the tape memory replaced by static magnetic core storage. Incidentally, the substitution can bring with it some useful circuit simplifications. As smaller (and cheaper) general-purpose computers come on the market the idea of using one for the above duty is becoming less controversial. It may eventually become practical to apply such a cheap computer to undertake this single task exclusively.

2. Operating Principles

2.1. Repetition

For economy of equipment, the correlation function is usually derived, one point at a time, by an iterative process, each time using a fresh value of lag. With economy and convenience again in mind, the information within each iteration is handled serially, one instantaneous value in each channel at a time. Unless the processes are known to be stationary, the same data will then have to be used over and over again. If, though, the signals were to be recorded in coded form, an alternative to repetition by tape loop or drum would offer itself.

A practice which lends itself well to long distance transmission of signals is the use of pulse code modula-

tion (p.c.m.) because, at each repeater station, regeneration of the pulse code to standard amplitude and timing is feasible¹⁵; the repeated signal is thus 'as good as new'. In much the same way, by using p.c.m. we are enabled to rewrite code on magnetic tape as soon as it has been read off elsewhere provided that, each time, we regenerate the code pulses.

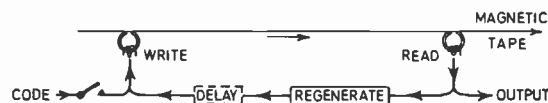


Fig. 1. Closed digital information loop using magnetic tape.

Figure 1 shows the principle used; write and read heads are located some distance apart along a moving magnetic tape and the code read off is passed to the regenerator and re-recorded. It will be appreciated that the amount of data carried by the length of tape between heads is held indefinitely in dynamic store, access being sequential. The principle is the same as that used in ultrasonic delay line stores, but the propagation speed is here much lower. With magnetic tape, however, there is the opportunity for varying the bit rate and, moreover, a number of channels each of identical propagation rate may be accommodated.

The practical necessity for a finite period for the averaging process places a zone of uncertainty about the 'true' infinite term average; the shorter the term, the lower the precision. Thus, the length of excerpt necessary is determined by the tolerable error in the correlogram.‡

Unlimited recirculation of information requires that any mutilation of the received code should not be so great that the original cannot be recovered, because an error, once made, would be perpetuated. Fortunately, in arriving at usable statistics, averaging must be applied over large populations, and the incidence of a few errors will have negligible influence upon the result. Some relaxation from perfect data preservation is therefore permissible, and redundant codes or the like will not normally be necessary.

2.2. Relative Scanning

Between successive repetitions, one channel must receive an increment in lag, although the lag must remain constant throughout any given repetition. That is, the signal in the second channel will precess with respect to that in the first. To provide the maximum resolution which the signal bandwidth will afford, the lag increment should be made equal to the sampling (digital word) period.

‡ When a maximum length binary sequence (or 'pseudo-random binary signal') is used as a perturbing test input to a system,¹⁶ an averaging period equal to a full sequence is clearly all that is necessary, since the system behaviour will thereafter repeat.

The above requirements may readily be met if the two inputs, which we may refer to as x and y , are written on parallel tracks, read at equal distances farther along the tape and recirculated as already described. In addition, however, the y data loop is arranged to include an extra element which introduces a delay of one word period. Thus the propagation speed will be the same for both channels, but the loop repetition period will be one word interval longer for y than for x .¹⁷

Figure 2 shows the progress of the x and y excerpts diagrammatically in analogue form, T being the repetition period for x while that for y is $(T + \Delta T)$; ΔT is shown greatly exaggerated. For clarity, the variables are shown as continuous functions of time

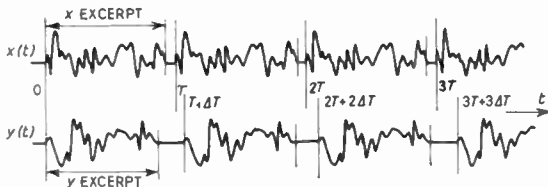


Fig. 2. Illustrative diagram of repetition and precession.

although, in practice, they will have been sampled and encoded. It will be seen that, at each repetition, the lag is successively $0, \Delta T, 2\Delta T, \dots$, and it will also be seen that the y excerpt is made rather shorter than for x . This has two advantages:

- (i) It prevents the end of the y excerpt eventually becoming associated with the beginning of the x and thereby avoids fictitious periodicities being associated with the signals.
- (ii) It results in the averaging interval (during which a word product is significant) remaining constant from repetition to repetition. This obviates a division process in computing the average product.

2.3. Word Length

With pulse code modulation, an input signal is sampled at regular intervals, and the amplitude of each successive sample is represented by a digital word to a resolution determined by the word length in bits. Thus, the amplitude represented by each word must be one of a number of discrete levels, whereas the original sample amplitude could generally have taken any value between the overload limits. This is illustrated in Fig. 3 in which a continuous function, $f(t)$, is sampled at regular time intervals. These samples are shown as bold vertical lines. The horizontal lines represent the borders between adjacent quantizing intervals, and any sample falling between a particular

pair of lines is represented digitally by a value corresponding to midway between them. The vertical dotted lines show the quantized version alongside each sample.

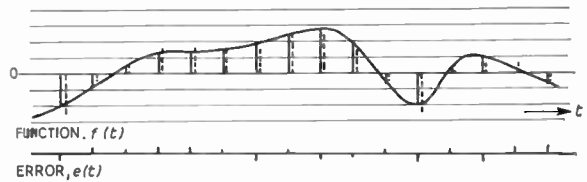


Fig. 3. Explanatory diagram of quantization and quantization noise.

Below $f(t)$ is shown the error, $e(t)$, between the quantized and true samples, which may be regarded as an extra sampled signal superimposed upon the original to give the numerical value. This error signal is preponderantly random, but of 'rectangular' (bounded uniform) amplitude probability distribution, and may be termed 'quantization noise'.

Whereas a superimposed noise is normally undesirable and must be minimized, a statistical process such as correlation is usually much more tolerant because of the averaging involved. The criterion for the noise to be tolerable is that it is only weakly correlated with either of the main inputs.

Watts,¹⁸ following Widrow,¹⁹ has investigated the conditions for the incoherence of quantization noise by considering the amplitude probability density of the input function and deriving a transform to detect periodicities of probability with respect to amplitude. By analogy with Nyquist sampling theory for regular time intervals, he obtains the maximum permissible difference between quantization levels. For instance, a function with a very smooth amplitude probability distribution (e.g. a Gaussian distribution) may be dealt with adequately by a one-bit word for which the threshold between the + state and the - state is located at the mean value. This is the case in polarity coincidence correlation.^{17, 20}

Noise (or noise-like) signals commonly encountered show a less even amplitude distribution but, for practical purposes, adequate precision can be obtained if the input signal exceeds the acceptance range of the input circuit not more than 1% of the time and if that range is made up of six or seven quanta. The mean value should first have been brought within plus or minus a half quantum or so of mid-range by means of added d.c.

It will be appreciated that the error in the instantaneous value consequent upon quantization could here be up to 7% of full range; it is only when averages of large populations of randomly variable quantities

are involved that the overall effect of such errors becomes acceptably low.

Although signals are usually expected to be random in amplitude, it is possible, even for functions with strong peaks in amplitude probability (e.g. square waves, or sinusoids) to be accommodated, with only moderately lowered precision, if they are accompanied by added random noise sufficient to round off and spread these peaks over about two quanta. Provided this auxiliary noise is quite incoherent, it will make no steady contribution to the output. The reduced precision may usually be made up by a modest increase in excerpt length.

Seven levels call for only three bits in each word and this small word length permits worthwhile simplification in encoding, multiplying and write/read circuits.

2.4. Autocorrelation of Added Noise

When two inputs are involved which are only partially coherent, their quantization noises generally will be substantially incoherent, both mutually, and with respect to the inputs. However, if the two signals are identical, as for autocorrelation, their quantization noises will also be identical and therefore mutually coherent. As a result, the correlation coefficient at zero lag will be too great by $q^2/12$, where q is the difference between adjacent levels. This will be recognized as a form of the well-known Sheppard's correction for statistics derived from grouped data.²¹

If, though, the linear gains of the stages feeding the encoders are made rather different for the two channels (e.g. one spans six levels as the other spans seven), the coherence of the quantization noises is sharply reduced, and no special corrections are usually required.

3. Magnetic Recording

3.1. Recording Mode

If a word is written with individual bits on separate parallel tracks, the permissible longitudinal packing density is often limited through variable skew in the tape and gap scatter in the write and read heads. The resulting time displacement can lead to clocking difficulties. Accordingly, when the word is only three bits long, writing the information and clock pulses serially on three adjacent tracks is attractive because the effect of skew is much reduced, and the increase of 3 : 1 in packing density easily accommodated by a write mode using two flux transitions per bit.²² Certain such modes are suitable for self-clocking, so it is possible to dispense with a separate clock train, and the correlation process would then take up only two tracks. The economy, both in tracks and in the accompanying write and read arrangements, more than compensates for the extra logic circuits required for staticizing and serializing.

3.2. Parameters

A number of system parameters will be assumed, as set out in Table 1, wherein the tape speed is high, but readily available, and the excerpt length sufficient to give moderate precision²³ while being easily accommodated by a tape mechanism. The bandwidth follows from the choice of a high, yet practical, bit packing density.

Table 1
System parameters

Input passband	70 Hz to 7 kHz
Word rate	20 000 w/s
Bit interval	15 μ s (min)
Tape speed	60 in/s
Longitudinal bit interval (min)	0.84×10^{-3} in $\approx 1/1200$ in $\approx 21 \mu$ m
Distance write/read	30 in
No. of words x channel	9.9×10^3
No. of words y channel	9×10^3
Max. lag	900 words or 45 ms
Repetition period	0.5 seconds

Several parameters apply to conditions during analysis only, and therefore it is open for data to be acquired at a lower rate, and over a correspondingly longer period, using a low tape speed to match the density parameters, followed by speeded-up playback.

Within the previously discussed limitations upon peakiness of the amplitude probability distribution of input signals, a population of 9000 samples corresponds, at the 90% confidence level, to an output error of not more than 2.5%. This error is inherent in the extraction of statistics from random data, and is exclusive of instrumental errors. Because most of the computation is performed digitally, however, the latter errors are confined to those circuits leading up to the digitizers, and are readily kept low.

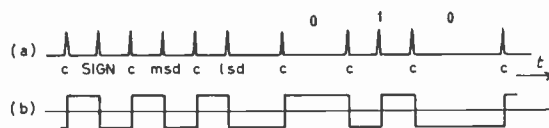


Fig. 4. Serial pulse code and write current waveform.

At the bit density quoted, a 'phase reversal' recording mode²² is apposite and can be arranged to provide both bit and word timing. Figure 4(a) shows the structure of the adopted pulse train due to be fed to a divide-by-two bistable circuit to give a write current waveform, (b). At playback, amplitude equalization, followed by limiting, recovers (b), from which (a) may

be derived through differentiation. The separation of clock from data pulses will be described in detail later.

3.3. Mechanism and Operation

When a long distance separates write and read heads along a magnetic tape, it becomes a practical necessity for 'decoupling', by means of a constant speed capstan, to be introduced close to each head if fluctuations in relative pulse timings are to be kept within bounds. This is readily accommodated on many standard instrumentation recorders by extending the path of that part of the tape which is normally guided by a 'turn around' roller, P, as shown in Fig. 5. Here, extra pulleys are incorporated to provide a bight (or

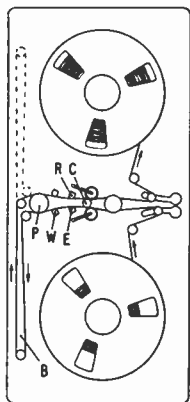


Fig. 5. Modified tape mechanism.

loop), B, giving a distance of 30 in between write, W, and read, R, heads. Approximately twice the length (and therefore duration of excerpt) is given if the tape also follows the extra path shown dotted. The use of gap-aligned multi-track write and read heads minimizes relative time displacements, and automatically ensures equal word storage capacity for the two digital channels (Sect. 3.2). It will be appreciated that only a small proportion of any variable stretch in B applies to the distance from R or W to the capstan, C, so that the relative time displacement at R and W is only slightly influenced. The residual variation may be dealt with electronically by means of a phase lock on the sample and clock pulse generator.

Erase head, E, carrying a d.c. erase current, applies only to the analysis tracks, and ensures that a clean tape is received by the write head, W. Because of this, the writing current can be rather less than that needed for satisfactory 'overwriting' of existing signals; less high frequency loss is therefore experienced.

In use, the *x* and *y* inputs may be provided 'live' or from a recording made previously; in the latter case,

as we have seen, accelerated playback offers the possibility of fast analysis of long, low-bandwidth excerpts. It is often economical and not unduly onerous to reserve two tracks on the acquisition tape, so enabling one to use the same tape transport for both playback and analysis. The other tracks would be recorded either directly or through, say, frequency modulation in the conventional way, and played back slowly to give a 'quick look' graphical output. When a region of interest was reached, a tone burst would be recorded on one of the analysis tracks at a wavelength suitable for subsequent detection.

After a short rewind, the tape would be started at full speed with no erase or writing currents on the 'marked' track; then, as soon as the tone burst was detected, the normal writing process would be started on the analysis tracks, taking signals derived from the information tracks selected.

4. Circuit Function

4.1. System Summary

Figure 6 shows in block form the main component features of the correlator; the *x* channel has been omitted for clarity. Those items for the *y* channel shown in the top and bottom rows are repeated for the *x* channel, with the exception of that marked 'register 1' and the OR gate controlling the up-down counter. In this figure only connections to and from the *x* channel are identified by the letter X.

Before the system is put into action, the tape deck is started and clock pulses obtained at the read head are compared in phase with those from the repetition pulse oscillator. The output of the comparator is used to adjust the frequency slightly so as to cause the relative phase of the pulses to settle at approximately 180 deg.

Both *x* and *y* analogue signals are first amplified to the working level, and then band limited in frequency by a low pass filter before being sampled regularly. The samples are next encoded to provide a three-bit code in which the first bit represents the sign and the remaining two bits the magnitude. Only seven discrete levels are represented by the eight possible combination codes because plus zero and minus zero refer to only one level. Normally zero is represented by 100, leaving 000 to be used for conveying other information (e.g. end of excerpt).

The three parallel bits in each channel are gated by 'three phase' clock pulses to give serial pulse trains which, on the start command, are passed to the write heads for measured periods of time, that for the *x* channel being 10% longer than for the *y*. From now on the 000 code is written until information appears at the read heads. Read signals are then gated into parallel form and staticized in *x* register 2 and *y* register 1 until cleared sequentially under master clock

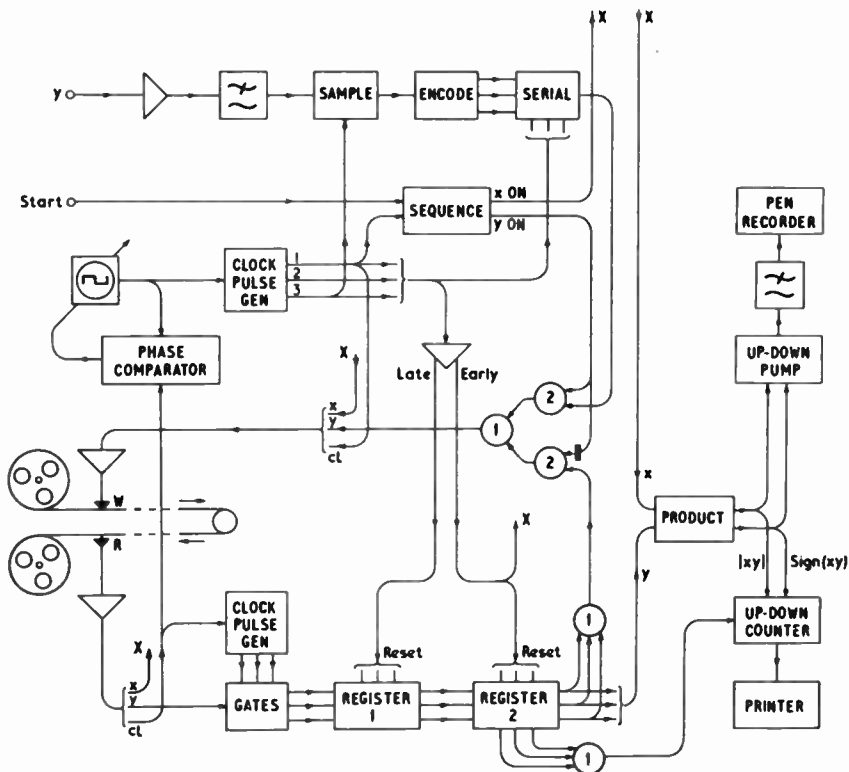


Fig. 6. Block diagram of correlator.

control. The resulting x code, now serial once more, is rewritten directly, accompanied by any code carried by y register 2 (000 at this time). This is quickly followed by the transfer to the latter of the contents of y register 1 which will then be rewritten at the next clock cycle. Thus, we have the one word extra delay referred to earlier on, and have set the two information loops recirculating.

Each time x and y registers 2 are cleared, they pass their codes to a multiplier circuit also, where the product of each word pair is derived. Because only two-bit words are involved, the normally rather slow binary rate multiplier²⁴ may be put to use to give a pulse train whose count at each word cycle is equal to the relevant product. With the product in this form, summation over the excerpt period involves simply adding or subtracting these pulses to or from the existing total in an up-down counter. The sense of the count is, of course, made to correspond to whether the respective signs of x and y are like or unlike.

If the counter has been cleared to zero when the y excerpts starts, the count accumulated by the time it finishes will be a measure of the appropriate correlation coefficient. As soon as the 000 code is detected, a 'print out and clear' instruction is therefore given so that the counter is ready for the next repetition.

Clearly, the excerpt repetition period must be made long enough for these operations to have been completed before the y excerpt reappears.

A visual record of rather lower precision may be obtained economically by causing the output pulses of the multiplier to operate upwards or downwards pump circuits as appropriate which feed the movement of a pen recorder. In this way, the mean current in the meter will furnish a measure of the average product, the dynamics of the movement ensuring that the majority of the fluctuation about the mean is filtered out. Some compromise is needed between the speed of response and the degree of smoothing but, with the full digital print-out available for reference, the consequent deficiency in the visual record is unimportant.

The analysis process continues until stopped, but it will be appreciated that the results are valid only until the finishes of the x and y excerpts coincide; that is, when the relative lag has reached the 10% excess duration given to the x excerpts over the y .

4.2. Detailed Circuit Description

For convenience in dealing with the circuit in more detail, it will be grouped into the following divisions:

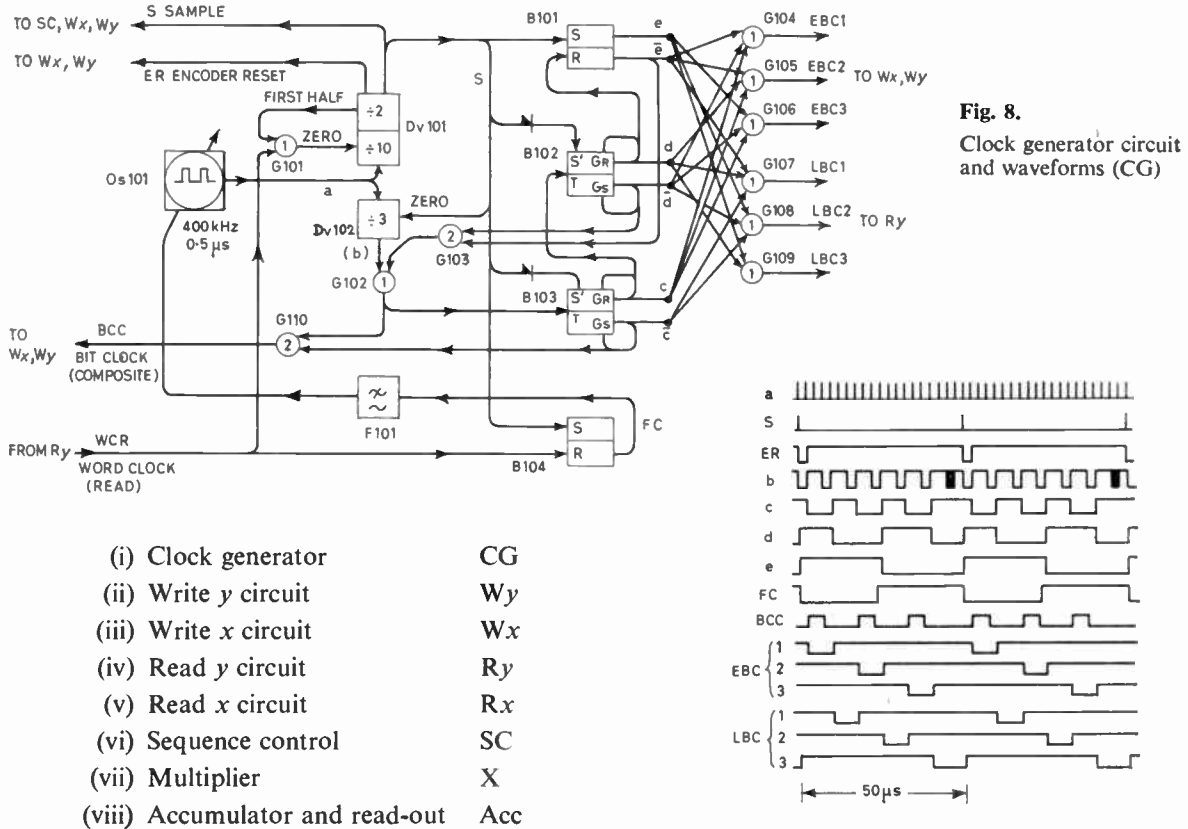


Fig. 8. Clock generator circuit and waveforms (CG)

The logical conventions assumed in their exposition are that '0' corresponds to earth, '1' to a positive voltage, and that changes of state in bistable elements take place when the appropriate input changes from 0 to 1. An asynchronous (i.e. not clocked) mode simplifies some of the clock recovery 'logic' and is adopted throughout.

In (vi) and (vii) the response times required are in many cases appreciably shorter than for (i) to (v), and it may be economic to use logical units of different types (and operating speeds) to suit the differing demands.

Binary stores will take the form of bistable units. Two types are called for; a simple set reset (RS)

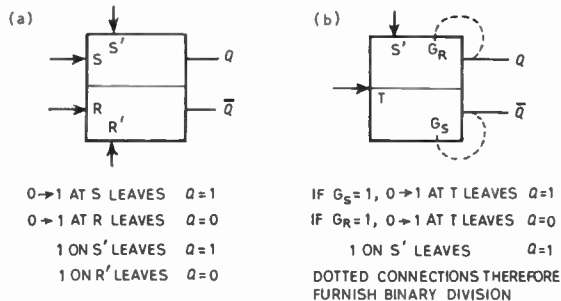


Fig. 7. Convention used for binary stores in logic diagrams.

memory, designated in Fig. 7(a), and the gated transfer device of Fig. 7(b) used for binary division. Nowadays, a variety of logic systems, 'integrated' and otherwise, have come on the market, but not all operating upon the same type of input stimulus. Although it may not apply directly to all, the behaviour of Fig. 7 should be readily achievable using only external connections as appropriate.

The waveforms to be given will be idealized, in that they show infinite rise and fall rates, but will convey adequately the timing of the various circuit functions.

4.2.1. Clock generator, CG

(a) Waveform derivation. This is shown diagrammatically in Fig. 8 together with the corresponding waveforms. A master oscillator, Os101, of slightly controllable frequency, provides a train, a, of 0.5 μs pulses at a repetition rate of 400 kHz. These pulses feed dividers Dv101, which gives an output at every twentieth input pulse (waveform S), and Dv102, which gives an output at one third of the input pulse rate. A second output, ER, is also given by Dv101, the duration being the interval between two pulses, a.

The S pulses pass to the x and y write circuits and control the sampling process; they also serve to start

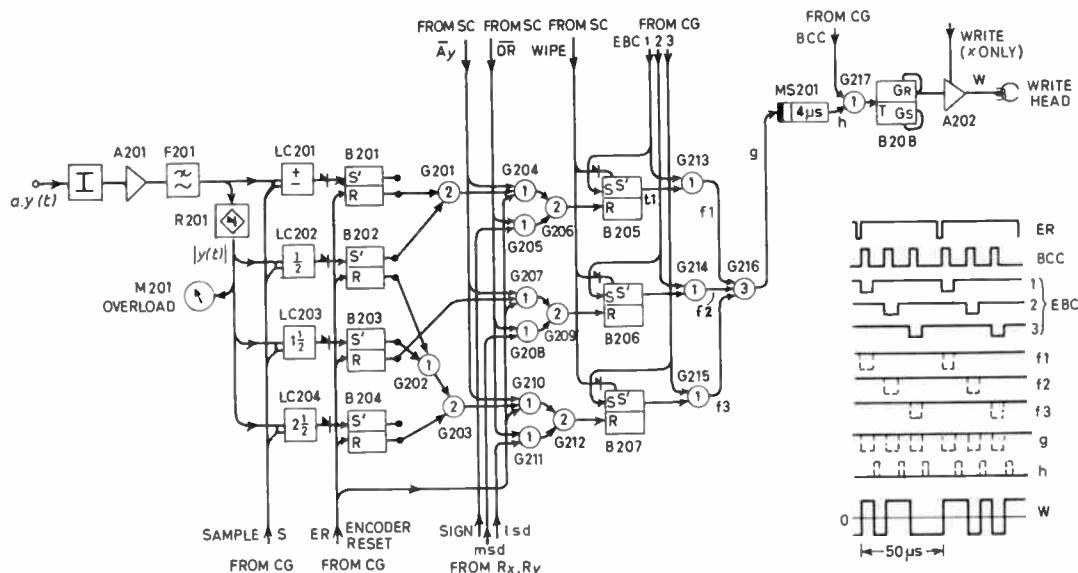


Fig. 9. Encoding and writing circuits, x and y (W_x, W_y).

each timing cycle from a standard condition by setting the bistable circuits B101 to 104. Circuit events are thenceforward controlled by the output of Dv102 which corresponds to waveform b, including the seventh pulse shown filled in. Whilst B101 and 102 are in the 1 condition, gate G103 is inactive, and pulses from Dv102 pass gate G102. Their rising edges trigger B103 into alternating states, giving the waveform, c, whose rising edges in turn cause B102 to alternate, giving waveform d. This output is used to reset B101 after the fourth pulse b.

After the sixth pulse, B101 and 102 are both in the 0 condition and gate G103 is able to give a constant 1 output, rendering G102 insensitive to further downward pulses from Dv102. The result is that B103 receives waveform b with the filled pulse ignored. Because 3 is not a factor of 20, the output of Dv102 would not be in the correct phase for the next word cycle if it were not for pulse S forcing it to the correct starting condition. Thus, in c, the cycle of 50 μ s duration is made up of five intervals of 7.5 μ s and one of 12.5 μ s.

From the waveforms, c, d, e and their negatives, gates G104 to 106 produce early bit clock pulses, EBC1, 2 and 3, and gates G107 to 109 produce late bit clock pulses, LBC1, 2 and 3, used for timing the rewriting of recirculating information. In addition, gate G110 combines b and \bar{c} to give a composite bit clock train, BCC, used in the writing circuits.

(b) *Phase lock.* It will later be seen that the relative timing of the reading and writing processes should be so arranged that the start of a word cycle appearing

at the read head occurs approximately midway through the cycle of the word currently being written. The former event is notified by a short word clock (read) pulse, WCR (Fig. 10), from the y reading circuit and is used to reset B104 to give a rectangular wave, FC, for exerting frequency control upon Os101. Obviously, abrupt changes in the pulse rate are unacceptable, so FC is first smoothed by means of a low-pass filter, F101. If, now, WCR should occur later than normal, the duration of the positive part of waveform FC decreases and the mean control voltage to Os101 drops. This would cause the pulse period to increase and tend to restore the phase relationship.

Unlike the conventional phase lock, the effect of the frequency change will not be felt at the read head until some 9000 words later, but stable functioning is ensured because F101 constrains changes to take place gradually. However, if a sudden phase jump should occur in WCR, the corrective action taken will depend upon the sense of the jump. Provided it is not too great, a forward jump may be disregarded, as the information will not be rewritten until the normal phase of the write cycle.

However, an abrupt lag may cause difficulty if the next word cycle has to start before the multiplying sequence is complete. Accordingly, G101 detects whenever WCR occurs in the second half (notified by the final binary stage of Dv101) of the word cycle, and applies a zero set to the $\div 10$ stage. This delays the start of the next word to the standard time interval after WCR, allowing the full time for the corresponding words to have been read and dealt with.

4.2.2. Write y circuit, W_y

(a) *Encoder.* The circuit configuration is shown in Fig. 9, together with the more important waveforms. The input analogue, $a.y(t)$, is attenuated as necessary to the required level, amplified by A201 and band limited by filter F201. The filtered signal is full-wave rectified in R201 to provide an analogue voltage, $|y(t)|$, monitored by overload meter, M201, which takes current only when $|y(t)|$ exceeds the working range. This current is, however, limited so that overloads, of whatever strength, will all carry the same weight.

Sampling pulse, S , whose duration is $0.5 \mu\text{s}$ and which occurs at the word repetition rate, is used to strobe simultaneously the level comparators LC201 to 204, and set bistable circuits B201 to 204 accordingly. The pulse duration is low, so that any change in $y(t)$ whilst the pulse is on would not be significant. LC201 notifies whether or not $y(t)$ exceeds zero and LC202 to LC204 whether $|y(t)|$ exceeds 0.5 , 1.5 and 2.5 quantum units respectively. Even though the quantization is coarse, the precision of the four threshold levels and the discrimination of the comparators should be no worse than 1% of the full range of seven quantum units, and preferably better.

(b) *Serializer.* Gates G202 and 203 are connected so as to give a 1 output if the less significant digit of $|y(t)|$ is to be a zero, and G201 to give a 1 output if $y(t) < 0$ and $|y(t)| > 0.5q$ (i.e. $y(t) < -0.5q$). These outputs, by saturating gate G204 (207 or 210), prevent the ER pulse affecting the output of G206 (209 or 212). If preferred, the first gate may be looked upon as an AND gate operating upon negated quantities. This manner of connection is called for when it is desired to work from the trailing edge of a pulse; the state during the pulse must then be 0 so that, at the end, there may be a $0 \rightarrow 1$ transition.

Given that input $\overline{Ay} = 0$ and input $\overline{DR} = 1$ (Sect. 4.2.6), the rising edge of ER resets or not bistable circuit B205 (206 or 207) according to whether the other input to G204 (207 or 210) was 0 or 1. This edge also serves to reset B201 to 204. Using the convention of Fig. 7(a), the \overline{Q} outputs of B205, 206 and 207 will thus carry in parallel the code of the current word. This code is serialized by gating the \overline{Q} output of each in turn with EBC1, 2 and 3 in gates G213, 214 and 215 respectively, at the same time restoring the bistable to the set state. The resulting waveforms f_1 , f_2 and f_3 are shown dotted to indicate that they may be present or absent in any one word. They combine in AND gate G216 to give a composite waveform, g , which operates a $4 \mu\text{s}$ monostable circuit, MS201.

Any resulting pulses, h , representing the word code, are combined with waveform BCC in OR gate G217 and the rising edges of its output used to alternate the

state of bistable circuit, B208. Amplifier A202 takes the output of B208 and gives a bipolar writing current, W , to the appropriate write head.

A 'wipe' input from the sequence circuit is able to override all input and recirculated signals and to clear the information loops to 000 words only.

4.2.3. Write x circuit, W_x

This circuit differs from W_y in a few minor respects only:

- (i) A DR input from the sequence unit replaces \overline{Ay} .
- (ii) The magnetizing current of either polarity in the write head remains zero until A202 receives an energizing voltage from the sequence unit. A previously recorded marker tone burst passing the write head would otherwise be largely erased.

4.2.4. Read y circuit, R_y

Figure 10 shows a suitable circuit configuration together with associated waveforms.

(a) *Clock recovery.* According to what code is being conveyed, the waveform at the read head will be of low amplitude whenever intervals between flux reversals are short, and of larger amplitude for the longer intervals† which occur when no data pulse falls between two timing pulses (Fig. 4). To recover the code, the read voltage is therefore amplified, fed to an equalizer, E , to yield a rounded version of the flux waveform and then to a limiter, LM , so as to give a delayed replica, R , of waveform W . Over all codes, the frequency spread of this rounded waveform covers about 3 : 1, so the equalization can be carried out with reasonably straightforward RC circuits. Its operation must be such that, for any possible pulse sequence, the relative time displacement of zero crossings of the output waveform is low.

Pulses of $2.5 \mu\text{s}$ duration are produced at each edge of R by monostable circuits MS301 and 302 and combined in gate G301, giving waveform k . Here the information pulses, once again shown dotted, may or may not be present according to the relevant code. The next task is to obtain a waveform from k in which all the information pulses have been suppressed, leaving only the always-present timing pulses. To this end, monostable circuit MS303 is triggered via OR gate G302 by those rising edges of k which occur more than $10 \mu\text{s}$ after the last one to trigger it. Even if a word such as '111' is present, the lengthened gap after the last information pulse of that word up until the first timing pulse of the following one ensures that the

† Discounting the basic 6 dB/octave rise of head output with frequency, this amplitude effect is a function of pole tip geometry and is not usually associated with a variation of delay with frequency. A 'linear-phase' amplitude equalizer is therefore required.

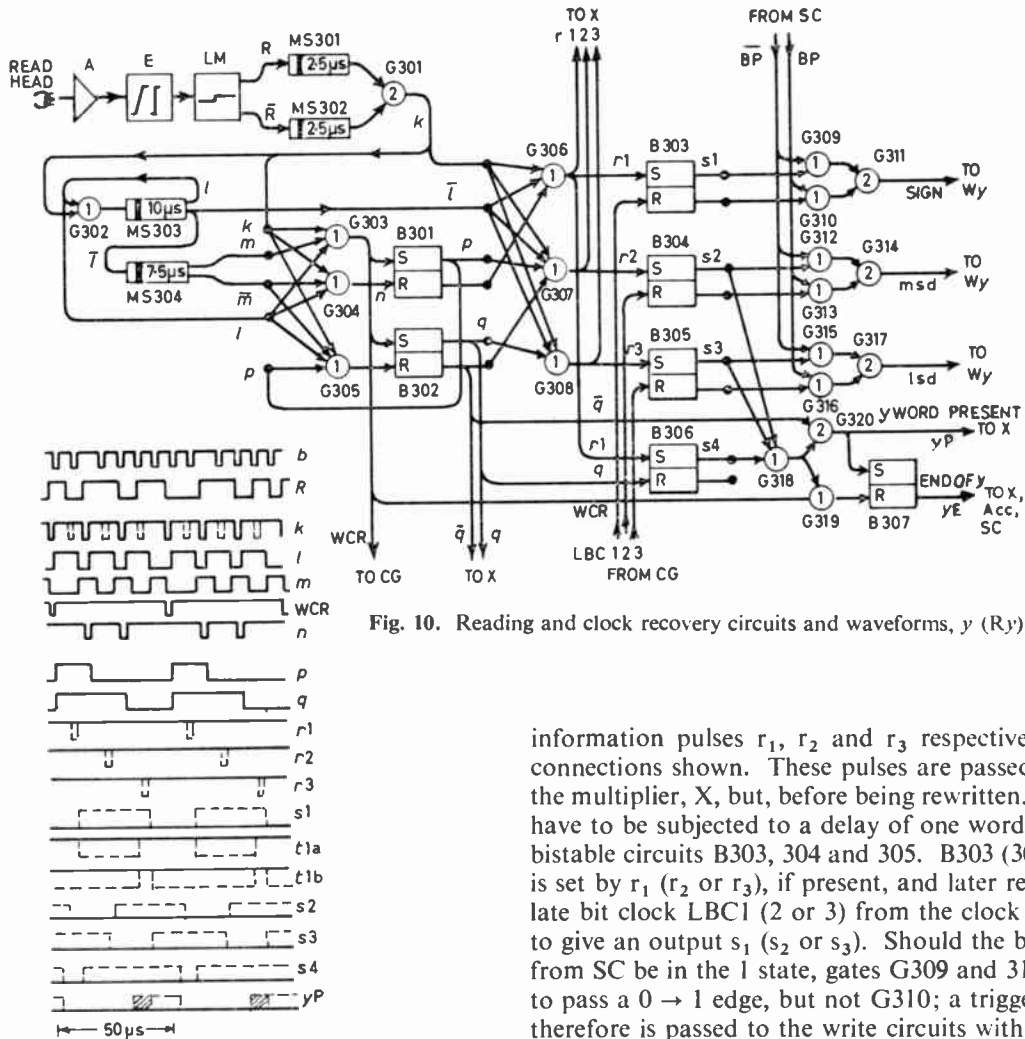


Fig. 10. Reading and clock recovery circuits and waveforms, y (R_y).

correct phase is quickly assumed. MS303 provides a gating waveform, l , suitable for the necessary pulse segregation.

To select, now, the first of the three timing pulses of each word, the recovery of MS303 is made to trigger a $7.5 \mu\text{s}$ monostable circuit, MS304, to produce a further gating waveform, m . Gate G303, fed with waveforms k , l and m gives as output the word clock (read) waveform, WCR, whilst G304 uses \bar{m} to select the alternative timing pulses as shown in waveform n . The WCR pulse is used to set bistable circuits B301 and 302, of which B301 is reset at the end of the first pulse of n , so giving waveform p . Up to now output p had prevented the fall and rise of the first pulse, n , from passing gate G305, and thus the reset of B302 will have been postponed until the next pulse of n . Waveform q results.

(b) *One word delay.* We now have enough gating waveforms for gates G306, 307 and 308 to extract the

information pulses r_1 , r_2 and r_3 respectively by the connections shown. These pulses are passed direct to the multiplier, X, but, before being rewritten, they may have to be subjected to a delay of one word period in bistable circuits B303, 304 and 305. B303 (304 or 305) is set by r_1 (r_2 or r_3), if present, and later reset by the late bit clock LBC1 (2 or 3) from the clock generator to give an output s_1 (s_2 or s_3). Should the bypass line from SC be in the 1 state, gates G309 and 311 are free to pass a $0 \rightarrow 1$ edge, but not G310; a triggering edge therefore is passed to the write circuits without delay. If, on the contrary, the bypass line is at 0, gates G310 and 311 do not pass a $0 \rightarrow 1$ edge until the end of s_1 .

Turning back to Fig. 9, we see that, via gates G205 and 206 (suitably conditioned), a $0 \rightarrow 1$ edge in s_1 will reset B205 only recently cleared to MS201 by EBC1. B205 thus gives an output t_{1a} in the bypass case, but gives t_{1b} (Fig. 10) when the delay is not to be bypassed. Comparing t_{1a} and t_{1b} , it will be seen that, for a given t_1 pulse present, the resulting $0 \rightarrow 1$ transition at G213 occurs one word period later in t_{1b} than it does in t_{1a} .

The presence of r_2 and r_3 pulses causes similar transfer processes to the writing circuits, in parallel and time echelon in B206 and 207. The outputs of G213 to 215 merge in G216 to give a serial regenerated word at MS201.

It will be seen from s_1 and s_3 (Fig. 10) that the clearing of B303 may quite possibly occur before B305 has been set, depending upon the relation of the write and read phases. In order to have all three digits of each word available simultaneously for a short time,

Fig. 11. Reading circuit, x (R_x)

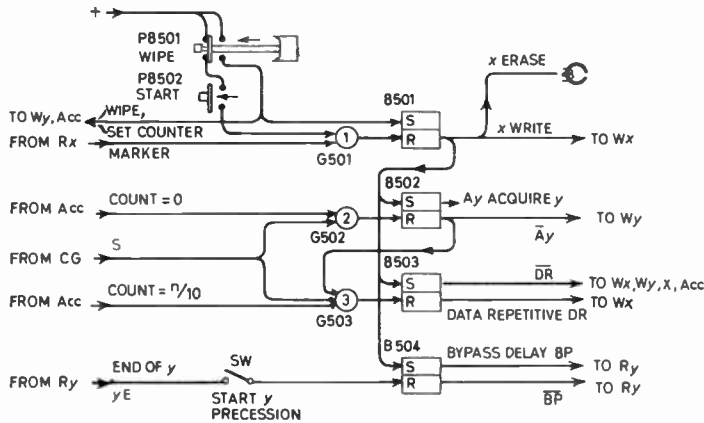
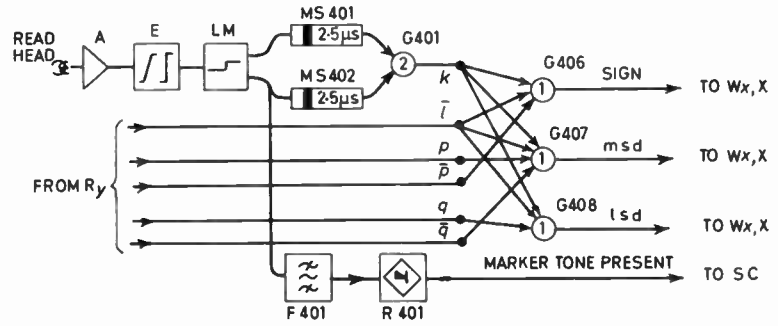


Fig. 12. Sequence control circuit (SC).

r_1 also sets bistable circuit, B306, which is in turn reset by waveform q , whose phase is entirely associated with the read signal. B306 gives an output, s_4 . In the presence of any one of s_2, s_3 or s_4 , gate G318 gives an output, curtailed in duration by \bar{q} via gate G320, to give a 'y present' pulse, yP , whenever a code which is not 000 is being handled.

The presence of a 000 code is detected by gate G319 to give a rising edge at the end of WCR. This edge nominally coincides with the falling edge of s_4 which could, in principle, deform the reset input to B307. However, the inherent delay in B306 allows WCR to have risen before s_4 falls. If insufficient margin for read/write phase error is afforded between WCR and the fall of s_2 , an inverter following G319 will make B307 sensitive to the leading rather than the trailing edge of the pulses. Bistable circuit B307 serves to remember that yP pulses have occurred until such time as it is cleared by a 000 code. It then produces a 1 output, yE , signifying 'End of y'.

4.2.5. Read x circuit, R_x

The circuit (Fig. 11) differs from R_y in respect of:

- (i) Waveforms \bar{l}, p and q can be obtained from R_y , provided the relative time displacement between the two tracks is small. This is readily assured by giving them adjacent locations across the tape.
- (ii) Pulses r_1, r_2 and r_3 pass direct to W_x and no delay system of B303 to 305, etc., is required.

- (iii) A tone burst detector circuit is added.

If a tone burst is to be used as marker to initiate the correlation process (Sect. 3.3), it is not permissible to put it on the y track which, prior to the start, is carrying and recirculating clock pulses, and whose erase head is therefore energized. However, the x track is available, and we have seen that provision has been made to put the write head current to zero so that it does not erase the tone.

The limited, amplified read signal is accordingly fed (Fig. 11) to a bandpass filter, F401, centred at about 6 kHz, to select any large amplitude tone of that frequency. This is passed to full wave rectifier R401 to give a suitable 'start' signal to the sequence control circuit. At the time when the location was originally marked by a tone burst, the tape would have had to be travelling much more slowly than 60 in/s and the impressed frequency would then have been that corresponding to a wavelength of 0.01 in.

4.2.6. Sequence control, SC

The circuit shown in Fig. 12 serves to ensure that the various functions can take place only when desired and that they should follow the correct sequence.

First of all the tape is rewound to some way in advance of the starting place and then set in forward motion. Push button PB501 is operated and passes a wipe signal to W_y , sets the starting value of the accumulator and sets bistable circuit B501. A dash-pot arrangement or its electrical equivalent delays the

restoration of PB501 until at least a full excerpt repetition period has gone by. Thereafter, push button PB502 is energized ready for use.

The arrival of a tone burst, or the operation of PB502, resets bistable circuit B501 via G501, and the resulting output restores the x write and erase circuits to normal. It also puts bistable circuits B502, 503 and 504 into the set state. Thus the 'acquire y ', Ay , output of B502 becomes 1 and the 'data repetitive', DR, of B503 becomes 0. The 0 signal of \overline{Ay} is sent to Wy (Fig. 9) where it connects the writing circuits to the encoding circuits, and the 0 state of DR performs the same duty for Wx .

In a manner to be described later, the number of words being written is counted in the accumulator circuit from a preset negative value and, when the amount registered reaches zero, an enabling signal is received by gate G502 and, at the next S pulse, B502 is reset, causing only '000' y words to be written henceforward. G503 is now ready for the time when the accumulated count reaches one tenth of the preset value, when it passes the following S pulse to reset B503, and so puts Wx and Wy to 'recirculate'. In this way the x excerpt is made 10% longer than the y excerpt as explained in Sect. 4.1.

During this time B504 has been sending Ry a 'bypass' signal (Fig. 10) and this is not cancelled until the y excerpt has been read through completely and has just finished. The yE signal from B307 serves to reset B504 (provided switch Sw is closed) and so removes the bypass of the one word delay. Sometimes, however, it is convenient to keep the relative delay zero (e.g. whilst the pen recorder movement settles initially, during system calibration, or whilst checking for tape drop-outs), and this is easily arranged by leaving Sw open. It should preferably be closed during a y repetition which may be identified from an oscilloscope monitoring the waveform h or an indicator fed by yE .

4.2.7. Multiplier, X

The x and y codes, read simultaneously, are passed in parallel form to the multiplier circuit shown in Fig. 13 where they are held in bistable registers. The respective sign digits (r_1 in Fig. 13) set B601 and 602 whose outputs are combined in the half-adder G608 to 613 to give one or the other of two outputs, according to whether the signs are like or unlike. These pass to the accumulator to determine the sense of pulse counting.

Bistable circuits B608 and 609 are set by the more and less significant bits of $|y|$ (r_2 and r_3 of Fig. 10) respectively, and the outputs later used to operate pulse gates G617 and 618. The remaining bistables, B603 to 607, are arranged with associated gates, G604

to 607, to form a subtractive binary counter, with r_2 and r_3 of $|x|$, inverted to give positive pulses, setting B604 and 605 respectively. B603 has previously been set into the 1 state by the 1 state of waveform q .

When q falls to 0, and \bar{q} consequently rises, the effect is postponed in gates G602 and 603 for 8.5 μ s by the operation of an inhibiting monostable circuit, MS601, so as to give time for any r_3 pulse to have registered. When fresh data are being written, the \overline{DR} input will be present but, if instead the y excerpt is being read, the yP input will be present for the relevant part of the word cycle; either way, gate G602 will receive an input via G601. Because B603 is in the set state, the content of the counter is not zero, and gate G616 provides the remaining input to gate G602, which therefore energizes the 2.5 MHz pulse generator, Os601, as soon as MS601 relaxes.

Pulses u now start to count the contents of B603 to 607 towards zero, carry pulses $v(c)$ and $w(c)$ operating B606 and 605 respectively. Now, u pulses gated by the other outputs of B607 and 606 may be termed 'non-carry' outputs and, according to the code of $|y|$, gates G618 and 617 produce waveforms v (n.c.) and w (n.c.).²⁴ For every four u pulses, there are two non-carry v pulses and one non-carry w and, to count $|x|$ down to zero, there would need to be $4|x|$ pulses. Thus, we will have $2|x|$ non-carry v pulses and $|x|$ non-carry w pulses. Clearly, if these are gated by the more and less significant bits of $|y|$ respectively, the total number of non-carry pulses will be $|xy|$. These are non-coincident and may be merged in gates G620 and 621.

Now, the count started with B603 set to 1 so, after $12|x|$ pulses u , the counter will have reached the 10000 state. This is detected by gate G614, which passes a signal via G615 and G603 to clear B601, 602, 608 and 609. B601 and 602 are now in a 'like' state, so G610 provides a 1 output. B608 and 609 no longer energize G617 and 618, and no further non-carry pulses are transmitted. (It should be noted that this 10 000 state is the starting point of the count cycle when the x and y excerpts are first being written in and only 000 codes have yet reached the read head.)

A further 16 pulses u are now required for the total to reach the 00000 from the 10000 state, when the output of G616 (and therefore of G602) falls to 0, and Os601 ceases to pulse. During this phase, G615 had been maintained by the negated output of B603 in the 0 state, and thus these 16 pulses were able to pass gates G619 and 620 on their way to Acc.

The maximum number of pulses required to reach to 00000 state will be seen to be $16 + 12 = 28$, which occupy $28 \times 0.4 = 11.2 \mu$ s. It will be appreciated, then, that the complete counting phase has finished by the time \bar{q} or yP revert to 0.

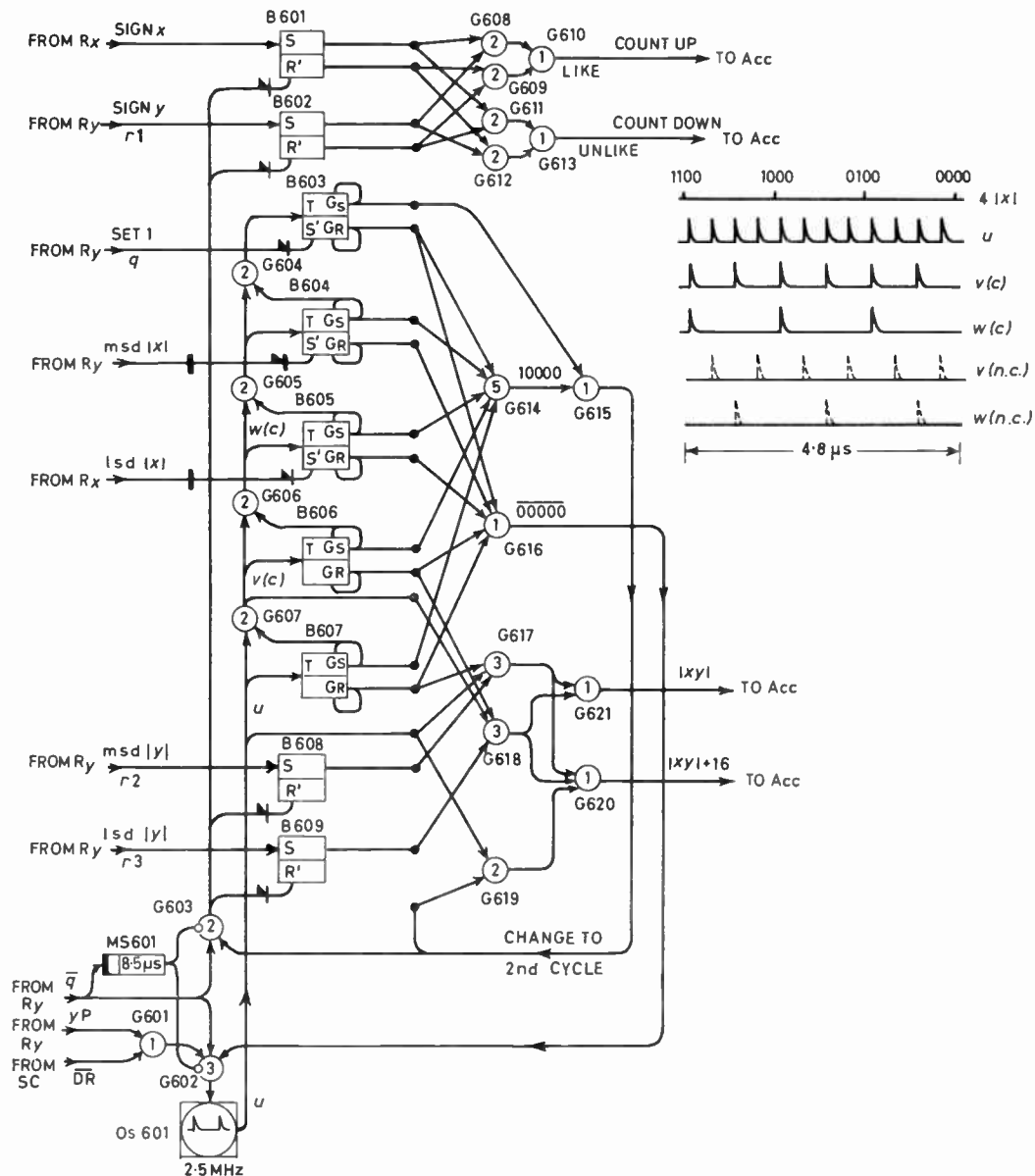


Fig. 13. Binary rate multiplier circuit and waveforms (X).

4.2.8. Accumulator, Acc

(a) *Digital summation.* This circuit, shown in Fig. 14, sums each individual product, xy , and delivers the total for each successive repetition. By also determining the lengths of the x and y excerpts, it ensures that the calibration remains the same should a correlation be repeated.

Bistable stages B701 to 704, together with associated gates G701 to 711, comprise a bidirectional 16 : 1 divider giving upward overflow pulses from G701 and downward from G702. The former pulses pass,

via G712, to a 10 : 1 divider, Dv701, which in turn feeds another, Dv702, comprising three decimal stages followed by a binary stage at the most significant end. Numerical displays are associated with Dv702, that for the binary stage reading 0 or $\bar{1}$.

Manual switches, Sw701, are provided for adjusting the length of the y excerpt so that, when the wipe push button PB501 (see Fig. 12) is operated at the start of the correlation procedure, a signal passes via G713 which sets in ($\bar{1} + \text{comp } n$) at Dv702. This is, of course, the equivalent of $-n$. During the initial writing phase

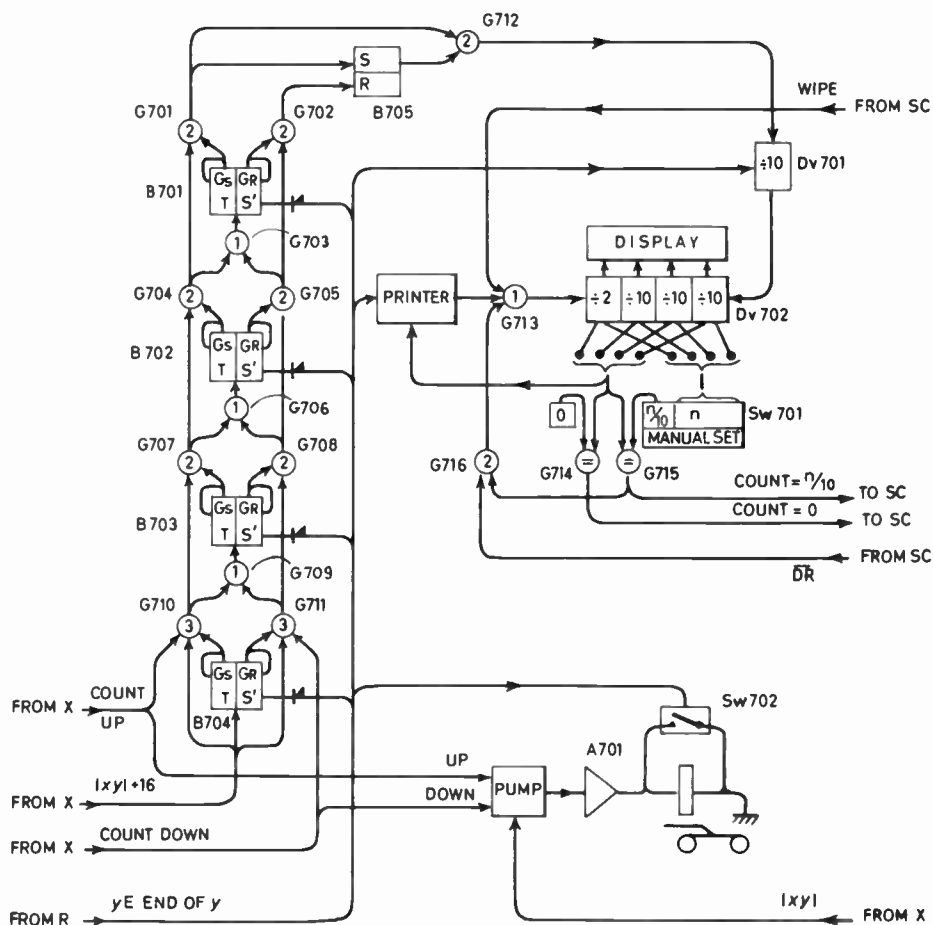


Fig. 14. Accumulator and read-out circuit (Acc).

the multiplier delivers only 16 pulses in the upwards sense at each word, there being no product xy . After the requisite number of y words, the count in Dv702 will have reached zero and gate G714 accordingly signals the sequence control circuit to suspend the writing of y words. When the count reaches $0.1n$, another signal is given, this time by gate G715, to stop the x words also. At the same time, it passes G716 and 713 to reset Dv702 to $(\bar{I} + \text{comp } n)$ ready for correlation. The DR signal immediately afterwards falls to 0 and G716 thereafter blocks any further response to a count of $0.1n$.

Once information starts to recirculate, the output of the multiplier at the r th word becomes $(16 + x_r y_r)$, in which the second term may be positive or negative, but will not exceed 9. Clearly, there is a preponderance of upward counting, and those stages beyond the first 16 : 1 reduction need provide unidirectional counting only. This greatly simplifies their carry arrangements

and invites the use of a commercially-available decimal instrument.†

Occasionally, an opportunity for false operation could arise; consider the situation when, towards the end of a counting cycle, G701 gives an upward overflow and the next word produces a substantial downward count. As a result the count in B701 to 704 will fall below zero and G702 will give a downwards overflow pulse. However, the 'negative' pulses are quickly followed and exceeded by 16 'positive' ones and G701 again gives an upward overflow although, at that time, the input increment would, in fact, be zero. To remedy this, bistable B705 is arranged to remember

† During a given $50 \mu\text{s}$ interval, Dv701 may receive up to two pulses separated by $6.4 \mu\text{s}$; if it comprises a 2 : 1 stage followed by a 5 : 1, the latter will receive no more than one pulse every $50 \mu\text{s}$, a rate within the capabilities of modern, neon-filled, decade stepping tubes. Hydrogen-filled types²⁵ will, of course, accept pulse intervals of much less than $6.4 \mu\text{s}$.

the occurrence of a downward overflow and to suppress the next upward one at gate G712. The maximum number of consecutive downward pulses is nine, so a downward overflow is invariably followed by an upward one, and the unit storage capacity of B705 is sufficient.

When the last word of the y excerpt has passed, no further pulses arrive from the multiplier and, if all the product xy had been zero, the supplementary 16 pulses would have brought the displayed total to exactly zero. With finite xy , then, the algebraic total will be correctly displayed, negative numbers by a characteristic of \bar{I} with a positive 'mantissa'.

A yE signal initiates a print-out cycle and clears B701 to 704 and Dv701, followed by a reset signal via G713 to Dv702 from the printer when the print-out cycle is complete.

Suppose all 9000 words of x and y to be $+3$ or, alternatively, -3 ; the total count in the accumulator would therefore be $\pm 81\,000$. This, divided by 160, corresponds to a displayed total of $\bar{I}493$ or 0506. These represent 'full scale' but, in practice, the value of $|xy|$ will often be less than nine and the total displayed is more likely to fall between $\bar{I}850$ and 0150. This precision matches that expected of the correlation (see Sect. 4.2).

Of course, the number printed out is proportional, though not equal to, the average value. However, the averaging time is known and fixed, so the system is amenable to calibration. Switch Sw of Fig. 12 may be left open, and known simple periodic signals (e.g. triangular or sine waves, *not* rectangular waves) applied to the x and y input terminals. The resulting output will not change and may be used to derive the calibration constant.

(b) *Graphical output.* To provide a pen record to supplement the digital print-out, it would be possible to provide digital storage of the accumulated total followed by a digital/analogue convertor to operate the pen movement. The precision of the quantities being dealt with, however, hardly justifies the equipment required, and the following analogue arrangement is more in keeping.

Each product $|xy|$ is fed in its pulse form from G621 (Fig. 13) to a pump circuit which releases a fixed amount of charge at each input pulse. The polarity signals are arranged to steer these packets of charge into or out of amplifier A701 supplying the movement of the pen recorder. The inertia of the movement together with damping serve to reduce the ripple superimposed upon the mean deflection and, so long as the information repetition period does not vary, the latter provides a useful measure of the variation from one correlation coefficient to the next.

The ripple caused by the periodic loss of torque at the end of each y excerpt may be reduced without the need for a large natural period for the movement. Switch Sw702 (which could take the form of a symmetrical transistor) is energized by the yE signal to place a short circuit across the meter coil. The circulating current, set up as the movement seeks zero, maintains the torque through the gap in supply current, and the deflection hardly changes.

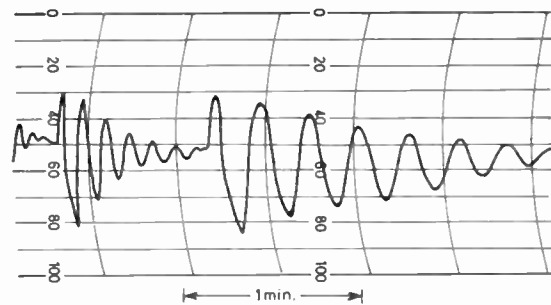


Fig. 15. Autocorrelograms of noise in damped resonant circuit.

Figure 15 shows two autocorrelograms of the voltage across a parallel LC circuit fed by wide-band, approximately white noise through a series resistor. Changes in component values give rise to changes in both natural period and damping. The derivation of the left-hand correlogram occupied roughly 55 seconds.

5. Discussion

5.1. Static Core Storage

The instrument described is particularly suited to the off-line correlation of signals which are, or could be, acquired and stored most conveniently on magnetic tape, possibly at a very different speed from that used for analysis. Here, a single device provides both the play-back and the sequential storage, etc., required for correlation.

In some applications, the signals are available 'live', and the intermediate step of tape storage is not necessary. The present-day economics of core stores are such that a case can be made for the use of a random access structure even for what are essentially sequential access operations. For this purpose, each word may remain in parallel form and the read/write processes are timed from a common reference clock. This, incidentally, eliminates the need for staticizer, serializer, clock recovery and phase lock circuits, with obvious economy. The address registers may be connected as sequential counters so that information is inserted and extracted successively from adjacent addresses. There is also a much greater freedom of choice of clock rate and, therefore, in the ratio of acquisition to analysis time.

5.2. Information Bandwidth

Let us compare the bandwidth of the analogue and digital channels on the tape, assuming a maximum resolvable frequency at the playback head of f_m . Taking the conventional deviation of $\pm 40\%$ for tape f.m., the carrier centre frequency would be $f_m/1.4$ corresponding to a signal cut-off (-0.5 dB) at $0.123 f_m$. The maximum frequency, f_m , would also correspond to two $7.5 \mu\text{s}$ intervals in Fig. 8, so the word rate would be $(15/50)f_m = 0.3 f_m$. The maximum permissible component frequency of the signals to be analysed would be less than half the above, say $0.125 f_m$. This is comparable with the above figure, although we could reasonably expect to utilize components beyond the -0.5 dB point, and still sample them correctly. For the parameters adopted, then, the p.c.m. bandwidth is slightly inferior to f.m., and would require a corresponding increase of packing density before it could give a close match.

5.3. Alternative Clocking

The reasons leading to the use of self-clocking were given in Section 3.1. Nevertheless, it is possible to adopt the code described and yet eliminate the clock recovery circuits of Fig. 10 should circumstances require it. A third track on the tape, placed between the two data tracks, could be made to carry a suitable, common timing signal. Extra read and write circuits and heads would, of course, have to be provided.

5.4. Tape Speed Flutter

The signals played back from a continuous loop in the type of recorder described in Section 1.2 have suffered from the cumulative effect of speed imperfections on two recording and two playback occasions. Those instruments in which subsequent re-recording of one channel is used to provide coarse lag increments will accumulate further flutter in the signal.

With p.c.m., on the other hand, the samples of the signal were taken at intervals determined by a stable clock generator, and repeated subsequent displacement in and correction of bit timing will have no effect. The total flutter to be expected arises, therefore, from one recording and one playback occasion only.

At each repetition, the appropriate value of lag is in no way dependent upon a known physical separation along the tape, or upon its time equivalent. Such dependence applies to the travelling head types of correlator, and attention is necessary in their design to minimize fluctuations of tape tension. The resulting variable tape stretch would coarsen the resolution of the measure, τ , of lag, corresponding to a loss of high frequency components of the input functions. In contrast, the lag in the digital case is equal to the word period, $\Delta\tau$, multiplied by the (integral) number of repetitions completed: both robust quantities.

5.5. Accelerated Playback

If digital information is in continuous recirculation, and the sampling and encoding processes lead to the 'up-dating' of appropriate words, we can, in principle, use our device in a different acquisition mode. By sampling at intervals of one word period greater than a whole number of recirculation cycles, we can obtain a 'time compressed' replica of the input function.^{17, 20} This method is appropriate where the propagation rate down the serial store cannot be varied. However, by making the original recording of the time function at a very low tape speed and playing back fast, the same goal is achieved with lower tape consumption. With a thin film or ferrite core store, of course, there are no low restrictions on the rate at which the store may be filled, and the difficulties in maintaining low tape speed flutter at low tape speed do not arise.

5.6. Precision

The statistical nature of the expected inputs to a correlator results in the output function being less regular than the results from coherent test signals might have led one to expect. Furthermore, analysis of a different excerpt will usually lead to an only approximately repeated result. Generally, the precision varies inversely as the square root of the population size,²³ so a compromise usually has to be struck between the time devoted to the experiment and the expected precision. For most purposes, results to within a few per cent are acceptable, and this makes no great demands on the linearity and stability of the signal handling circuits, culminating as they do in analogue/digital convertors. Demands would have been rather greater if the circuits had remained analogue throughout, including multiplier and integrator.

6. Acknowledgments

Thanks for interest shown are due to Dr. E. L. C. White, Chief Scientist, E.M.I. Electronics Ltd., by whose permission this work is reported. The practical assistance of W. D. Gilmour in constructing an experimental correlator to prove the method is also gratefully acknowledged.

7. References

1. J. G. Henderson and G. J. Pengilly, 'Experimental determination of system transfer functions from normal operating data', *J. Brit. Instn Radio Engrs*, 18, p. 179, March 1958.
2. J. G. Balchen and E. Blandhol, 'On the experimental determination of statistical properties of signals and disturbances in automatic control systems', 'Automatic and Remote Control' (ed. J. F. Coales). Proceedings of the 1st International Congress of the International Federation of Automatic Control, Moscow, 1960, Vol. 2, p. 788 (Butterworths, London, 1961).
3. F. D. Boardman, E. L. E. Harrington and D. J. A. Carswell, 'A correlator for investigating random fluctuations in nuclear power reactors', *The Radio and Electronic Engineer*, 30, No. 3, p. 161, September 1965.

4. A. N. Burd, 'Correlation techniques in studio testing', *The Radio and Electronic Engineer*, **27**, No. 5, p. 387, May 1964.
5. C. L. Gilford and M. W. Greenaway, 'The application of phase coherent detection and correlation methods to room acoustics', B.B.C. Engineering Division, Monograph No. 9, November 1956.
6. H. J. Jones and J. A. Morrison, 'Cross-correlation filtering', *Geophysics*, **19**, No. 4, p. 660, October 1954.
7. F. N. Tullos and L. C. Cummings, 'An analog seismic correlator', *Geophysics*, **26**, No. 3, p. 298, June 1961.
8. J. S. Barlow, 'Autocorrelation and cross-correlation analysis in electroencephalography', *Trans. Inst. Radio Engrs on Medical Electronics*, ME-6, No. 3, p. 179, September 1959.
9. R. B. Blackman and J. W. Tukey, 'Measurement of power spectra', *Bell Syst. Tech. J.*, **37**, p. 185, January 1958.
10. K. N. Stevens, 'Autocorrelation analysis of speech sounds', *J. Acoust. Soc. Amer.*, No. 22, p. 769, November 1950.
11. K. W. Goff, 'An analog electronic correlator for acoustic measurements', *J. Acoust. Soc. Amer.*, **27**, p. 223, March 1955.
12. A. R. Billings and D. J. Lloyd, 'A correlator employing Hall multipliers applied to the analysis of vocoder control signals', *Proc. Instn Elect. Engrs*, **107**, Pt. B, p. 435, September 1960.
13. R. V. Mathews, 'Data reduction—analogue or digital', *International Conference on Magnetic Recording*, p. 55. (I.E.E., London, 1964).
14. L. M. Saper, 'On-line auto- and cross-correlator realized with hybrid computer techniques', *International Convention Record of the I.E.E.E. Bio-Medical Electronics Session*, **11**, Part 9, pp. 120–130, 1963.
15. W. M. Goodall, 'Telephony by pulse code modulation', *Bell Syst. Tech. J.*, **26**, p. 395, July 1947.
16. J. D. Balcomb, H. B. Denmuth and E. P. Gyftopoulos, 'A cross-correlation method for measuring the impulse response of reactor systems', *Nuclear Science and Engineering*, **11**, No. 2, p. 159, October 1961.
17. W. W. Scanlon and G. Lieberman, 'Naval ordnance and electronics research', *Proc. I.R.E.*, **47**, p. 910, May 1959.
18. D. G. Watts, 'A general theory of amplitude quantization with applications to correlation determination', *Proc. I.E.E.*, **109**, Pt. C, p. 209, March 1962.
19. B. Widrow, 'A study of rough amplitude quantization by means of Nyquist sampling theory', *Trans. I.R.E. on Circuit Theory*, CT-3, p. 266, December 1956.
20. W. B. Allen and E. C. Westerfield, 'Digital compressed-time correlators and matched filters for active sonar', *J. Acoust. Soc. Amer.*, **36**, p. 121, January 1964.
21. W. F. Sheppard, 'On the calculation of the most probable values of frequency-constants, for data arranged according to equidistant divisions of a scale', *Proc. London Math. Soc.*, **29**, p. 353, 1898.
22. A. Gabor, 'High-density recording on magnetic tape', *Electronics*, **32**, p. 72, 16th October 1959.
23. J. S. Bendat, 'Principles and Applications of Random Noise Theory', Chapter 7 (John Wiley, New York, and Chapman & Hall, London, 1958).
24. Y. Lundh, 'Digital techniques for small computations', *J. Brit. Instn Radio Engrs*, **19**, p. 37, January 1959.
25. K. Apel, 'A 1 Mc/s bi-directional gas-filled counting tube', *The Radio and Electronic Engineer*, **28**, No. 3, p. 147, September 1964.

Manuscript first received by the Institution on 19th July 1965, and in final form on 9th December 1965. (Paper No. 1066/EA31.)

© The Institution of Electronic and Radio Engineers, 1966

A Three-Cavity Refractometer and Associated Telemetry Equipment

By

C. S. FOWLER, C.Eng.
(Member)†,

R. J. B. CHAMPION (Graduate)†

AND

J. N. TYLER†

Summary: The paper describes the construction and performance of a microwave, spaced-cavity refractometer designed for the measurement of the small-scale variations of refractive index in the lower atmosphere. The instrument has been used on a captive balloon at heights up to 2.5 km with telemetry equipment transmitting, to a ground station, information on variations in refractive index, temperature, wind speed and pressure.

1. Introduction

Measurements of the small-scale variations of refractive index in the lower atmosphere are an important requirement in research on tropospheric radio wave propagation. In forward-scatter experiments and in vertical-incidence radar soundings it is necessary to determine the differences in refractive-index which occur over vertical and horizontal distances of a few centimetres to a few metres. The equipment described in this paper was designed to measure these differences. It has been used on a captive balloon for soundings up to a height of 2.5 km.

Microwave refractometers operate by measuring the change in the resonant frequency of a microwave cavity through which the air passes and a second, closed cavity is generally used as a reference. The refractometer design described in this paper is a development of that due to Birnbaum,¹ modified to make provision for three microwave cavities.² These cavities are connected in two pairs and with each pair a measurement is made of the difference of the refractive index of the air in the cavities. Several different arrangements of the cavities are possible. With two in a horizontal line and the third below one of them (all open and in a plane normal to the wind direction) measurements of the differences in refractive index in the horizontal and vertical directions can be made simultaneously. This arrangement gives information on the degree of anisotropy in the fine-scale structure of refractive index. Two difference measurements can also be made with the three cavities in line vertically, or horizontally (in line with or perpendicular to the wind direction), and the results can be compared with theoretical values derived from analyses of the spectral properties of turbulent motion. If necessary, one of the cavities can be closed to give a measurement of the total variance in refractive index combined with a difference measurement. If the variance in refractive index measured by two open

cavities 1 m apart is $\overline{\Delta N_1^2}$ and the total variance, measured by an open and closed pair, is $\overline{\Delta N_t^2}$ then the value of the spatial correlation function for a distance of 1 m, ρ_1 , is given by

$$\rho_1 = 1 - \frac{\overline{\Delta N_1^2}}{2\overline{\Delta N_t^2}} \quad \dots\dots(1)$$

If a specific form is assumed for the correlation function, then the scale size (distance at which $\rho = 1/e$) of the irregularities can be estimated, and this is an important requirement in theories of tropospheric propagation.

Adjacent cavities in any configuration can be spaced by distances of 0.1 to 1 m. Changes in refractive index of 1 part in 10^7 occurring at frequencies up to 30 Hz can be recorded.

2. Principle of Refractometer Operation

A block diagram of the refractometer is shown in Fig. 1 and Fig. 2 shows the three cavities in a triangular array. The cavities were constructed from special invar (prepared for this requirement by the Metallurgy Division of the National Physical Laboratory) having a temperature coefficient of expansion of about 0.4 parts in 10^6 per deg C, approximately one third of the value for commercial specimens of invar. The invar was gold-plated to minimize corrosion of the cavity walls which would reduce the Q -factor. The end-plates of the cavities were constructed with about 90% of the cross-sectional area removed to allow free movement of the air through the cavity. This type of cavity is an improvement on that described in a previous paper, the modified design being based on work carried out at the National Bureau of Standards, Boulder, Colorado. A sketch of an end-plate is given in Fig. 3. The removal of part of the end-plates in cylindrical cavities has the effect of lowering both the Q -factor and resonance frequency. The radial thickness of the ring (shown in Fig. 3) and the distance it projects axially from the cavity were determined empirically to reduce fringing effects to a minimum and to obtain a Q -factor of the order of 7000 with the maximum amount of material removed from the end-plate.

† Science Research Council, Radio and Space Research Station, Slough, Buckinghamshire.

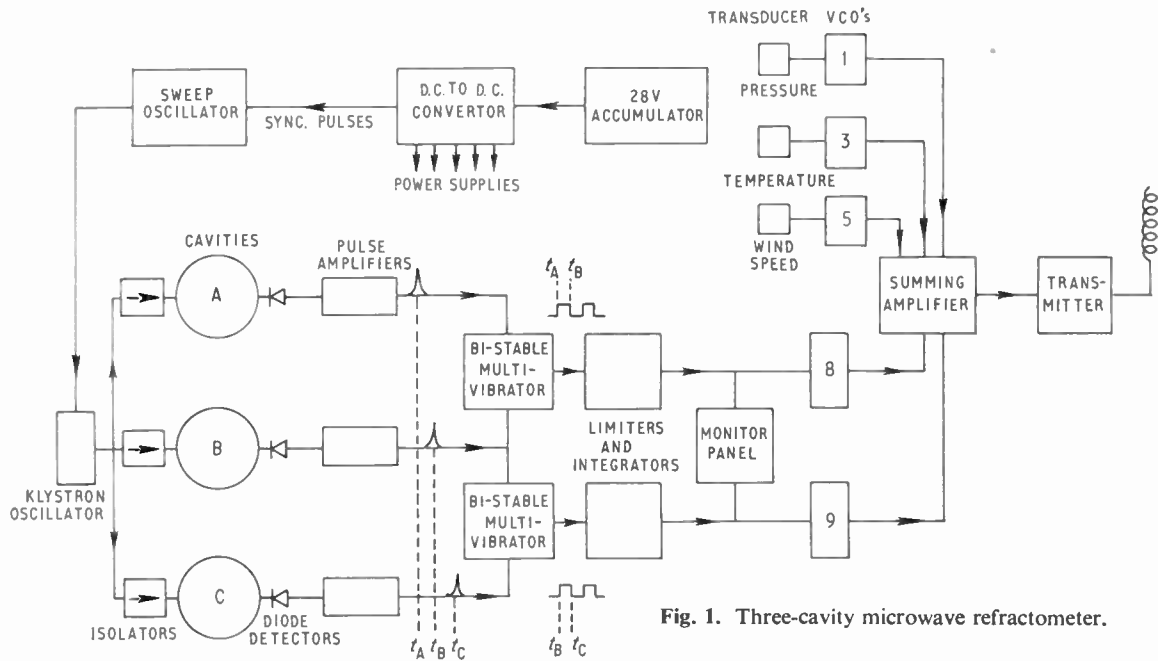


Fig. 1. Three-cavity microwave refractometer.

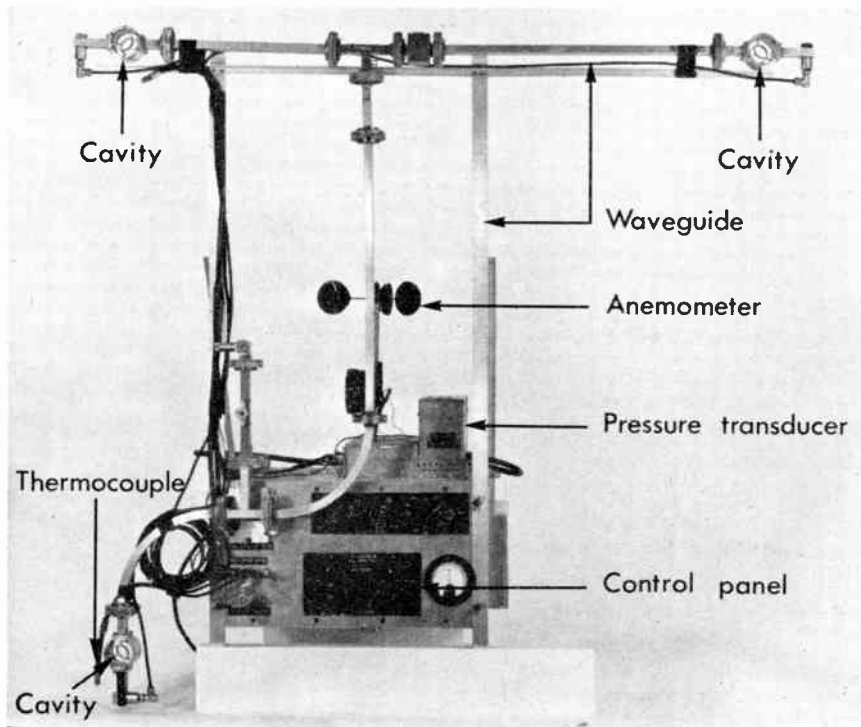


Fig. 2. The three cavities arranged in a triangular array and the associated equipment.

The nominal resonance frequencies of the cavities used are 9455, 9452 and 9449 MHz (cavities A, B and C respectively). The resonance frequencies of A and C can be compared simultaneously with that

of B the reference cavity. The change in the resonance frequency of a cavity, Δf , is related to the change in refractive index n , thus: $\Delta f/f = -\Delta n/n$. In terms of N units [where $N = (n-1)10^6$] we have, at a centre

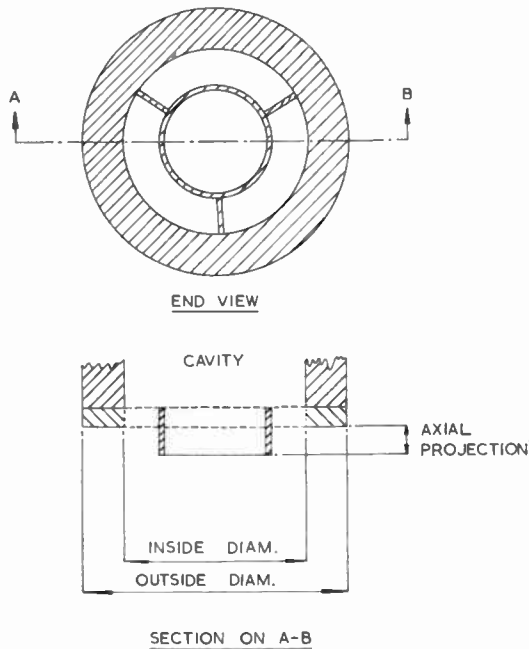


Fig. 3. Cavity end-plates.

frequency of 9.45 GHz, $\Delta N = -106\Delta f$, where f is in MHz.

The cavities are connected to a klystron oscillator by waveguides containing ferrite isolators which attenuate any reflected power by about 20 dB. The isolators minimize the effects of mismatched impedances on the klystron oscillator and of coupling between the cavities. The klystron is frequency-modulated by means of a saw-tooth voltage applied to the reflector and was chosen to have a frequency-versus-voltage characteristic which was linear over as large a frequency range as possible—of the order of 30 MHz.

The resonant condition in each cavity is detected by a crystal diode loosely coupled to it. The pulses are amplified and differentiated to form trigger pulses, the timing of which in relation to the maximum of the resonance response is made independent of input amplitude over a range of at least two to one.

The output of the saw-tooth or sweep generator causes the klystron frequency to be swept from a high to a low frequency at a p.r.f. of approximately 2300 Hz. To prevent unwanted modulation of the output signals due to beating between harmonics of the power-supply frequency and the sweep-frequency, the sweep-frequency generator is locked to the second harmonic of the power-supply frequency. The first trigger pulse occurring in each sweep is obtained from cavity A and the pulse switches on a bistable multivibrator which is turned off by the pulse from cavity B (the reference cavity). The latter pulse also turns on a second bistable multivibrator which

is turned off by the pulse from cavity C. Two square wave voltages are thereby produced at the p.r.f. of the sweep generator.

Changes in width of the square wave obtained from each pair of cavities (A-B), (B-C) are proportional to the changes between the resonance frequencies of the two cavities and hence to the difference in refractive index of the air filling them. The two square-wave voltages are limited to a constant amplitude and integrated. Provided the amplitude of the sweep remains constant, the p.r.f. can change without affecting the mean d.c. level.

The final d.c. amplifiers are of the differential type. The refractive-index analogue voltage is applied to one input and accurate direct-voltage steps equivalent to ± 20 or $\pm 2 N$ to the other input; by this means a total change of 200 N -units can be measured. However, when the equipment is flown, the zero setting steps cannot be altered and a total change of only ± 10 or $\pm 20 N$ must be preselected.

3. Telemetry

The telemetry system, built with transistors to reduce size and weight, has provision for five information channels. A single-valve u.h.f. oscillator is amplitude-modulated by the combined outputs of five voltage-controlled oscillators (v.c.o.'s). The instantaneous frequency of oscillation of a given v.c.o. is, over a limited band, linearly related to the input voltage. The input voltages are in turn proportional to the parameters being measured.

The centre frequencies of the oscillators are those recommended by the American Inter-Range Instrumentation Group (I.R.I.G.); they are selected to minimize inter-channel interference and are given in Table 1.

Table 1
Telemetry channel frequencies

I.R.I.G. Channel No.	Centre frequency (Hz) and % deviation	Corresponding maximum modulation frequency (Hz)	Channel use
1	370 (+15%)	6	Pressure (height)
3	730 ($\pm 7.5\%$)	11	Temperature
5	1300 ($\pm 7.5\%$)	20	Wind speed
6	1700		Timing-mark oscillator (ground)
7	2300		Sweep oscillator
8	3000 ($\pm 7.5\%$)	45	Refractive index
9	3900 ($\pm 7.5\%$)	60	Refractive index
10	5400 ($\pm 7.5\%$)	80	Spare
Ref.	6400		Reference frequency (ground)

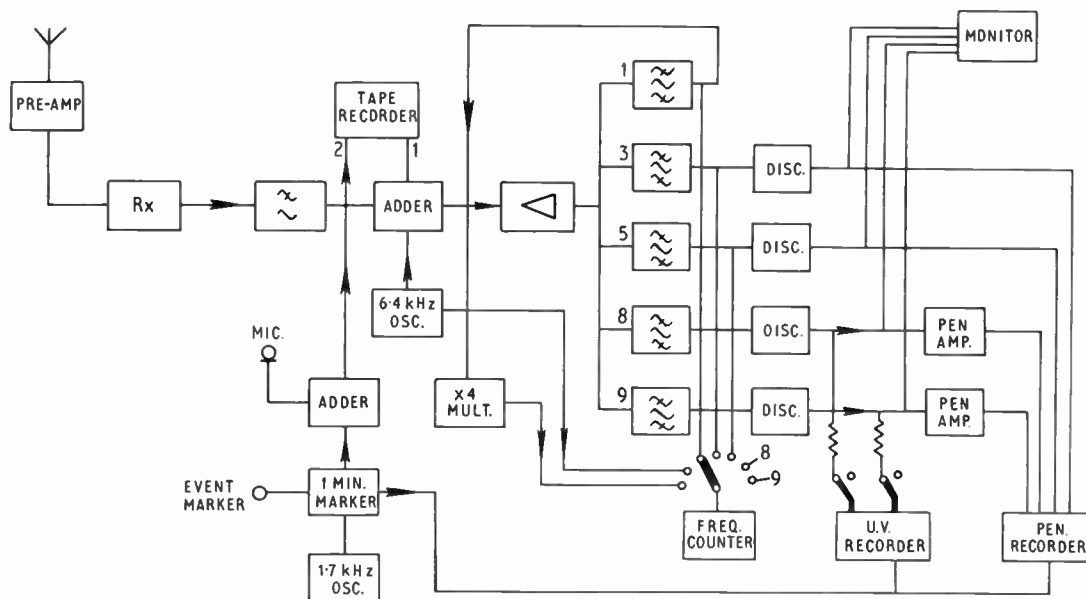


Fig. 4. Telemetry ground equipment.

The output of the u.h.f. transmitter is fed to a helical aerial with a 3 dB beam-width of 70 deg and 8 dB gain. The circular polarization prevents large fluctuations in amplitude if the aerial swings.

4. Measurements of Temperature, Pressure and Wind Speed

4.1. Temperature

Differences in air temperature over a chosen spacing in the vertical or horizontal are indicated by thermocouples connected to a transistor differential amplifier, the output of which controls one of the v.c.o.'s. Drift is 0.25 deg C for a 20 deg change in ambient temperature.

4.2. Pressure

The height of the instrument is monitored in terms of atmospheric pressure changes, based on the model atmosphere of the International Civil Aviation Organization (I.C.A.O.). A sensitive aneroid capsule is linked mechanically to a potentiometer which controls the direct voltages applied to a v.c.o. The maximum frequency-deviation of the v.c.o. corresponds to a height of approximately 1.8 km and the resolution of the measurement is ± 2 millibars or ± 15 metres. To make full use of this resolution at the ground station the instantaneous frequency of the appropriate telemetry channel is multiplied by four and displayed on a digital frequency meter.

4.3. Wind Speed

A lightweight cup anemometer, mounted forward of the refractometer to avoid eddy-effects, drives, via

reduction gearing, a set of make-break contacts. A voltage source applied to the appropriate v.c.o. is interrupted by these contacts. The rate of interruption is proportional to the wind speed. The accuracy is that of the anemometer calibration and is of the order of $\pm 10\%$ at 5 knots and $\pm 3\%$ at 30 knots.

5. Ground Equipment

A block diagram of the equipment is shown in Fig. 4. A steerable helical aerial similar to the airborne one is coupled to the input of a sensitive u.h.f. receiver. The amplitude-demodulated output from the receiver consists of the combined v.c.o. frequencies to which a stable reference is added to enable a correction to be made for the effect of speed variations in the tape recorder (input 1). A speech commentary, time marks, and marks to identify the occurrence of significant events are recorded on the other tape channel (input 2). In parallel, the combined frequencies are separated by band-pass filters and frequency-demodulated.

The filter characteristics are such that frequencies differing from the centre frequency by $\pm 15\%$ are 30 dB down and frequencies differing by $\pm 25\%$ at least 55 dB down.

Each filter output is amplified and limited in a Schmitt trigger-circuit to provide pulses of equal amplitude and shape irrespective of the input frequency. These pulses are rectified and smoothed to produce a voltage proportional to the original transducer voltage and, after amplification, are recorded on a five-pen, quick-response chart recorder. The pens

recording the refractive index variations require ± 55 V into 4200 ohms for full-scale deflection, the amplifiers being designed so that no current flows in the pens at the centre frequency of the channel; however, if the input or discriminator circuits fail, the pens will be deflected heavily off-scale in a negative direction. As a precaution the pens are shunted by a Zener diode which conducts heavily at a voltage sufficiently in excess of 55 V to avoid non-linearity near full-scale deflection.

To enable detailed examination to be made of the small-scale refractive-index changes, provision is also made to record on a quick-response, galvanometer type recorder with a high chart speed. The maximum sensitivity and chart speed are five times those of the pen recorder.

6. Power Supplies

The stabilized voltages required for the refractometer are obtained from a series-regulated, air-cooled, transistor d.c. to d.c. converter. The primary supply is a 30 Ah, 28 V accumulator which supplies 4.5 A. The stabilized voltage is 18.6 V which is used to supply the valve heaters and the converter square-wave oscillator. The output of the oscillator at the transformer secondaries is rectified and smoothed to provide the high-tension supplies of 160, 300, -260 and -85 V. The negative voltage is further stabilized to supply the klystron reflector potential. The overall stability is such that a change of accumulator voltage from 30 to 23 V causes a fall of 0.5 V on the -260 V line. The efficiency of the high tension converter is 85%.

The ground equipment requires 400 W at 230-240 V 50 c/s. The a.c. supply is stabilized in addition to the various h.t. supplies. Furthermore, the heater supplies to the discriminators are obtained from a highly-stabilized source.

7. Performance

The equipment which weighs 140 lb (63 kg), has been flown on a captive balloon (capacity 45 000 ft³; 128 m³) for a total period of about one hundred and fifty hours to heights of 2.5 km, the normal duration of a flight being between two and three hours.

The overall 'noise' level, with sealed cavities, is less than 0.05 *N* units and changes of about 0.1 *N* unit can be detected. The limiting frequency-response, set by the R-C filters following the discriminators, is about 0.6 of the theoretical maximum for each channel. To increase this, more elaborate L-C filters would be required. A specially-designed cavity

wavemeter with a resolution of better than ± 10 kHz (corresponding to ± 1 *N* unit) is used for overall calibration of the two refractive index channels, the reference cavity being replaced by the wave-meter. Slow drifts, after an initial warm-up period of thirty minutes, are not normally greater than 10 *N* units and are not important in the determination of differences in refractive index in the balloon soundings.

The accuracy of the equipment in measuring differences of refractive index is of the order of $\pm 10\%$ of the full scale deflections of ± 20 or ± 10 *N* units. Water droplets in the cavities will, however, cause the system to fail due to the fall in *Q* and the large change in resonance frequency. This limitation has only been encountered so far in clouds with temperatures near 0°C.

Facilities have been provided to sample the magnetic tape recordings at rates up to 400 Hz. These samples are digitized and stored on magnetic data tapes for statistical analysis by a *Pegasus* computer.

6. Acknowledgments

The soundings with the refractometer were carried out with the co-operation of the Meteorological Office, the Ministry of Aviation and the R.A.F. Balloon Unit at Cardington, Bedfordshire. Information on design of cavity resonators was kindly supplied by Dr. M. C. Thompson, Jr., of the N.B.S. Laboratories, Boulder, Colorado, U.S.A. The authors are indebted to Mr. B. E. Hopkins of the Metallurgy Division, National Physical Laboratory, for his help in preparing the specimens of invar used in the construction of the cavities. The outline proposals for the design of the spaced-cavity refractometer are due to Mr. J. A. Lane, to whom the authors are indebted for advice in the experiments and in the preparation of the paper. The work described was carried out as part of the programme of the Radio and Space Research Station, and the paper is published by permission of the Director.

7. References

1. H. B. Bussey and C. Birnbaum, 'Measurement of variations in atmospheric refractive index with an air-borne microwave refractometer', *J. Res. Nat. Bur. Stand.*, **51**, p. 171, 1953.
2. J. A. Lane, 'Small-scale irregularities of the radio refractive index of the troposphere', *Nature*, **204**, p. 438, 1964.
3. J. A. Lane, D. S. Froome and G. J. McConnell, 'The construction and performance of an airborne microwave refractometer', *Proc. Instn Elect. Engrs*, **108**, Pt. B, p. 398, 1961.

Manuscript first received by the Institution on 20th October 1965 and in final form on 23rd March 1966. (Paper No. 1067)

© The Institution of Electronic and Radio Engineers, 1966

A Transistor-Diode Feedback Type Logic Circuit

By

J. B. EARNSHAW, M.Sc.(Eng.)†

AND

P. M. FENWICK, M.Sc.†

Presented at the New Zealand National Electronics Conference sponsored jointly by the New Zealand Section of the I.E.R.E. and the New Zealand Electronics Institute, in Auckland, in August 1966.

Summary: The paper describes an improved form of saturated transistor logic circuit in which rectifier diodes are used to provide non-linear current feedback from collector to base of the transistor. The resulting arrangement has many advantages over the basic saturated circuit, particularly with respect to speed and logical versatility. Due to the ability of the circuit to handle two levels of logic in each stage, mean delays approaching 1 ns per logical decision can be obtained using non-selected components.

1. Introduction

A basic saturated transistor logic circuit is shown in Fig. 1(a) with the collector characteristics and nominal load line in Fig. 1(b). Although this type of logic circuit is well described in the literature, a brief explanation of its operation is appropriate here to facilitate comparisons between it and the feedback-type circuit which has been developed.¹⁻³

When the input level is at V_1 , sufficient current flows through R_1 to supply the current defined by the $R_2 - V_{bb}$ source, and to provide enough base current to drive the transistor into the saturation region. The output level is $V_0 = V_{cs} \approx 0$ volts, and the output impedance is only a few ohms.

When the input level drops to V_0 , the current defined by the $R_2 - V_{bb}$ source, and supplied via R_1 , is sufficient to reverse bias the emitter-base junction of the transistor, whereupon the collector current is reduced to its leakage value, i.e. approximately 0 mA. The output level is then $V_1 \approx V_{cc}$ and the output impedance is R_c .

Logical operations between a number of inputs to the circuit (shown dotted in Fig. 1(a)) are carried out by current summing at the transistor base. By suitably selecting the values of R_1 and R_2 the circuit may be made to perform NOR, NAND or NOT-MAJORITY logic. In general, however, the circuit is used for NOR logic as the associated design conditions are less stringent than those for NAND and NOT-MAJORITY logic.

In order to provide adequate current definition and thereby ensure reliable circuit operation, the difference between the '0' and '1' levels must be comparatively large, often several volts. The large collector voltage 'swing' combined with the fact that the transistor is driven from cut-off into saturation, and vice versa, renders the basic saturated circuit incapable of opera-

tion at very high speeds. A further limitation is that the transistor input capacitance loads the attenuator formed by R_1 and R_2 so that base voltage changes are delayed with respect to the input signals.

The use of a collector clamping diode, as shown in Fig. 1(c), improves the transient response of the circuit at the expense of current definition and fan-out capabilities. An anti-saturation germanium diode, used as in Fig. 1(d), can reduce the turn-off delay in

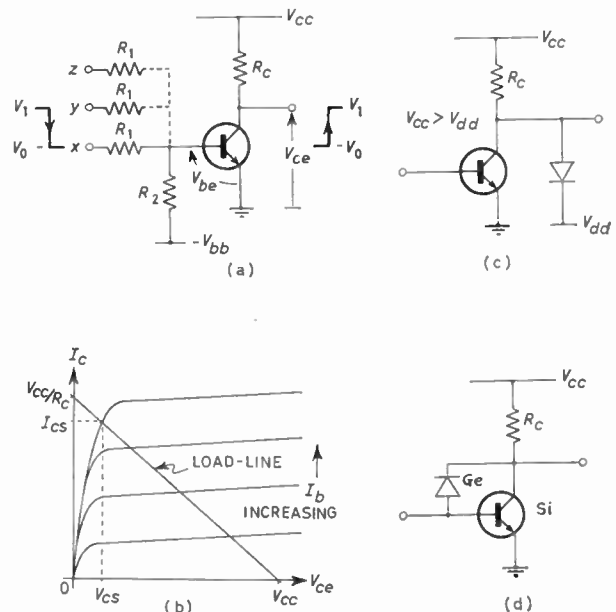


Fig. 1. (a) Basic saturated transistor logic circuit. (b) Collector characteristics and nominal load-line. (c) Collector clamping diode. (d) Anti-saturation diode.

† Physics Department, University of Auckland.

silicon transistors provided that the minority carrier storage in the diode is sufficiently low. Finally, the 'attenuator delay' may be eliminated by connecting 'speed-up' capacitors across the R_1 resistors, although this results in some loss of isolation between different inputs to the same circuit.

2. Basic Transistor-Diode Feedback Circuit

Some very significant changes in the characteristics of the basic saturated transistor circuit occur when non-linear current feedback is applied via a diode connected from collector to base of the transistor, as shown in Fig. 2(a).† The resulting transfer characteristic is illustrated in Fig. 2(b), and its shape is explained as follows.

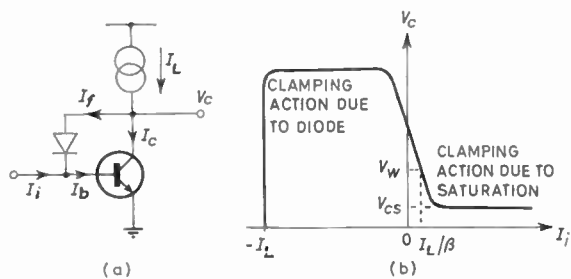


Fig. 2. (a) Basic transistor-diode feedback circuit.
(b) Transfer characteristic.

When the input current $I_i = 0$, all the base current, I_b , is supplied via the feedback path, so that $I_f = I_b = I_L/(1 + \beta)$ where $I_f =$ feedback current $I_L =$ load current, and β is the current gain. In these circumstances the collector potential V_c , is equal to V_w (the forward conduction potential of the base-emitter diode) plus the potential developed across the feedback diode by the current of $I_L/(1 + \beta)$.

When $I_i = I_L/\beta$, the base current necessary to maintain the collector current of I_L is supplied solely by the input, so that the current through the feedback diode is zero and the collector potential is equal to that of the base, i.e. $V_c = V_b \approx V_w$. Further increases in I_i cause the transistor to saturate with $V_c = V_{cs}$.

For negative values of I_i where $|I_i| < I_L$, the current through the feedback diode is $(I_L + \beta|I_i|)/(1 + \beta)$, and V_c is then determined mainly by the characteristics of the diode. When $I_i \leq -I_L$ the collector current is reduced to zero, so that transistor action ceases and the value of V_c is undefined.

† A version of this circuit with a feedback resistance in place of the diode is discussed in the Appendix, which should be read in conjunction with this section.

If the range of input currents is limited to $|I_i| \ll I_L$, consistent with the transistor saturating, then the value of I_c is approximately constant and equal to I_L for all values of I_i . Under these circumstances, which correspond to normal operating conditions, the outstanding features of the circuit are:

- (i) The clamping action of the feedback diode limits the collector voltage 'swing' and thereby maintains the collector current at very nearly the saturation value.
- (ii) Since the feedback current limits any changes in base current to $1/(1 + \beta)$ times the corresponding changes in input current the base potential is maintained approximately constant and equal to V_w .
- (iii) With similar type semiconductors for both the feedback diode and transistor, the high and low collector output levels are symmetrical about the constant base potential. For silicon devices these levels are typically 1.4 volt and 0.2 volt.
- (iv) Except for a small range of values of I_i in the vicinity of I_L/β the transistor is either saturated or operated with negative current feedback. Both these conditions provide low input and output impedances of typically 15–25 ohms.

Improvements in the switching speed of this circuit, as compared with the basic saturated transistor circuit, are a direct consequence of the features set out above. For example, when the output level is switched from high to low and back to high again by an input current pulse, then:

- (i) Since in this circuit V_b is virtually constant it is not necessary for the 'turn-on' input current to charge the base circuit capacitances before the output level can be lowered. It is, however, necessary to supply some charge to overcome minority carrier storage in the feedback diode before it can be reverse biased.
- (ii) Because the transistor is never cut-off, it is not necessary to establish conduction, and comparatively little charge is required to drive the transistor into saturation. In addition, the limited output voltage swing reduces the charge required by the collector circuit capacitances.
- (iii) Removal of the excess base charge by the 'turn off' input current is unaffected by the feedback diode since it is cut-off during this phase of the switching operation.
- (iv) Taking the transistor from the edge of saturation to the condition where the output voltage is again clamped by the feedback diode requires approximately the same charge as for phase (ii).

Clearly the 'turn-on' delay is determined largely by the storage characteristics of the feedback diode, and

the 'turn-off' delay by those of the transistor. For optimum operation, the storage characteristics of the two semiconductor devices should be similar, and as low as possible.

3. Actual Transistor-Diode Feedback Circuit

The actual feedback circuit, as shown in Fig. 3 uses a Fairchild 2N709 silicon planar epitaxial n-p-n transistor with a pair of Mullard AAZ13 gold-bonded germanium diodes in the feedback path. The use of a pair of germanium diodes is a temporary expedient

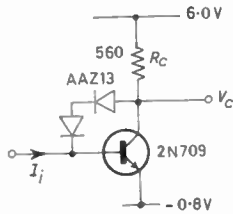


Fig. 3. Actual transistor-diode feedback circuit.

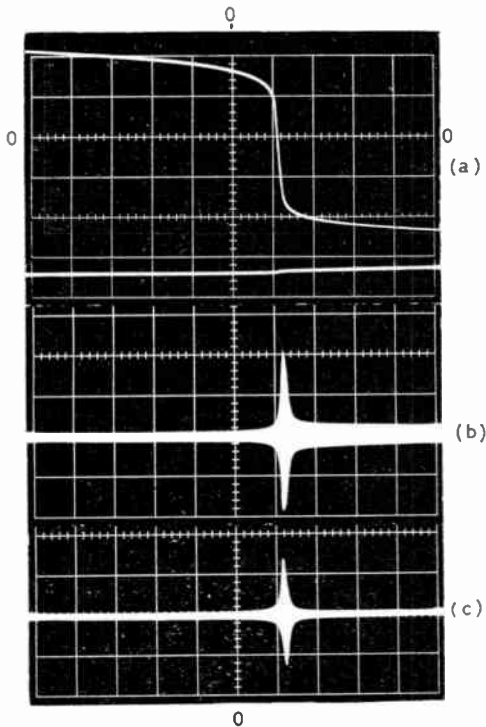


Fig. 4. Feedback circuit characteristics ($I_1 \dots 0.2$ mA/div).

- (a) Upper trace: transfer characteristic V_c vs I_1 ($V_c \dots 0.25$ volt/div).
Lower trace: input characteristic V_b vs I_1 ($V_b \dots 0.25$ volt/div).
- (b) Input resistance R_i vs I_1 ($R_i \dots 50$ ohm/div).
- (c) Output resistance R_o vs I_1 ($R_o \dots 50$ ohm/div).

until a suitable silicon diode becomes available at comparable cost. By returning the emitter to -0.8 volt the base is maintained at approximately earth potential, so that the upper and lower output levels are $+0.5$ volt and -0.6 volt respectively.† The ideal current source I_L in the basic circuit is replaced by a resistance R_c in the actual circuit. In order to achieve optimum switching speeds the value of R_c is selected so that the mean collector current is about 10 mA, since this maximizes the gain-bandwidth product for the 2N709 transistor.

The oscillograms in Fig. 4 show the circuit characteristics. The transfer characteristic is close to ideal, with a sharp transition between two well-defined output levels, and the input characteristic shows the almost constant base potential which is expected from the discussion in the previous section.

The input and output impedance oscillograms are obtained by modulating I_i or I_L , as appropriate, at 500 kHz with a current of 10 μ A. The relevant impedance is indicated by the peak-peak amplitude of the 500 kHz signal. The oscillograms show that except in the immediate vicinity of the transition region where they rise to 200 ohms and 150 ohms respectively, the small signal input and output impedances are comparatively low, i.e. 15-25 ohms.

4. Inter-circuit Coupling

The nearly constant value of the base potential makes the feedback circuit apparently very suitable for use with resistive coupling, but when account is taken of the various component and supply tolerances, the difference of only 1 volt between the output levels leads to unacceptably poor current definition. An alternative and superior form of inter-circuit coupling is provided by the current steering diode gates shown in Fig. 5. These gates rely for their operation on the low input and output impedances of the feedback

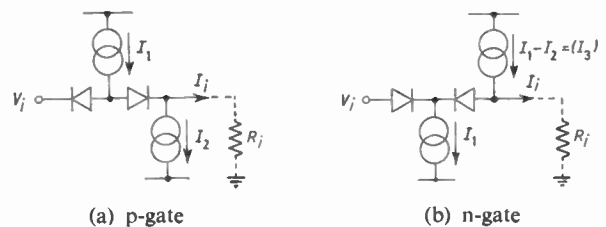


Fig. 5. Current steering diode gates.

† Returning the emitter to a negative supply line so that the base is at earth potential is clearly not necessary for the operation of the circuit, but it does facilitate the observation of circuit waveforms using a sampling oscilloscope with low impedance d.c. probes.

circuit, together with the symmetry of the output levels about the nearly constant base potential.

Both the gates are designed so that the current I_i supplied to the feedback circuit is $I_1 - I_2$ when V_i is high and $-I_2$ when V_i is low. The differences between the two types of gate lie mainly in their demands on the input voltage source V_i , and in their applications. With a p-gate, the voltage source must accept a current I_1 when V_i is low, whereas with an n-gate it must supply a current I_1 when V_i is high. By employing additional input diodes p-gates can be used to perform AND operations between a number of inputs with positive logic, whilst n-gates can be used for AND operations with negative logic. Upon reversing the sign of the logic both the diode gates perform OR operations.

5. Complete Logic Circuit

By combining the transistor-diode feedback circuit with an appropriate diode gate a complete logic circuit is formed. Two such circuits are shown in Fig. 6. With positive logic, circuit (a) performs the NAND operation between inputs x and y , whereas circuit (b) performs the NOR operation.

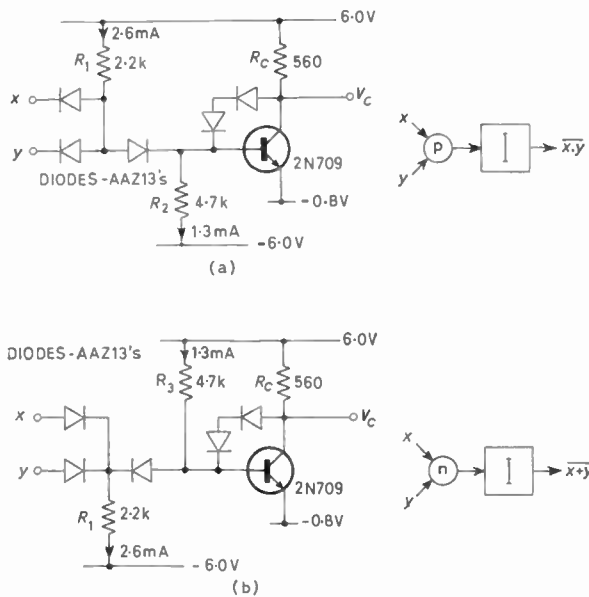


Fig. 6. Complete logic circuits with (a) p-gate and (b) n-gate. (Indicated logical operations apply only for positive logic.)

In the actual logic circuit the ideal current sources in the gates are replaced by resistances R_1 , R_2 and R_3 , defining currents of about 2.6 mA, 1.3 mA and 1.3 mA respectively. Since the smallest of these resistances is about 100 times greater than the input and output

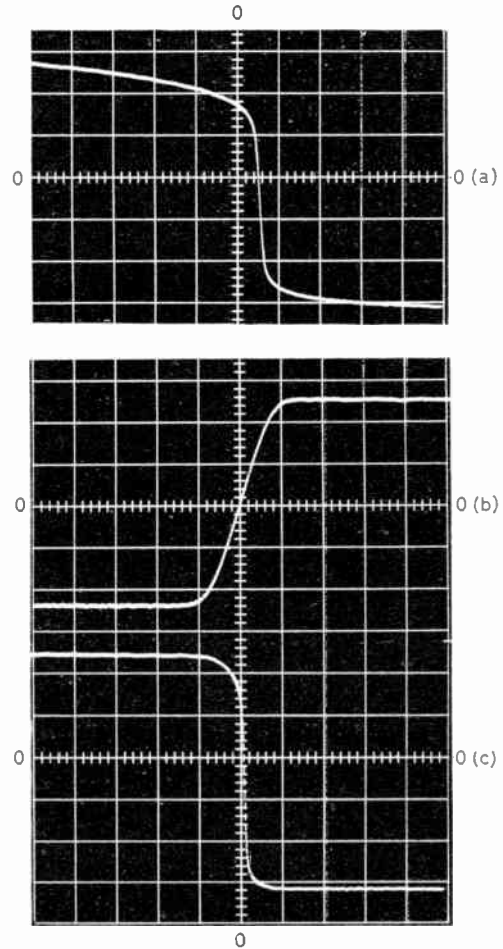


Fig. 7. Circuit transfer characteristics.

- (a) Feedback circuit, V_c vs I_i ($V_c \dots 0.2$ V/div; $I_i \dots 0.5$ mA/div).
- (b) Gate circuit, I_i vs V_i ($I_i \dots 0.5$ mA/div; $V_i \dots 0.2$ V/div).
- (c) Overall, V_c vs V_i ($V_c \dots 0.2$ V/div; $V_i \dots 0.2$ V/div).

impedances of the feedback circuit, the concept of ideal current sources can be retained.

Actual transfer characteristics of the feedback circuit, diode gate and the complete logic circuit are displayed by the oscillograms in Fig. 7. The double limiting actions of the feedback circuit and diode gate result in a very sharp transition between the output levels in the overall transfer characteristic, the output being undefined only for input voltages in the range -100 mV to $+100$ mV. Since the output levels are $+500$ mV and -600 mV, one very important feature resulting from the narrow transition region is immunity from noise of many tens of millivolts.

The power requirements of the circuit are quite moderate, the mean dissipation being about 100 mW.

6. Constructional Details

In view of the high speed operation which the circuit is capable of attaining, the control and reduction of unwanted stray capacitances and inductances is most important. For this reason the circuits are constructed on double-sided copper laminate, one copper layer being used as a ground plane. The signal paths through the semiconductors are arranged to be as short as the components permit, but due to the negligible variations in the currents flowing through the collector load and gate resistors the leads of these components may be comparatively long, thereby enabling the power supply lines to be well removed from the signal circuitry. Extensive decoupling of the ± 6 volt supply lines is unnecessary and small blocks of 6 or 8 logic circuits may be operated with only one 50 nF bypass capacitor on each line. The -0.8 volt supply line is bypassed with a 50 nF disk ceramic capacitor at each emitter.

Interconnections between spatially separated logic circuits are greatly simplified by the low input impedance of the feedback circuit which, with the inclusion of an appropriate series resistor, provides a reasonable match for 50 ohm miniature coaxial cable. The current steering diode gates operate without modification as cable drivers.

7. Logic Delays

Evaluation of the dynamic characteristics of the logic circuit, under conditions which simulate as far as possible those in an infinite chain of asynchronous logic, can be made by observing its performance in a ring oscillator, constructed by connecting an odd number of logic circuits in a continuous loop. Such a configuration is inherently unstable, its period of oscillation being equal to twice the loop delay. Provision of 'dummy' fan-out loading for each logic circuit extends the degree of environmental simulation, and thereby enables the effects of such loading on the circuit's performance to be studied. By arranging that the various defined currents can also be varied it is possible to optimize the design of the logic circuit for minimum logic delay. The component values given earlier are those for the optimum design when R_c is selected according to the fan-out to provide a mean collector current of about 10 mA.

The unloaded delay of the logic circuit is 2 ns and this increases with fan-out as shown in Fig. 8. The increased delay is brought about partly by the varying current requirements of the diode gates which cause the collector current to change as the output switches from one level to the other, and partly by the extra capacitive loading which is introduced.

For a given fan-out the logic delay with p-gates is observed to be larger than that with n-gates. One

factor contributing to this is that with p-gates the logic circuit must accept current from the gates when V_{cc} is low, whereas with n-gates the circuit supplies current to the gates when V_{cc} is high. Therefore with p-gates the transistor is operated under more adverse conditions than with n-gates, so that its switching

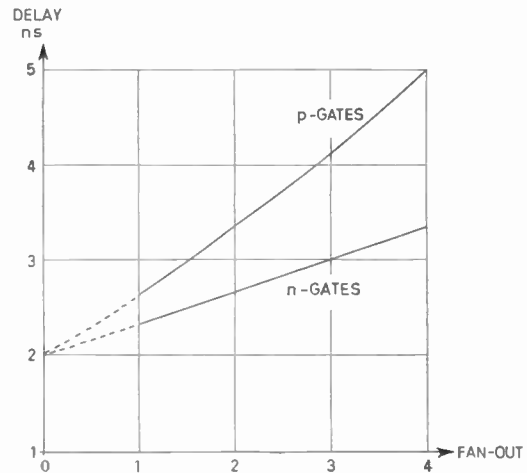


Fig. 8. Graph of mean logic delay vs fan-out.

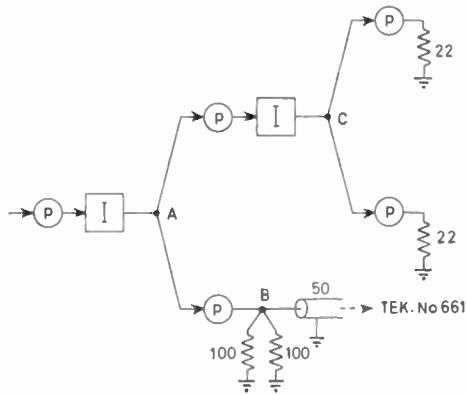
speeds are consequently slower. Obviously to minimize logic delays n-gates are used wherever possible.

8. Circuit Waveforms

Using the circuit arrangement in Fig. 9(a) the waveforms in Fig. 9(b) were observed with a sampling oscilloscope. Correct relative timing exists between the different waveforms so that events in various parts of the circuit can be correlated.

The decrease in switching speed and associated increase in logic delay when a logic circuit is loaded by two p-gates may be clearly seen by comparing waveforms (i) and (ii).

The overshoots in waveform (iii), which shows the gate output current at B, are due partly to minority carrier storage in the gate diodes and partly to capacitive feed-through. These overshoots have a significant effect on the output of the following feedback circuit, especially when it is loaded, as in waveform (v). During the initial stages of the rise and fall of the output voltage the feedback circuit is driven by an input current which overshoots to nearly twice the steady state value; consequently the voltage transition in these initial stages is faster than in the final stages where the input current recovers to its steady state value.



(a) Arrangement for observing circuit waveforms.

Fig. 9.

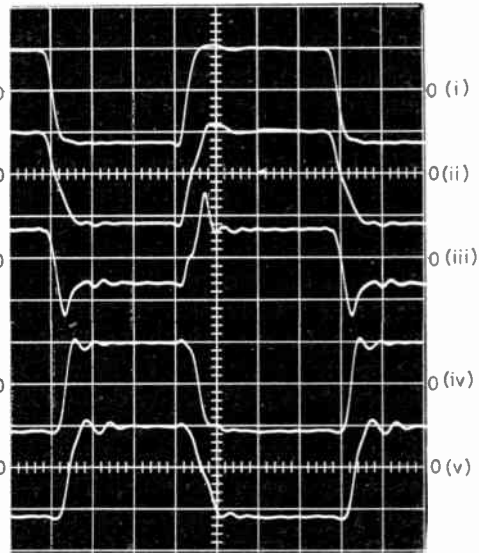
Some minority carrier storage in the gate diodes is clearly desirable, for without it the initial faster switching of the output voltage disappears and the logic delay is increased; however, as it also places additional loading on the driving circuit the optimum amount is difficult to assess. The diodes selected for the gate circuit are the same type as those employed in the feedback circuit, and in this way neither the gate circuit nor the feedback circuit unduly limits the speed capabilities of the other.

The output voltage waveforms from the second logic circuit show a delay, relative to the loaded output of the first, of about 2 ns for no loading increasing to about 3.5 ns for a loading of two p-gates. The slight ringing on these waveforms is due to a resonance of the feedback loop. It is somewhat dependent upon the transistor used and the collector current, but it is of insufficient amplitude to affect the operation of any following gates.

9. Fan-in and Fan-out Limitations

The main limitation on fan-in is imposed by the problem of providing satisfactory interconnections between associated logic circuits rather than by reverse conduction in the gate diodes, which is the more usual limitation. For example, with a fan-in of four the reverse conduction at 25°C is less than 5% of I_1 . On the other hand the fan-out is limited largely by the input current requirements of the following gates (see Section 4). With n-gates the limitation is that $I_c > 0$ when the output level is high, whereas with p-gates it is that $I_c < \beta(I_1 - I_2)$ when the output level is low.

A worst case analysis to determine the maximum fan-out indicates that with resistor and power supply tolerances of $\pm 5\%$ and strictly worst-case semiconductors, complete reliability is guaranteed for fan-outs of up to 3 n-gates, 3 p-gates, or 2 n-gates together with 2 p-gates, when R_c is chosen so that the



(b) Circuit waveforms (scales 0.5 V/div; 2 mA/div; 10 ns/div).

- (i) Unloaded output voltage at A with gates disconnected.
- (ii) Loaded output voltage at A with fan out of 2 p-gates.
- (iii) Gate current at B, equal to that supplied to the feedback circuit.
- (iv) Unloaded output voltage at C with gates disconnected.
- (v) Loaded output voltage at C with fan-out of 2 p-gates.

mean value of I_c is about 10 mA. With some selection of components and reduction in operating speed, fan-outs of 4 n-gates and 4 p-gates are possible.

10. Logical Capabilities

By combining the basic p- and n-gates with additional diodes and with each other, as shown in Fig. 10, their logical capabilities may be considerably extended.

For the purposes of defining the logical operations performed by the various arrangements, it is convenient to consider the logic to reside in the transfer current I_i , which is supplied to the following feedback circuit (inverter). Table 1 is a truth table in terms of I_i for the arrangements (a), (b), (c) and (d). It may be extended to include (e) and (f) by noting that (e) simplifies to (d) if $x = pANDq$ and $y = rANDs$; similarly (f) simplifies to (b) if $x = pORq$ and $y = rORS$.†

The logical operations performed by the various arrangements are indicated in Fig. 10 assuming positive logic. With negative logic the operations AND and OR are interchanged.

† Arrangements such as (e) and (f) are often referred to as two-level logic gates, because they perform two logical operations. With such arrangements the delay per logical decision is effectively half the normal stage delay. When these gates are incorporated in the present logic circuit mean delays approaching 1 ns per logical decision can be obtained.

Table 1

Truth table for diode gates (a), (b), (c) and (d) in Fig. 10 (Nominal current values are $I_1 = 2.6 \text{ mA}$, $I_2 = 1.3 \text{ mA}$).

Inputs		I_1			
x	y	(a)	(b)	(c)	(d)
low	low	$-I_2$	$-I_1 - I_2$	$-I_2$	$-I_2$
high	low	$-I_2$	$-I_2$	$I_1 - I_2$	$I_1 - I_2$
low	high	$-I_2$	$-I_2$	$I_1 - I_2$	$I_1 - I_2$
high	high	$I_1 - I_2$	$I_1 - I_2$	$I_1 - I_2$	$2I_1 - I_2$

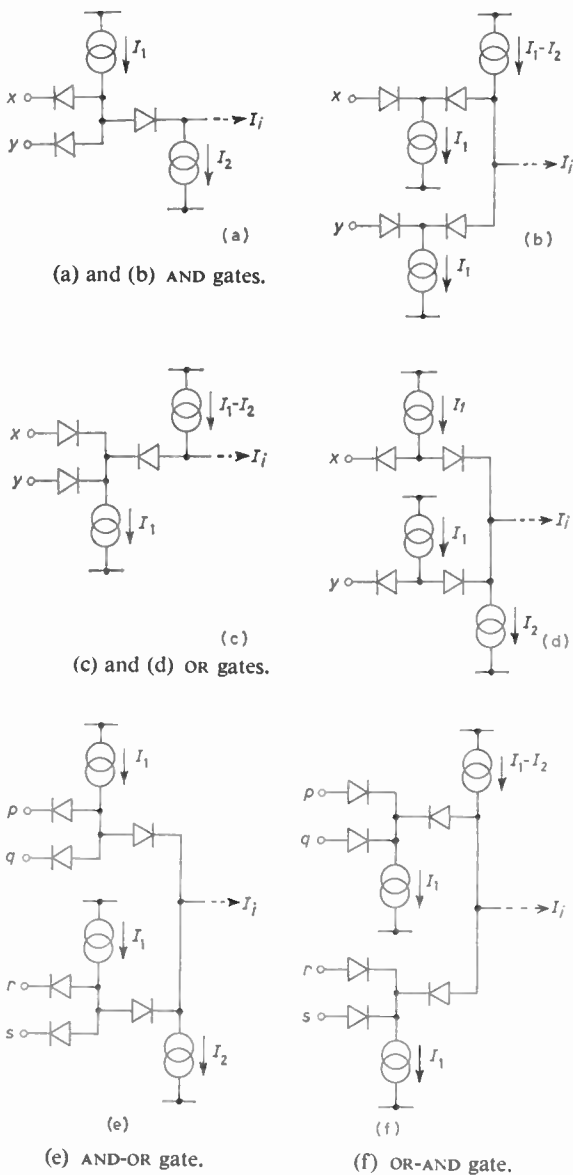


Fig. 10. Logical operations with current steering diode gates for positive logic. (For negative logic, operations AND and OR are interchanged.)

For certain input combinations the (b)-type and (d)-type arrangements demand and supply respectively over-drive currents of 3.9 mA, assuming $I_1 = 2I_2 = 2.6 \text{ mA}$. With the (b)-types, where the demanded over-drive current is supplied via the feedback diodes of the following inverter, allowance must be made for this current in the selection of R_c . Increased delays due to excess stored charge in either the transistor or the feedback diodes will only occur in the unlikely event where the inputs are changed simultaneously from their overdrive condition values.

Notwithstanding the problems associated with the over-drive currents and the cost of extra components, there are some applications where, because of the different loading conditions they impose on the preceding inverters, the (b) and (d) arrangements may be preferred to the simpler (a) and (c) arrangements which perform the same logical operations.

11. Alternative Feedback Circuits

Smith and Pohm⁴ have described a logic circuit in which backward diodes or low peak current (1 mA) tunnel diodes are used as feedback elements from collector to base of the associated transistor. The bi-directional conduction characteristics of these tunnelling devices ensure that not only is the transistor never cut-off, but also it is kept out of saturation. By using tunnel diodes with peak currents which are less than the input driving currents, the logic circuit does not suffer from the latching properties normally characteristic of circuits employing these devices. Because the collector output levels are asymmetric about the base potential the use of current steering diode gates is precluded and conventional resistor coupling is employed. With similar type transistors the Smith and Pohm circuit has comparable operating speeds to the transistor-diode circuit that has been described herein, but it is more expensive, less versatile, and requires closer tolerance components for reliable operation.

Another circuit which uses tunnel diodes in a feedback path from collector to base of a transistor has been described by Scarrott and Mitchell.⁵ In their circuit the tunnel diode peak current is comparable with the transistor collector current variation, so that the tunnel diode provides part of the current gain and thereby enhances the switching speed of the circuit. This feedback circuit is potentially the fastest of those mentioned in this paper; however, in addition to having similar disadvantages to the Smith and Pohm circuit, it is also a latching type circuit. This latter feature limits its applications almost entirely to synchronous systems.

A version of the transistor-diode feedback circuit has been developed with the transistor emitter earthed

and the current defining resistors returned to ± 9 volt supply lines. Although this version has the disadvantages of having output levels that are asymmetric with respect to earth (0.2 volt and 1.3 volt), and increased power dissipation (approximately 150 mW per stage), it has the advantages of requiring one less supply voltage, no emitter decoupling capacitor, and being somewhat less restricted by semiconductor tolerances. The circuits of the gates and the inverter are illustrated in Fig. 11.

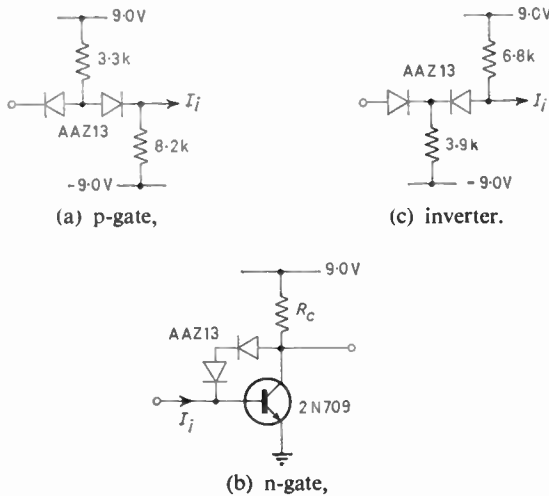


Fig. 11. Logic circuit with earthed emitter.

One immediate application for the transistor-diode feedback type logic circuits is in the carry path of a high speed parallel adder. The sum generation time for words of 16 bits is expected to be about 45 ns. The design of this adder, which is based on the Kilburn adder,⁶ will be described elsewhere.

12. Acknowledgments

The use of a feedback diode for collector-base voltage clamping was suggested to one of the authors (J. B. E.) by Dr. M. J. Lanigan in 1963 when this author was a Turner & Newall Research Fellow in the Electrical Engineering Laboratories at the University of Manchester. Both authors thank Dr. Lanigan for his suggestion which had arisen from his previous discussions with Mr. E. T. Warburton of International Computers and Tabulators Ltd., West Gorton, Manchester, who subsequently presented details in a contribution (not published) at a Joint I.E.R.E.-I.E.E. Colloquium on 'Logic Circuits' in January 1965.

The generous financial support of the New Zealand Universities Research Grants Committee during the design and development of this logic circuit is gratefully acknowledged.

The provision of suitable research facilities in the Physics Department at the University of Auckland is greatly appreciated.

13. References

1. J. B. Earnshaw, 'Design for a tunnel diode-transistor store with non-destructive read-out of information', *I.E.E.E. Trans. on Electronic Computers*, EC-13, pp. 710-22, December 1964.
2. P. M. Fenwick, 'The Design, Analysis and some Applications of a High Speed Transistor Logic Circuit', M.Sc. Thesis, University of Auckland, September 1965.
3. J. B. Earnshaw, 'Some High Speed Tunnel Diode and Transistor Digital Circuits', Ph.D. Thesis. University of Auckland, December 1965.
4. W. R. Smith and A. V. Pohm, 'A new approach to resistor-transistor-tunnel diode nano-second logic', *I.R.E. Trans. on Electronic Computers*, EC-11, pp. 658-64, October 1962.
5. G. G. Scarrott and R. W. Mitchell, 'High speed logic circuits using a tunnel diode transistor feedback amplifier', *J. Brit. I.R.E.*, 26, pp. 485-91, December 1963.
6. T. Kilburn, D. B. G. Edwards and D. Aspinall, 'A parallel arithmetic unit using a saturated-transistor fast carry circuit', *Proc. Instn Elect. Engrs*, 107B, pp. 573-84, November 1960 (I.E.E. Paper No. 3302M).

14. Appendix

Approximate Analysis of a Transistor Feedback Circuit

Figure 12(a) shows a simple transistor circuit in which direct current feedback is applied from collector to base via a resistance R_f . The input current I_i and the load current I_L are supplied from ideal current sources. Interest in the circuit is centred in the transfer relationship between V_c and I_i for I_L constant.

For the purpose of this approximate analysis the action of the transistor is represented by the equations

$$I_c = \beta I_b \quad \dots\dots(1)$$

and
$$V_b = V_k + R_b I_b \quad \dots\dots(2)$$

for $V_c > V_{cs}$ and $I_b > 0$

where V_{cs} is the collector-emitter saturation voltage, V_k is the knee-voltage of the base-emitter diode characteristic and R_b is the slope resistance (assumed constant) of this characteristic.

From an inspection of the circuit,

$$I_c = I_L - I_f \quad \dots\dots(3)$$

$$I_b = I_i + I_f \quad \dots\dots(4)$$

and
$$V_c = V_b + R_f I_f \quad \dots\dots(5)$$

Solving eqns. (1), (3) and (4) for I_f , I_b and I_c in terms of I_i and I_L :

$$I_f = \frac{I_L - \beta I_i}{1 + \beta} \quad \dots\dots(6)$$

$$I_b = \frac{I_L + I_i}{1 + \beta} \quad \dots\dots(7)$$

and
$$I_c = \beta \frac{I_L + I_i}{1 + \beta} \quad \dots\dots(8)$$

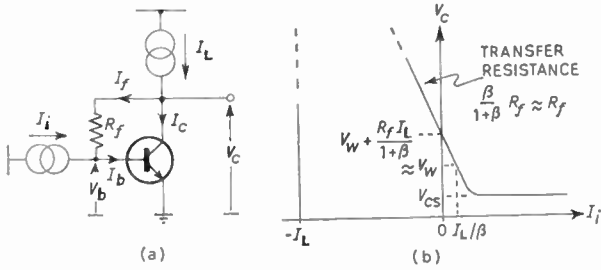


Fig. 12. (a) Transistor feedback circuit.
(b) Transfer characteristic.

Accordingly eqn. (2) becomes

$$V_b = V_k + R_b \frac{I_L + I_i}{1 + \beta} \quad \dots\dots(9)$$

and assuming that $R_f \gg R_b/\beta$, as will normally be the case, eqn. (5) becomes

$$V_c = V_k + \frac{R_b + R_f}{1 + \beta} \cdot I_L - \frac{\beta \cdot R_f}{1 + \beta} \cdot I_i \quad \dots\dots(10)$$

For constant values of I_L it is convenient to rewrite eqn. (10) as

$$V_c = V_w + \frac{R_f}{1 + \beta} (I_L - \beta I_i) \quad \dots\dots(11)$$

where V_w is the forward conduction potential of the base-emitter diode when $I_i = 0$, i.e.

$$V_w = V_k + R_b I_L / (1 + \beta)$$

The transfer characteristic in Fig. 12(b) follows directly from eqn. (11) and significant features associated with it are:

(i) when $I_i \leq -I_L$:

$$I_b = 0, \quad I_c = 0$$

and the transistor is cut-off with V_c undefined.

(ii) when $I_i = 0$:

$$I_b = I_L / (1 + \beta)$$

and this base current is all supplied via R_f ,

so that

$$V_b = V_w$$

and

$$V_c = V_w + R_f \cdot \frac{I_L}{1 + \beta}$$

(iii) when $I_i = I_L/\beta$:

$$I_f = 0$$

i.e. the feedback current is cut-off and

$$V_c = V_b \approx V_w$$

(iv) when $I_i > I_L/\beta$:

$$V_c \rightarrow V_{cs}$$

and the transistor is driven into saturation as I_i

is increased to approximately

$$I_L/\beta + (V_w - V_{cs})/R_f.$$

For $-I_L < I_i < I_L/\beta$ the circuit has a transfer resistance

$$-\frac{\partial V_c}{\partial I_i} = \frac{\beta}{1 + \beta} \cdot R_f \quad \dots\dots(12)$$

and because only a fraction $1/(1 + \beta)$ of any input current change is supplied to the base, the associated changes in V_b , compared with those in V_c are small, namely,

$$\frac{\partial V_b}{\partial I_i} / \frac{\partial V_c}{\partial I_i} = -\frac{1}{\beta} \cdot \frac{R_b}{R_f} \quad \dots\dots(13)$$

The input impedance, at frequencies much less than f_r , for I_L constant is

$$\frac{\partial V_b}{\partial I_i} = \frac{R_b}{1 + \beta} \dots (= R_i) \quad \dots\dots(14)$$

Similarly the output impedance, for I_i constant is

$$\frac{\partial V_c}{\partial I_L} = \frac{R_b + R_f}{1 + \beta} \dots (= R_o) \quad \dots\dots(15)$$

The apparently anomalous result in equation (14), namely that the input impedance is independent of the value of the feedback resistance, arises from the initial assumptions regarding the ideal nature of the transistor and current sources. In practice R_f must be significantly less than the current defining resistance in the collector circuit current source for the above analysis to be valid. Under these circumstances the input impedance of the circuit is approximately the same as that of a grounded base transistor, and the output impedance is similar in magnitude to the input impedance.

Many of the results derived above still apply, subject to some limitations, even when the feedback element is non-linear. For example, if the voltage drop across the non-linear element is $F(I_f)$ for a current of I_f , and the slope resistance at this current is R_f , eqns. (6) to (8) remain unchanged, whilst eqns. (13) to (15) are valid for small changes about a specific operating condition. The most significant modification is to eqn. (5) which becomes

$$V_c = V_b + F(I_f) \quad \dots\dots(16)$$

Accordingly eqn. (11) becomes

$$V_c \approx V_w + F\left(\frac{I_L - \beta I_i}{1 + \beta}\right) \quad \dots\dots(17)$$

which clearly indicates that the shape of the transfer characteristic is determined mainly by the characteristics of the non-linear feedback element.

*Manuscript received by the Institution on 27th May 1966.
(Paper No. 1068/C87)*

Radio Engineering Overseas . . .

The following abstracts are taken from Commonwealth, European and Asian journals received by the Institution's Library. Abstracts of papers published in American journals are not included because they are available in many other publications. Members who wish to consult any of the papers quoted should apply to the Librarian, giving full bibliographical details, i.e. title, author, journal and date, of the paper required. All papers are in the language of the country of origin of the journal unless otherwise stated. Translations cannot be supplied.

NOISE IN PARAMETRIC AMPLIFIERS

The reduction of signal/noise ratio of a parametric amplifier which has a noisy pumping source has been discussed in a Japanese paper. The p.m. noise in the pumping source is cancelled out through the two conversion processes, and therefore the reflection type parametric amplifier is shown to be the most suitable for f.m. transmission. The a.m. noise in the pumping source is converted to p.m. noise in the parametric amplifier and the succeeding stages, but this noise can be countered by the saturation effect of the gain relating to the pumping power. Consequently, it is shown that it is possible to use noisy microwave power generated from the multiplier for a pumping source without any decrease in the signal/noise ratio.

'Signal/noise ratio diminishing of parametric amplifier due to noisy pumping source in the case of f.m. transmission', T. Okajima, T. Kamata and H. Komagata, *Review of the Electrical Communication Laboratory, NTT*, 14, Nos. 5-6, pp. 400-405, May-June 1966.

V.I.F. PROPAGATION

The shape and order of the recorded regular undisturbed diurnal phase change of the v.l.f. signals is discussed in a recent German paper. The signals were received at Lindau, Harz (Germany) from the 18.6 kc/s transmitter at Jim Creek (NPG/NLK) near Seattle, Washington, over the transpolar propagation path. The largest regular diurnal change in phase is about 2λ radians and occurs at the time near equinox, and the smallest change occurs at the time near summer and winter solstice. Through the spherical v.l.f. waveguide, in which the earth and the ionosphere are considered to be sharp boundaries, the second mode (in addition to the first mode) can propagate over long paths under special conditions and, after having travelled about 8100 km, often arrives with amplitudes of the same order as those of the first mode, so that phase deviations by interference of the first and second mode can occur. The impact of solar plasma and the phenomena caused by it in the polar ionosphere (aurora, geomagnetic activity and an increase of ionospheric absorption of h.f. radio waves) obviously affect the regular diurnal phase change only at those times of the day when most of the propagation path is in darkness. Polar cap absorption events have not been observed in the phase records during the observation period from June 1964 to August 1965 (sunspot minimum epoch). Events of this kind should be observed in the approaching years of increased sunspot activity.

'Results of phase variation measurements on v.l.f. signals propagated through the Arctic Polar cap', G. Lange-Hesse and K. Rinnert, *Archiv der Elektrischen Übertragung*, 20, No. 2, pp. 123-29, February 1966.

DISTRIBUTION OF AUDIO FREQUENCY SIGNALS ON TELEVISION LINKS

A paper by two authors with Nederlandsche Radio Unie describes a system which provides for the simultaneous distribution of monophonic and stereophonic programmes using a television radio-relay link.

With a modern television link, six a.f. programmes may be transmitted simultaneously in the video-frequency band. Three of these programmes may be multiplex stereophonic signals; in this case, sub-carriers are frequency-modulated with a deviation of 8%. For the three monophonic programmes, amplitude-modulation with suppressed sub-carriers is used, and pilot-tones whose frequencies are half the sub-carrier frequencies are added for the demodulation.

Outside the video band, several additional sound programmes might be accommodated if necessary, the normal television-sound channel being already available.

This system offers many advantages over the conventional method of distributing sound signals, both for a broadcasting organization's own needs and for exchanges between broadcasting organizations. The distribution of stereophonic signals, which was once considered to be almost impossible, may be effected easily and the flexibility of the method is equal to the handling of normal sound programmes.

'Distribution of monophonic and stereophonic audio-frequency signals on television links', H. J. van der Heide and J. J. Geluk, *E.B.U. Review*, 96-A, pp. 46-51, April 1966. (In English.)

HIGH-SPEED SHIFT REGISTER

If a digital computer can shift the numerical information of one word by several positions at a time, higher speed logical operations can be obtained.

The author of a Japanese paper describes an experimental model of the high-speed shift register which operates with a clock frequency as high as 5 MHz and yields a shift time of over 20 digits in 40 nanoseconds. It uses a multi-winding pulse transformer.

The use of a taper line for propagation of shift signal is a method for parallel drive in many high-speed circuits, and a pulse transformer constructed from parallel lines was found useful for these high-speed operations. The author states that the device uses only about half the number of circuit elements used in conventional diode logic.

'A forty nanoseconds high-speed shifter', N. Kuroyanagi, *Review of the Electrical Communication Laboratory, NTT*, 14, Nos. 5-6, pp. 381-99, May-June 1966.